LONG-TERM ANALYSIS APPLIED TO MOORING SYSTEMS DESIGN

Pedro de Amorim Seabra

Dissertação de Mestrado apresentada ao Programa de Pós-graduação em Engenharia Oceânica, COPPE, da Universidade Federal do Rio de Janeiro, como parte dos requisitos necessários à obtenção do título de Mestre em Engenharia Oceânica.

Orientadores: Paulo de Tarso Themistocles Esperança
Luis Volnei Sudati Sagrilo

Rio de Janeiro
Setembro de 2019

LONG-TERM ANALYSIS APPLIED TO MOORING SYSTEMS DESIGN

Pedro de Amorim Seabra

DISSERTAÇÃO SUBMETIDA AO CORPO DOCENTE DO INSTITUTO ALBERTO LUIZ COIMBRA DE PÓS-GRADUAÇÃO E PESQUISA DE ENGENHARIA (COPPE) DA UNIVERSIDADE FEDERAL DO RIO DE JANEIRO COMO PARTE DOS REQUISITOS NECESSÁRIOS PARA A OBTENÇÃO DO GRAU DE MESTRE EM CIÊNCIAS EM ENGENHARIA OCEÂNICA.

Examinada por:

_____

Prof. Paulo de Tarso Themistocles Esperança, D.Sc.

_____

Prof. Luis Volnei Sudati Sagrilo, D.Sc.

_____

Dr. Paulo Mauricio Videiro, D.Sc.

_____

Dr. Mauro Costa de Oliveira, D.Sc.

RIO DE JANEIRO, RJ - BRASIL
SETEMBRO DE 2019

Seabra, Pedro de Amorim

Long-Term Analysis Applied to Mooring Systems Design / Pedro de Amorim Seabra. – Rio de Janeiro: UFRJ/COPPE, 2019.

XXI, 120 p.: il.; 29,7 cm.

Orientadores: Paulo de Tarso Themistocles Esperança
Luis Volnei Sudati Sagrilo

Dissertação (mestrado) – UFRJ/ COPPE/ Programa de Engenharia Oceânica, 2019.

Referências Bibliográficas: p. 83-86.

1. Long-Term Analysis. 2. Mooring Systems Analysis. 3. Offshore Platform Mooring Systems. I. Esperança, Paulo de Tarso Themistocles, *et al*. II. Universidade Federal do Rio de Janeiro, COPPE, Programa de Engenharia Oceânica. III. Título.

"In fact, it is doubtful whether men who would not be ready to fight for a high principle would be good for anything at all."

- Nikola Tesla

ACKNOWLEDGMENTS

First of all, I thank to my wife Karina Brito de Mattos Seabra for the companionship, support and encouragement during this journey, without her this work would not have been accomplished. I also thanks to my family, my father, mother and brothers for their understanding, their love and friendship endures no matter de distance.

I would like to thank the advisors and supervisors Luis Volnei Sudati Sagrilo and Paulo de Tarso Themistocles Esperança for guiding me to achieve the results presented in this paper. The knowledge I have acquired from both of you, especially during these last two years, is invaluable. In particular I would like to thank the Professor Sagrilo for the patience, insistence and dedication.

My thanks to Fabio Gouveia Telles de Menezes, a friend that is also an advisor in my professional life. I would also like to remember the importance of the professional Ronaldo Rossi in my early years in PETROBRAS, an example to be followed.

I am grateful for the contributions I have received from the professionals from CENPES/PETROBRAS, thanks to Mauro Oliveira for the support, especially in relation to software Dynasim and to Eric Oliveira for the explanations about metocean data.

Finally, I am thankful for the opportunity given to me by PETROBRAS, in special by the managers Maiza, Yves and Christino that provide me everything I need to start and finish this work. I hope to be able to return the investment made in me by the Company with the knowledge I have acquired.

Resumo da Dissertação apresentada à COPPE/UFRJ como parte dos requisitos necessários para a obtenção do grau de Mestre em Ciências (M.Sc.).

ANÁLISE DE LONGO-PRAZO APLICADA A PROJETO DE SISTEMAS DE ANCORAGEM

Pedro de Amorim Seabra

Setembro/2019

Orientadores: Paulo de Tarso Themistocles Esperança
Luis Volnei Sudati Sagrilo

Programa: Engenharia Oceânica

Esta dissertação propõe um procedimento numérico/computacional alternativo aos procedimentos atualmente utilizados na indústria para obtenção de carregamentos extremos em linhas de ancoragem de plataformas offshore. Neste contexto, a dissertação está fundamentada na metodologia de análise de longo-prazo da resposta, aplicada no projeto de dimensionamento de sistemas de ancoragem convencionais fixos: FPSOs e Semi-Submersíveis em configuração tipo spread-mooring e FPSOs tipo turret (single point mooring).

Através da aplicação da metodologia proposta, espera-se que os sistemas de ancoragem possam ser projetados com adequado e similar nível de confiabilidade em todas as linhas - uma vez que o procedimento pressupõe utilização de dados ambientais medidos simultaneamente, específicos da locação onde será instalada a plataforma.

O trabalho foi realizado com auxílio do software Dynasim [1] para gerar as séries de tração no domínio do tempo, que posteriormente foram pós-processadas através de códigos computacionais desenvolvidos através do software Python [2]. Sendo assim, outro resultado deste trabalho é o conjunto de códigos compilados especificamente para realizar o gerenciamento das análises e obter as respostas de longo-prazo baseadas em sinais de tração no domínio do tempo.

Abstract of Dissertation presented to COPPE/UFRJ as a partial fulfillment of the requirements for the degree of Master of Science (M.Sc.)

LONG-TERM ANALYSIS APPLIED TO MOORING SYSTEMS DESIGN

Pedro de Amorim Seabra

September/2019

Advisors: Paulo de Tarso Themistocles Esperança
Luis Volnei Sudati Sagrilo

Department: Ocean Engineering

This dissertation proposes a numerical/computational procedure alternative to the currently procedures used in the industry to obtain the extreme loads on offshore platforms' mooring lines. In this context, the dissertation is based on the long-term response analysis methodology, applied to the design of conventional fixed mooring systems: FPSOs and Semi-Submersible in spread mooring configuration and turret–moored FPSOs (single point mooring).

By the application of the proposed methodology, it is expected that offshore platforms' mooring systems will be able to be designed with an appropriated reliability level for all lines – since the procedure presupposes the use of environmental data measured simultaneously, specific from the location where the Platform will be installed.

The work was carried out using Dynasim software [1] to generate the time domain tension series, which were later post-processed by using computational codes developed with Python software [2]. Thus, another result of this work is the set of codes compiled specifically to perform the mooring analyses management and obtain the long-term responses based on tension time series.

SUMMARY

SYMBOLOGY

ABBREVIATIONS

API	American Petroleum Institute
CDF	Cumulative Density Function
CoV	Coefficient of Variation
DNVGL	Det Norske Veritas Germanischer Lloyd
DOF	Degrees of Freedom
FEM	Finite Element Method
FPSO	Floating Production Storage and Offloading
ISO	International Organization for Standardization
ISSC	International Ship Structures Congress
ITTC	International Towing Tank Conference
JONSWAP	Joint North Sea Wave Project
LOA	Length Overall
MPV	Most Probable Value
NPD	Norwegian Petroleum Directorate
PDF	Probability Density Function
POSMOOR	Position Mooring
TLD	Teste de Longa Duração (Long Duration Test)
ULS	Ultimate Limit State
VLCC	Very Large Crude Carrier

ROMAN SYMBOLS

c	System damping matrix
EA_{DIN}	Dynamic axial stiffness (synthetic ropes)

$f_X(x)$	PDF of the random variable X
$f_{\boldsymbol{Y}}(\boldsymbol{y})$	PDF of the short-term conditions
$f_{\boldsymbol{C}}(\boldsymbol{c})$	PDF of the environemtal conditions
$f_K(k)$	PDF of the floater drafts
$f_{R_P\|\boldsymbol{Y}}(r_P\|\boldsymbol{y})$	PDF (peaks distribution) for the peaks of total tension, associated with the short-term condition $\boldsymbol{y}$
$f^E_{R_P\|\boldsymbol{Y}}(r_P\|\boldsymbol{y})$	Extreme PDF (extreme peaks distribution) for the peaks of total tension, associated with the short-term condition $\boldsymbol{y}$
$F_X(x)$	CDF of the random variable X
$F_{R_P\|\boldsymbol{Y}}(r_P\|\boldsymbol{y})$,	CDF (peaks distribution) for the peaks of total tension,
$F_{R_P\|K,\boldsymbol{C}}(r_P\|k,\boldsymbol{c})$	associated with the short-term condition $\boldsymbol{y} = k, \boldsymbol{c}$
$F^E_{R_P\|\boldsymbol{Y}}(r_P\|\boldsymbol{y})$	Extreme CDF (extreme peaks distribution) for the peaks of total tension, associated with the short-term condition $\boldsymbol{y}$
$F^{LT}_{R_P}(r_P)$	Long-term CDF (peaks distribution) for the peaks of total tension
$\tilde{F}^{LT}_{R_P}(r_P)$	Estimated long-term CDF (peaks distribution) for the peaks of total tension
$F^{LT}_{R_{D\|Y}}\left(r_{p_D}\right)$	Long-term CDF (peaks distribution) for dynamic parcel of peaks of total tension
$F^{LT}_{R_P}\left(r^{MPV}_{P_{Nyr}}\right)$	Probability of non-exceedance of the most probable long-term extreme response for a return period of N_{yr} years ($r^{MPV}_{P_{Nyr}}$)
$\boldsymbol{F}(t)$	Resulting force vector acting over the system
H_i	ith wave height
H_S	Significant wave height
k	Nonlinear stiffness matrix

$\boldsymbol{m}$	System mass matrix (structural + hydrodynamic)
m_X	Mean statistical estimator of the random variable X
m_n	nth order of the spectrum moment
N	Total size of a sample
$N_p(\boldsymbol{y})$	Number of tension peaks of the short-term condition $\boldsymbol{y}$
N_{yr}	Number of years
N_{cond}	Number of short-term environmental conditions for a period of 1-yr
$\overline{N}_p$	Expected number of response peaks within long-term period of N_{yr} years
N_B	Total number of Bootstrap simulation
p_i	Relative frequency of occurrence of the ith floater draft (k_i)
r_P, x_p	Peaks values of total tension
r_S	Static tension
r_{p_D}	Dynamic parcel of peaks values of total tension
$r_P^{MPV}(\boldsymbol{y})$	MPV of tension for the short-term condition $\boldsymbol{y}$
$r_{P_{Nyr}}^{MPV}$	Most probable long-term response for a return period of N_{yr} years
$\tilde{r}_{P_{Nyr}}^{MPV}$	Mean estimator of the most probable long-term response for a return period of N_{yr} years
$\hat{r}_{P_{Nyr}}^{MPV}$	Upper bound estimator of the most probable long-term response for a return period of N_{yr} years
$R_{\boldsymbol{Y}}(t\|\boldsymbol{Y}=\boldsymbol{y})$	Total short-term tension time-series, conditioned to the short-term condition $\boldsymbol{Y} = \boldsymbol{y}$
$R_{PT}(K=k)$	Line pre-tension conditioned to the draft condition $K = k$

$R_{D\|\boldsymbol{Y}}(t\|\boldsymbol{Y}=\boldsymbol{y})$	Dynamic short-term tension time-series, conditioned to the short-term condition $\boldsymbol{Y} = \boldsymbol{y}$
s_X	Standard deviation statistical estimator of the random variable X
$s_{\tilde{r}}$	Standard deviation statistical estimator of the most probable long-term response
s_{m_X}	Mean stardard error of the random variable X
$S_X(\omega)$	Spectrum density function of the random process X
t	Time
t_j	Specific time "j"
T_{sim}	Total simulation time
T_{st}	Short-term period duration
T_i	ith wave period
T_Z	Mean up-crossing wave period
T_P	Spectrum peak period
T_μ	Mean tension
T_{MBL}	Minimum break load tension
$T_{Max}, T_{Original}$	Maximum extreme most probable tension occurred in the short-term analysis
T_{LT}	Long-term total tension
T_{100}	Centenary total tension, after the Bootstrap procedure
T_{Target}	Target tension
T_{Eq}	Maximum extreme most probable tension for the equivalent condition
T_{QS}	Quasi-static tension (catenary characteristic curves method)
T_{Dyn}	Quasi-static tension (explicit FEM method)

T_{3hr}	Any kind of tension related with the short-term return period of 3hr
T_{15hr}	Any kind of tension related with the short-term return period of 15hr
T_{30hr}	Any kind of tension related with the short-term return period of 30hr
$u(.)$	Weibull location parameter of a random variable
$u_P^W(\boldsymbol{y})$	Weibull location parameter of peaks distribution associated with the short-term condition $\boldsymbol{y}$
V_W	Wind velocity
V_C	Current velocity
$\boldsymbol{x}(t)$	Displacement vector of the system
$\dot{\boldsymbol{x}}(t)$	Velocity vector of the system
$\ddot{\boldsymbol{x}}(t)$	Acceleration vector of the system
$X(t)$	Random process
$X_i(t_j)$	Random variable "i", at the specific time "j"
$\boldsymbol{y}(k, \boldsymbol{c})$	Specific short-term condition, associated with the specific draft k and specific environmental condition $\boldsymbol{c}$
$\boldsymbol{y}$	Short-term condition
Z_i	Long-term most probable response ($r_{P_{Nyr}}^{MPV}$) for the ith Bootstrap simulation
$\boldsymbol{Z}$	Sample of long-term most probable values

GREEK SYMBOLS

$\alpha(.)$	Weibull scale parameter of a random variable
$\alpha_P^W(\boldsymbol{y})$	Weibull scale parameter of peaks distribution associated with the short-term condition $\boldsymbol{y}$

$\gamma_{\{.\}}$	Skewness associated with any variable {.}
$\Gamma(.)$	Gamma function
ε	Spectrum bandwidth-related parameter
$\eta(t)$	Sea level surface elevation
η_{a_n}	nth wave amplitude component
θ_W	Wind direction of propagation
θ_C	Current direction of propagation
θ_1	Sea (wave) direction of propagation
θ_2	Swell (wave) direction of propagation
$\kappa_{\{.\}}$	Kurtosis associated with any variable {.}
$\lambda(.)$	Weibull shape parameter of a random variable
$\lambda_P^w(\boldsymbol{y})$	Weibull shape parameter of peaks distribution associated with the short-term condition $\boldsymbol{y}$
$\mu_{\{.\}}$	Mean associated with any variable {.}
$\nu_p(\boldsymbol{y})$, or $\nu_p(k, \boldsymbol{c})$	Rate (frequency) of tension peaks of short-term condition $\boldsymbol{y} = k, \boldsymbol{c}$
ν_p^M	Mean rate (frequency) of tension peaks
$\tilde{\nu}_p^M$	Estimated mean rate (frequency) of tension peaks
$\sigma_{\{.\}}$	Standard deviation associated with any variable {.}
ϵ_n	nth wave phase component
$\Phi(.)$	CDF of a standard Gaussian random variable
ω_n	nth angular frequency

LIST OF FIGURES

LIST OF TABLES

1 INTRODUCTION

1.1 BRIEF HISTORICAL REVIEW

With the beginning of oil exploration in deeper waters of more than 400m, came up the necessity to handle with compliant structures; in other words, more flexible structures able to support large offsets (displacements on sea water level) without being damaged when exposed to the environmental forces induced by waves, winds and currents. In this context, it is possible to highlight structures such as Spars, Semi-Submersibles and FPSOs.

One important difference between this type of structures previously mentioned and fixed platforms is the great nonlinearity involved when it is intended to identify important characteristics of designed system (offsets in the horizontal plane, line geometry, tensions in the mooring lines and other responses related to the environmental loads).

Although major engineering problems related to wave loading can be solved by using the linear theory, the main responses of floating units, such those related to the mooring system, shall consider nonlinear aspects in order to better estimate their offsets and tensions along the mooring lines. Consequently, systems with large nonlinearities cannot be properly solved using linear theories and frequency-domain analysis approaches since they tend to misrepresent the responses of the moored platforms.

Besides the steady forces generated by current and steady wind, moored platforms are affected by the first and second order wave excitations. The first order wave forces present frequencies in the same range of the wave spectrum frequencies. The second order forces appear due to high-order combinations of wave components, resulting in wave force components with frequencies associated to differences and sums of wave spectrum frequencies. These second order wave forces are small, however, those ones related to the difference of frequencies (or low frequencies) cannot be disregarded since they are in resonance with platform natural periods in the horizontal plane. In practical terms, speaking in terms of periods instead of frequencies, the first order forces are in the range of 3 to 25s and the second order ones can be in the range of 100 to 400s. Due to large motions in the horizontal plane the structural response of the mooring system is also nonlinear. Therefore, the best away to perform the analysis of a moored platform unit is

to carry out time-domain numerical simulations, where all the nonlinear effects related to waves, current, wind and those related to system itself can be properly accounted for.

However, a time domain computational analysis is very costly, requiring considerable processing power. Thus, at the beginning of the development of mooring systems designs, it was common to use frequency domain analysis, considering an uncoupled analysis methodology. The hull motions (first and second order) were obtained in a first step and then used as inputs to compute the final mooring system behavior - mainly mooring line tensions and platform offset. Using dedicated frequency domain softwares, the frequency-domain analyses were performed separately for the slowly-varying and wave-frequency motions. The tensions due to the mean offset and slowly-varying motion were calculated using a quasi-static approach. In that way, the slowly-varying motion was analyzed taking into account the resonance frequency of moored platform at the mean drift position. Thereafter, approximately considering a linear behavior, the frequency-domain dynamic tension would be added to those ones previously estimated. Extreme responses were estimated based on linear-Gaussian stochastic processes theory.

A very important characteristic of the responses of nonlinear systems is that it is not possible to represent their statistics behavior by a Gaussian process. In order to better estimate statistical parameters of the responses of a nonlinear mechanical system non-Gaussian statistical procedures must be employed.

Due to worldwide advance in the use of moored units, mainly in offshore oil industry, appeared the necessity to create rules and standards related to the design of such units. In this context, rules such as POSMOOR [3], API RP-2SK [4] and, later, ISO 19901-7 [5] were formulated for the design of the mooring systems of floating units. The first one was modified and became the DNVGL-OS-E301 [6] and the latter two are currently in force and - in order to ensure suitable reliability of mooring systems - they bring a set of specifications, such as: the necessity of applying corrosion rates; the application of safety factors to determine maximum tension; parameters for calculations of fatigue life, etc.

Although there are two main rules (API RP-2SK [4] and ISO 19901-7 [5]) as a reference for designing mooring systems, the issue about the combinations of environmental conditions is still a subject of discussion. The rules require that the permanent mooring systems shall be designed considering the most unfavorable

combination of wind, wave and current with a return period of no less than 100 years for the combination. Moreover, the directions of these environmental actions shall be defined according to collected data from the specific area. For extra-tropical locations the rules accept the combination of 100-year return period for both wind and wave in association with 10-year return period for current and vice-versa.

In that way, for southeast Brazilian areas, for example, oil companies have made agreements with Classification Societies (the part that represents the authorities and insurers interests), creating methodologies to define combination of environmental conditions, that shall be used in the design aiming to an adequate level of robustness for the mooring system during its whole lifetime. Such agreements are attempts to estimate the system responses to those possible extreme environmental conditions that, for example, a production platform (and its mooring lines) will have to withstand during 20 or 25 years of operation in the same location.

It is also worth mentioning that evolution in the increase of the computers' processing power and the development of more sophisticated computer tools for coupled analysis of the floater and the lines connected to it has made possible to design structures by a fully coupled time-domain analysis, representing the mooring lines and risers by finite elements (bar/beam elements) and the floater by 6-DOF rigid body. This type of analysis brings greater accuracy and reliability in the results of the simulations.

The high processing power of modern computers and clusters has also made it possible to use more advanced modelling of environmental conditions that the floating production units will possibly face during their lifetime. In this way, more robust methodologies, which consider a huge amount of environmental conditions, can be used during the mooring system design process.

In order to better understand how the environmental conditions occur, campaigns to obtain meteo-oceanographic data, specific to each location, have been done for many years in the Brazilian coast: specifically in the Campos Basins, Santos Basin and, in the last years, also in the Sergipe-Alagoas Basin. Thus, companies such as Petrobras and others have at their disposal a considerable volume of simultaneous observed environmental data related to current, wind and wave (intensities and directions), allowing designers to take more consistent steps in the improvement of the currently used design methodologies.

More specifically, the advances in both quantity and quality of collected environmental data and the increase of the computers processing power has enabled to consider the approach of long-term methodologies for mooring systems design. Nowadays, the most used methodology to predict line tensions and floater offsets is the short-term coupled analysis, where the mooring system responses are obtained by a time-domain analysis for only some specific design combinations of extreme environmental conditions. As mentioned before, this short-term analysis demands certain considerations and agreements with the responsible authorities and, as clearly mentioned in rules, as ISO 19904-1 [7], it is not the best way to obtain the offshore structure responses.

The series of International Standards applicable to offshore structures (ISO 19900 to ISO 19906) constitutes a common basis covering those aspects related to design requirements and assessments of all offshore structures used by the petroleum, petrochemical and natural gas industries worldwide. According to ISO 19904-1 [7], the state of art for determining global responses is to undertake a long-term analysis, based on the site-specific environmental data. The long-term method considers all current, wind and wave intensity environmental parameters and theirs real directional combinations, measured along various years at the specific location where the platform will be installed. The higher the quality and quantity of measured data is, the more reliable the long-term analysis will be.

1.2 PURPOSE OF THE WORK

The main purpose of this dissertation is to develop a numerical/computational procedure that aims to increase the accuracy on the estimation of the extreme tension responses of mooring lines connected to offshore platforms, compared to those estimated by procedures currently employed by the offshore industry. In this context, the work will be based on the methodology of long-term analysis, employing a 10-year long environmental conditions database. As case studies, the methodology is applied to the analysis of three different mooring systems: a) spread-moored FPSO, b) Semi-Submersible platform and c) turret-moored FPSO.

The reliability analysis (or failure probability) of the system is out of the scope of this work, then appropriate safety factors for this methodology will be not discussed (it is

a suggestion for a future work). Thus, this dissertation is devoted just to the development of a long-term design methodology to estimate the extreme response (tension) of mooring lines of moored platforms.

An additional study included in this dissertation is related to the influence of the short-term numerical simulation length on the final extreme long-term top tension of each mooring line of the platform types mentioned above. Simulations lengths of 3-hr, 15-hr and 21-hr have been investigated. Therefore, a total of 8 case studies have been evaluated in this work:

1) Spread-moored VLCC FPSO with 20 mooring lines in 4 clusters. Simulation lengths of 3-hr, 15-hr and 21-hr;
2) Turret-moored Suezmax FPSO (single point mooring) with 6 mooring lines evenly far apart. Simulation lengths of 3-hr, 15-hr and 30-hr;
3) Spread moored Semi-Submersible with 16 mooring lines in 4 clusters. Simulation lengths of 3-hr and 15-hr;

The work was carried out using Dynasim software [1], [8]-[11] to simulate the short-term environmental conditions and extract the associate mooring lines top tension time-series, which are later post-processed by using a code developed in Python [2], [12]. In the Dynasim model, the mooring lines and risers connected to the floater were modeled using the standard catenary equations. A cluster composed by 12 computers (Core i7, 32G Ram) were used to process the analyses.

1.3 LITERATURE AND RULES REVIEW

As previously mentioned, the API RP-2SK [4] and ISO 19901-7 [5] are the most used rules for the design of floating units mooring systems.

Although mooring design methodologies have experienced considerable consolidation in the 90's, important discussions and relevant contributions continue to occur, particularly in regard to long-term and reliability analyzes.

The books by Faltinsen [13], Ochi [14] and Chakrabarti [15], [16] are initial references concerning the subject of long-term analysis in the field of naval/offshore industry. However, in general, they focus on the estimation of long-term motions on floating units subject to random waves. The book by Naess and Moan [17] is an up-to-date reference on the topic.

Long-term analysis is recognized [17] as the most appropriate methodology for estimating the long-term extreme response of a marine structure since it takes into account the response in all short-term conditions that it will face during its lifetime. There are many ways of performing of a long-term analysis, such as [17], [18]: all-short term peaks approach, all short-term extremes and the long-term extreme value. The long-term response distribution is obtained by means a multi-dimensional integral over the domain of the environmental parameters modeled by their joint probability distribution.

Specifically related to long-term analysis of mooring systems, few works are reported in literature, most of them related to reliability analysis of these systems [19]-[24]. In general, the long-term analysis is the base for the development of reliability-based studies. In that way, although one of the focus of reliability procedures is to find more appropriate safety factors to be used in the design, the calibration process must be based on a long-term analysis procedure. Concerning the mooring systems, consistent steps have been occurred in relation of reliability analysis, where since the late 1990s and early 2000s significant works have been presented (Ref. [19], [20], [21] and [25]), with rules as DNVGL-OS-E301 [6] already incorporating the results of this type of analysis. The studies about reliability of moored systems have not stopped [22], [23] looking at site-specific safety factors calibration.

In this work, a specific procedure for long-term analysis for estimating the long-term extreme mooring line tension is developed based on a discrete integration procedure of the long-term integral using a large database of simultaneous observations of the wave, wind and current environmental parameters. It is based on the all short-term peaks procedure. For each short-term simulation a probability distribution is fitted to the peaks of tension time series simulated by Dynasim. Based on Ref. [26], the short-term peaks distribution model chosen for the devolvement of this work was the Weibull distribution with three parameters (Weibull-3P). Ref. [26] also indicates appropriate details for the numerical simulations, such as: minimum level of sea spectrum discretization, simulation length, etc.

2 RANDOM ANALYSIS

2.1 RANDOM PROCESS

A random process (or stochastic process) is defined as a family (a set) of random realizations (random time series) of a parameter of interest, such as: wave elevation in a given location, a structural response of a structure subject a stochastic loading process and so on. An illustration of a random process is given in Figure 2-1.

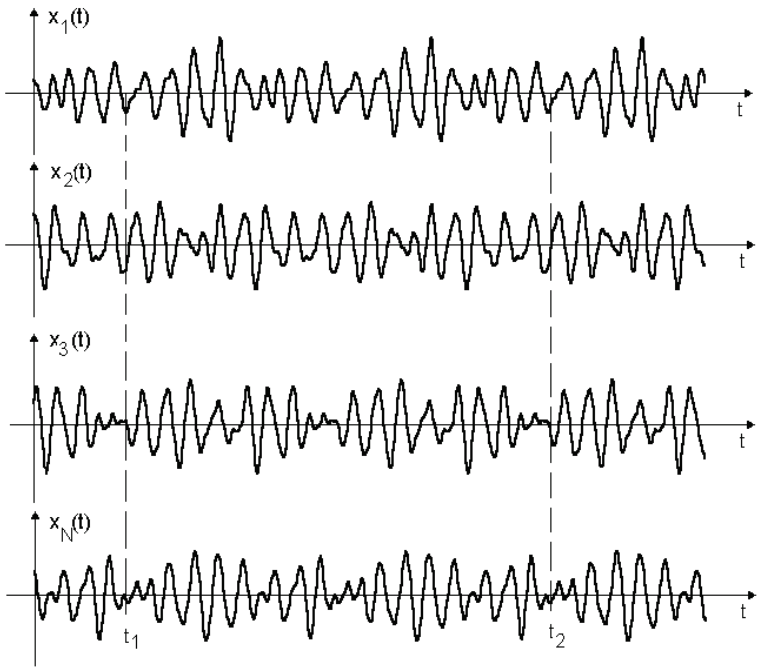

Figure 2-1 – Random process realizations

In physical terms, a good illustration of a random process is the sea surface elevation in a given offshore location area. Now, suppose the area in which the irregular sea is observed can be divided by "N" other small areas, where the sea elevation will be measured and recorded, every pre-determined time step, as exposed in Figure 2-2.

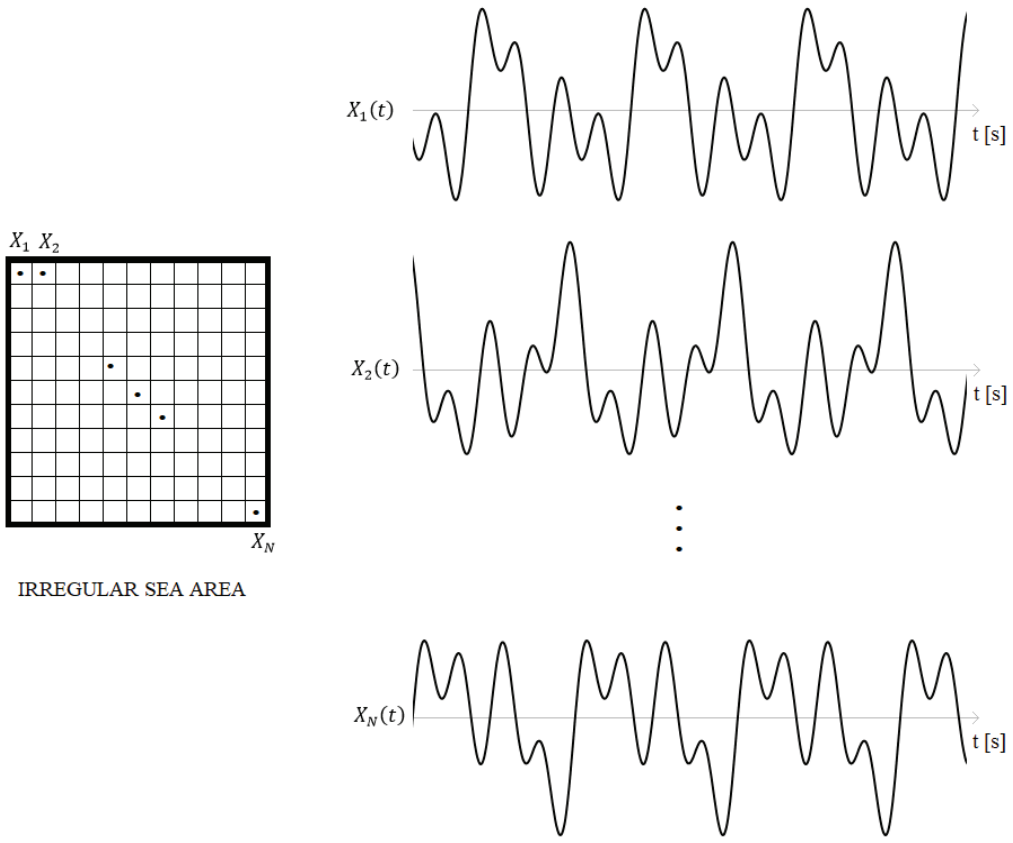

Figure 2-2 – Random sea observations

The random process $X(t)$ that will represent the irregular sea of that specific area will be composed by a set of random time-series $(X_1(t), X_2(t), \dots, X_N(t))$, the "N" recorded wave elevation records. It means that, at any time "t_j", the ensemble of random variables $(X_1(t_j), X_2(t_j), \dots, X_N(t_j))$, describes statistically the random process $X(t)$ at the time t_j. At any time t_j some statistical parameters, such as sample mean and standard deviation, can be computed:

$$\mu_{t_j} = \frac{\sum_{i=1}^{N} X_i(t_j)}{N} \tag{2.1.1}$$

$$\sigma_{t_j} = \left(\frac{\sum_{i=1}^{N} \left(X_i(t_j) - \mu_{t_j} \right)^2}{N} \right)^{1/2} \tag{2.1.2}$$

If the statistical parameters computed at different points in time are equal, i.e., the statistical parameters are independent of time, the process is said to be a stationary random process. Additionally, the statistical parameters can be computed along the time axis of a single realization of a stationary process, for instance, the mean and standard deviation are given by:

$$\mu_i = \lim_{T_{sim}\to\infty} \int_0^{T_{sim}} x(t)dt \tag{2.1.3}$$

$$\sigma_i = \left(\lim_{T_{sim}\to\infty} \int_0^{T_{sim}} (x(t) - \mu_i)dt \right)^{1/2} \tag{2.1.4}$$

where T_{sim} is the time series length, or total simulation time.

In case the statistical parameters computed are the same for all realization and additionally are equal to as computed by the ensemble sample, the process is also called ergodic.

In practical terms, it is very common to assume that the random processes under investigation are stationary and ergodic because in this case just a single realization of the stochastic process is enough to describe it statistically. This hypothesis is assumed in the present study.

2.1.1 GAUSSIAN AND NON-GAUSSIAN PROCESSES

An important aspect in the analysis of stochastic ergodic process is its representation in the frequency domain by the corresponding Fourier transform of its single realization. This representation is defined as the spectral density function or simply spectrum $S_X(\omega)$ of the random process. An illustration of a spectrum is shown in Figure 2-3.

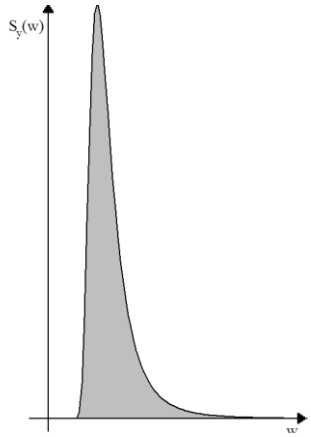

Figure 2-3 – Spectrum of a random process

From the spectrum its possible to define the so-called spectrum moments, which are defined as:

$$m_n = \int_0^\infty \omega^n S_X(\omega) d\omega \tag{2.1.5}$$

where "n" is the order of the spectral moment. An important characteristic of any stochastic process is that the zeroth spectral moment corresponds to the process variance, i.e.:

$$m_0 = \sigma_X^2 \tag{2.1.6}$$

From a realization of an ergodic random process it is also possible to identify, at least, three probability distributions: a) the distribution of process itself; b) the distribution of the process peaks (maxima) and c) the distribution of the largest (extreme) peak, as shown in Figure 2-4.

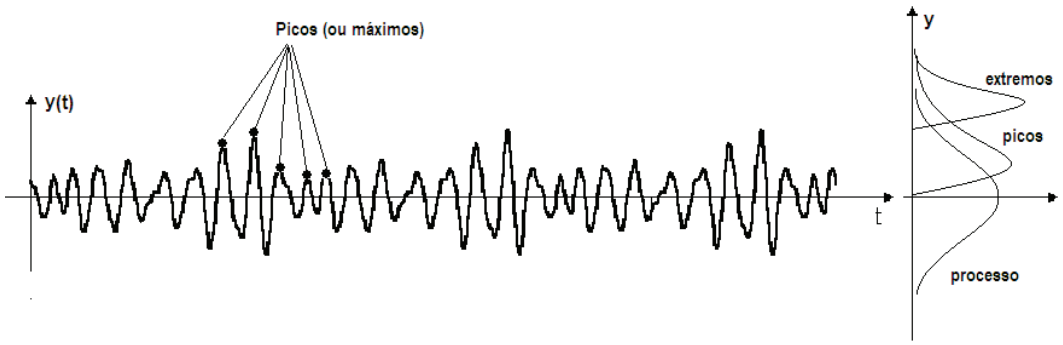

Figure 2-4 – Probability distributions associated to an ergodic process

Several random processes observed in the nature, when observed during a specific time interval, can be modelled as Gaussian processes. An example is the sea elevation variation around the mean sea level, in deep waters: putting the origin system on the sea mean level and measuring the sea elevation it will be clear that all data could be represented by Normal distribution, with zero mean. This was first found by Philip Rudnick, in 1951, by the analysis of measured waves from the Pacific Ocean and can be mathematically proved using the *Central Limit Theorem*, for more details, see, for instance, reference [14].

The Gaussian distribution has also its great value in the engineering when representing processes that can be treated by the linear theory, i.e., any linear combination of Gaussian processes is also another Gaussian process. This principle can be applied in some floater response analysis, which have the characteristics of being governed by the first order wave effects. The heave motion of an FPSO is a good example of response that can be well represented by the linear theory and, so, by a Gaussian process.

When a phenomenon, as the sea surface elevation in deep waters, can be represented by a Gaussian distribution, its peaks (maximum) distribution is theoretically given the Rice distribution (see Appendix A). Moreover, if the process spectrum is limited in a narrow bad of frequencies, i.e, a narrow-band process, the peaks distribution converges to Rayleigh distribution, which in turn is a particular case of Weibull distribution (Appendix A). Besides, the largest peak distribution is given by the Gumbel distribution independently of the spectrum bandwidth (Appendix A). Moreover, all this distributions mentioned above can be derived from the process spectrum. In other words, there are analytical solutions for all distributions of interest for random process if it is Gaussian and the only information needed to establish them is the process spectral density function; for more details, for instance, see [14] and [17].

Although a wide range of problems in naval engineering can be solved by the linear theory, using the theory of Gaussian stochastic processes, there are still some situations, including for instance the surface elevation in shallow waters and nonlinear structural responses of floating units to environmental forces (mooring lines tension, riser cross-section stress, etc.) that cannot be classified as Gaussian processes. In this case, these processes are classified as Non-Gaussian ones.

In general, there is no theoretical solution for the peaks and extreme peak distribution of a Non-Gaussian process and some numerical procedure based on the available realization of the process are employed to get them. One of the most important distribution for the stochastic analysis of a Non-Gaussian process is the process peaks distribution [17]. From this distribution, using the Order Statistics theory (Appendix A), the extreme peak distribution can be derived. Many procedures have been investigated lately in order to establish the best statistical model to represent the peaks response parameter of a marine structure [26]. The most practical approach has been identified as the one that fits a 3-parameter Weibull distribution to the time-series peaks sample [26] using the method of moments based on the three first statistical moments of data: mean, standard deviation and skewness coefficient. In this work, this procedure is used to deal with the peaks distribution of mooring line tension processes.

See Appendix A for more details about probability distributions and statistics of extremes.

2.1.2 SEA SURFACE ELEVATION PROCESS

The waves are one of the most important source of random loads acting on any offshore structure. So, it is important to briefly discuss its statistical modelling.

In the long-term the sea surface elevation (wave) random process cannot be characterized as a stationary random process since its statistical parameters change with time. Then, in the analysis of marine structures the common procedure adopted is to assume that this process maintains some characteristics of stationarity just within some limited period of the time, i.e., the so-called short-term period. Then the long-term representation of the sea surface elevation process is modeled as a sequence of "pseudo-stationary" short-term random processes. The common practice, which was followed in this work, is to adopt a short-term period equal to 3-hr.

Besides being stationary, the short-term sea surface elevation process is assumed, by physical evidences [14], to be also ergodic and Gaussian represented by a known spectral density defined as function of some environmental parameters, as described bellow.

In practical terms, for each short-term, a record of the sea surface elevation is observed, as shown in Figure 2-5.

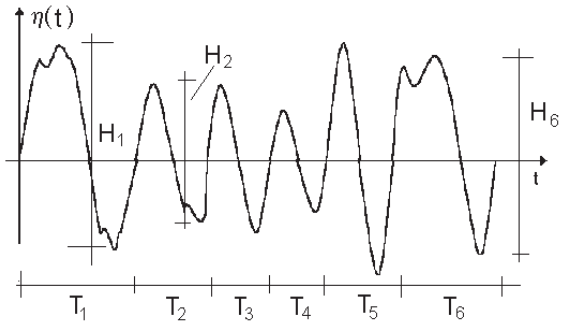

Figure 2-5 – Sea surface elevation record

From the measured record one identifies all single waves with the corresponding heights (H_i) and periods (T_i), see Figure 2-5. From this initial data analysis, the significant wave height (H_S) and mean up-crossing wave period (T_Z) can be computed. The H_S is taken as the mean value of 1/3 largest individual heights H_i and T_Z is computed as mean value of all individual wave periods T_i.

The short-term sea spectrum could be computed from the Fourier transform of sea surface elevation record. However, many researchers worked to get an analytical equation for the sea spectrum based on the H_S- T_Z pair. One of them is the so-called Modified ISSC spectrum which is given by (first accepted by the 2nd ISSC in 1967 - see, for instance [13] and [14]):

$$S_\eta(\omega) = \frac{4\pi^3 H_S^2}{\omega^5 T_Z^4} e^{-\left(\frac{16\pi^3}{\omega^4 T_Z^4}\right)} \tag{2.1.7}$$

There other sea spectrum formulae currently used in the analysis of marine structures, as the JONSWAP spectrum (recommended by the 17th ITTC – see, for instance [13] and [14]) which is defined in terms of H_S and T_P, with the latter being spectral peak period (inverse of the frequency associated to the largest value of the spectrum). The relationship between $T_Z$and T_P can be found, for instance, in reference [14].

Then, together with the mean incidence direction, H_S and T_Z (or T_P) are the main short-term environmental parameters used to characterize the sea surface elevation in a single short-term period. Without going into more details, similar treatment is also given to the wind velocity, as be seen in Ref. [14]. More details about the sea and the wind spectra used in this work are presented in Appendix B.

Nowadays, a more advanced modelling has also been used to represent the sea surface elevation. One of them, for each short-term is the separation of sea and swell wave components. The sea waves are those generated by the local wind while swell waves are those arriving at the location of interest but were generated very far from it. Then each one of these types waves is represented by the corresponding incidence direction, H_S, T_Z (or T_P) and a proper spectrum model.

2.1.3 WIND AND WAVE GENERATION

Many times in the numerical analyses of marine structures it is necessary to generate artificially a time-series (a random realization) of wave train or wind velocity from a given spectrum model (representation in frequency domain). In what follows one technique used for this goal will be described for the generation of the wave elevation record, however, it can equally be used for the generation of a wind velocity time series representing a given wind spectrum.

The most common technique used to artificially generate a random wave train, which is incorporated, in the vast majority, of computer codes for analysis of marine structures, is the spectral decomposition technique. Basically, as shown in Figure 2-6, it corresponds a superposition of regular waves with random phases, as described below.

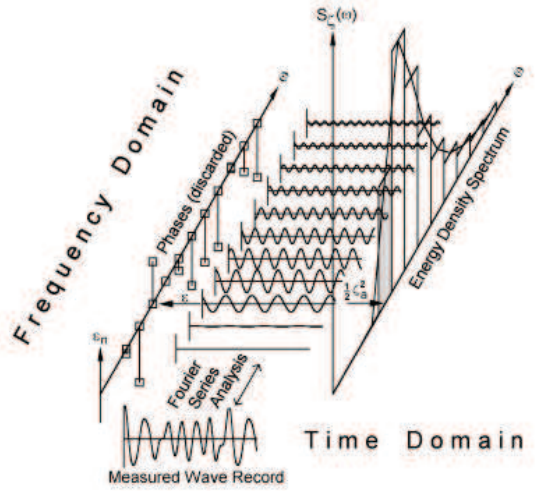

Figure 2-6 –Irregular sea surface generation by a linear superposition of regular wave components [27]

The surface elevation $\eta(t)$ can be modelled as (for instance, see [13]):

$$\eta(t) = \sum_{n=1}^{N} \eta_{a_n} \cos(\omega_n t + \epsilon_n) \tag{2.1.8}$$

Remembering that the sea surface elevation is assumed to be Gaussian, then the variance of the generated time series must be equal to spectrum area. So, the following relationship can be established:

$$\sum_{n=1}^{N} S_\eta(\omega_n)\Delta\omega = m_0 = \sigma_\eta^2 = \sum_{n=1}^{N} \frac{1}{2}\left(\eta_{a_n}\right)^2 \tag{2.1.9}$$

Then for a given band of the frequency spectrum (see Figure 2-7) the corresponding regular wave amplitude can be taken from:

$$S_\eta(\omega_n)\Delta\omega = \frac{1}{2}\left(\eta_{a_n}\right)^2 \tag{2.1.10}$$

Leading to:

$$\eta_{a_n} = \sqrt{2S_\eta(\omega_n)\Delta\omega} \tag{2.1.11}$$

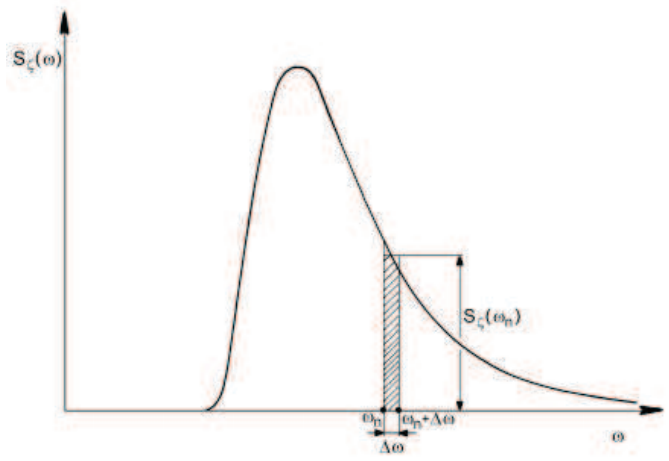

Figure 2-7 – Spectral density decomposition [27]

In summary, the spectral density function is divided into N frequency bands and a regular wave with the same variance of each spectrum band is generated. The frequency associated to each spectrum band can be that associated to interval mean value, however, it generates a periodic time-series [4], [13] and [27] after a period of time of $2\pi/\Delta\omega$. To avoid such problem the range of discrete frequencies of the spectrum should be less then:

$$\Delta\omega \leq \frac{2\pi}{T_{sim}} \tag{2.1.12}$$

Another way of avoid the periodicity in the generated time-series is to define a random frequency value within each frequency band and an important aspect in this numerical generation is to guarantee that the generated time-series is Gaussian. Based on the *Central Limit Theorem* this condition is achieved when *N* is large, in practice larger than 500-1000 components [17].

In the formulation described above the random phases ϵ_n are just used to generate distinct realizations for the same wave elevation process. In other words, for each distinct realization of the process, a distinct fixed set of random phases ϵ_n must be used.

Therefore, the sea and wind spectrums must be defined in order to represent the environmental conditions on a mooring analysis. The sea and the wind spectrums that will be used in this work are presented in Appendix B.

2.2 RANDOM DYNAMIC ANALYSIS OF MARINE STRUCTURES

2.2.1 TIME DOMAIN ANALYSIS

Nonlinear time domain stochastic analysis is a general approach to analyze offshore structures since it can take into account properly the randomness of loads and also the nonlinearities of the structural system. The focus of the present work and so of this section, is on the analyses of mooring lines.

Nonlinear time domain analysis is the state-of-the-art to design mooring systems. This procedure allows the coupled modelling of the whole system where the floater, mooring lines, risers, buoys etc. are all included in a single numerical model. The floater is modelled as a 6-DOF rigid body and all lines are modelled by finite elements. In this model the motion equation of the system is solved at each time-step and the nonlinearities present in it can be are properly updated. The dynamic interaction between the floater and slender structures connected to it are also accounted for. However, this model is very computer demanding which is a characteristic that in the everyday design practice limits its usage only for some more specific analysis.

However, in order to speed up the numerical simulations of a floater system some other techniques can be applied to get a good cost benefit between the processing time and the quality of results. For example, in the initial design phases, where many uncertainties are present, it is possible to simplify the analysis by modeling all lines using the catenary equation, making a large scan of design possibilities in relatively quicker analyses. Even when checking the as-laid condition (installed condition), if the focus is to obtain the tensions along the mooring lines, when the software allows, the designer can

choose to use the FEM (Finite Element Method) only in these kind of lines, using catenary equation to represent, for example, the risers.

Available computer codes, as Dynasim [1], are capable to run not only a full coupled dynamic analysis (with all lines discretized by the FEM) in time domain, but also a quasi-static analysis that uses the catenary equation to estimate the tensions along the lines. Although the quasi-static analysis are not able to catch some non-linear effects and the line dynamics, it can be very useful to identify, for example, the critical environmental conditions to be analyzed through a full dynamic analysis.

Independently of the line modelling used (catenary equation or finite element discretization), the environmental loads acting on the floater can be modelled as random processes and the responses obtained at each time step of the numerical simulation will also be random processes. The basic inputs for a dynamic stochastic time domain analysis are wave elevation and wind velocity generated time-series for the corresponding environmental parameters (Hs, Tz, mean wind velocity, directions, etc.).

In general terms, the motion equation to be solved at every time-step of a stochastic nonlinear time-domain simulation of a floater system is defined by:

$$\boldsymbol{m}\ddot{\boldsymbol{x}}(t) + \boldsymbol{c}\dot{\boldsymbol{x}}(t) + \boldsymbol{k}\boldsymbol{x}(t) = \boldsymbol{F}(t) \tag{2.2.1}$$

where:

$\boldsymbol{m}$ = system mass matrix (structural+hydrodynamic)

c = system damping matrix;

k = nonlinear stiffness matrix;

$\boldsymbol{F}(t)$ = forces acting over the system;

$\boldsymbol{x}(t), \dot{\boldsymbol{x}}(t), \ddot{\boldsymbol{x}}(t)$ = displacement, velocity and acceleration of the system;

One important aspect related to a stochastic analysis is the composition of the force vector acting on the system. $\boldsymbol{F}(t)$ can be expressed by (see references [8]-[11] and also [28]-[33]):

$$\boldsymbol{F}(t) = \boldsymbol{F}_{Wind}(t) + \boldsymbol{F}_{Current} + \boldsymbol{F}_{W1}(t) + \boldsymbol{F}_{WMD} + \boldsymbol{F}_{W2}(t) + \boldsymbol{F}_{Res}(t) + \boldsymbol{F}_{PD}(t) + \boldsymbol{F}_{WD}(t) + \boldsymbol{F}_{Line}(t) + \boldsymbol{F}_{LDrag}(t) + \boldsymbol{F}_{LD}(t) \quad (2.2.2)$$

where:

$\boldsymbol{F}_{Wind}$ = Wind-induced forces;

$\boldsymbol{F}_{Current}$ = Current-induced forces;

$\boldsymbol{F}_{W1}$ = Wave-induced first order forces;

$\boldsymbol{F}_{WMD}$ = Wave-induced mean drift forces;

$\boldsymbol{F}_{W2}$ = Wave-induced second order forces;

$\boldsymbol{F}_{Res}$ = Floater restoring forces;

$\boldsymbol{F}_{PD}$ = Potential damping forces;

$\boldsymbol{F}_{WD}$ = Wave drift damping forces;

$\boldsymbol{F}_{Line}$ = Line resroting forces;

$\boldsymbol{F}_{LDrag}$ = Line hydrodynamic-induced (drag) forces;

$\boldsymbol{F}_{LD}$ = Line damping forces.

The action of the environmental forces over the floating moored system and the system characteristics lead to time-series of responses (such as mooring tensions, floater motions, etc.) with the pattern shown in Figure 2-8. In this figure it is possible to identify three kinds of components: steady, first order and second order components.

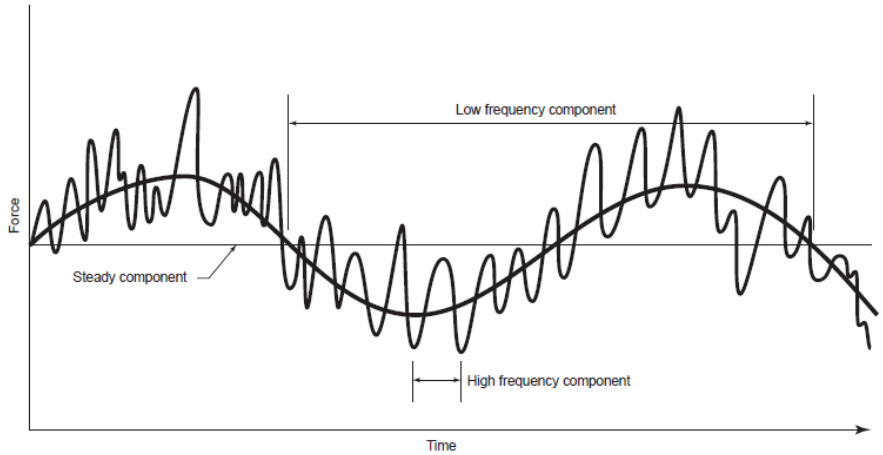

Figure 2-8 – General pattern of a response time history obtained in a stochastic nonlinear time domain analyses [4]

The steady component of the response is related to steady force components while the first order (or high frequency) and second order (or low frequency), respectively, are related to forces with frequency content in the wave spectrum band and to second-order wave forces.

In general, the low frequency response component of the moored system is associated to its resonant period which is in the order of 100s~400s, depending on the system. The wave frequency component of the response presents period content in the range of 3s-25s depending on the wave characteristics.

As in the characterization of sea surface elevation, since the response time series obtained by the numerical simulation is related to a fixed set of environmental parameters of wave, wind and current it is a short-term analysis. Moreover, assuming that the sea surface elevation and wind velocity processes are ergodic, the response stochastic process is also ergodic.

2.2.2 SHORT-TERM AND LONG-TERM ANALYSES

In offshore structures responses (tensions on lines, tethers, bracings; floater motions like offsets on the plane, Heave, Pitch, Roll, etc.) will be related with environmental conditions of the location where the structure will be installed. So, as the wave elevation process is characterized by a collection of short-term pseudo-stationary processes, the structural analyses can be defined in terms of two time length scales: short-term and long-term analysis.

A short-term analysis predicts the responses of an offshore structures within a short-term environmental condition, usually of 3-h, according to the corresponding environmental parameters of wave, wind and current for such condition. The long-term analysis, in practical terms, looks at (and treats statistically) the responses for all short-term conditions that the structure will be subject to in a long-term period.

These structures shall be designed to resist the extreme responses that could occur during its operational lifetime and it is common practice to design for extreme responses associated to a return period of 100-yr. In practical terms, there are basically two kinds of analysis that can be performed to predict these extreme situations: the short-term design methodology and the long-term design methodology. Both of them are based on short-

term analyses, a stochastic analysis for any set of short-term environmental and draft parameters.

The short-term design methodology is related with a unique extreme environmental situation, where the structure will be designed to support this extreme event. The idea that governs this methodology is that, once the structure is able to resist to the worst possible condition, it will be able to withstand all other operational conditions.

Therefore, in relation to the short-term design methodology, although the analyses can be done considering a set of environmental conditions, it will be classified as short-term methodology because the response is obtained from just one extreme condition: at one specific draft; considering just one wave spectrum, one wind spectrum, one current profile and their angle of incidence.

The long-term design methodology, or just long-term analysis, on the other hand, aims to predict the extreme response considering the influence of each short-term condition that the structure could be submitted during its operational lifetime. These conditions will encompass the floater unit's drafts, a large set of different environmental conditions (wave, wind, current and their directions) and will be associated with probability of occurrence of such events (drafts and environmental conditions).

In that way, structures designed by long-term methodology will present extreme responses based on all the short-term responses that are predicted to occur during a long exposition period of the platform operating in a specific location. Although this methodology is classified as the state-of-the-art [7] to design offshore structures, it also demands large investments on metocean campaigns and good computational processing power; since this procedure requires to deal with a big amount of data such as a large set of environmental conditions and the operational profile of the unit (to extract the drafts distribution).

It must be emphasized that there are some approximate design approaches that try to compute the long-term response by means of short-term design analyses, such as the environmental contour (see Chapter 2.3.2.1) and the equivalent short-term environmental condition approaches (the proposed methodology in this work). In these approaches a set of design short-term environmental conditions are defined in such a way that their largest short-term extreme response is approximately equal to the long-term response.

The Chapter 2.3 will present how the short-term and long-term analyses can be applied in the design of mooring systems while the Chapter 3 will bring the mathematical concepts involved in these analyses.

2.3 MOORING SYSTEM ANALYSIS

All developments made in this work were based on the use of the computer code Dynasim [1] and [8]-[11]. This is a software for the dynamic analysis of floater incorporating the characteristics described in the previous section. As outlined before, the focus of this work is on mooring line analysis. So, in what follows, more details are given about the modelling of mooring lines using Dynasim.

2.3.1 MOORING LINE MODELLING IN DYNASIM

In what follows, a summary of mooring line modelling in Dynasim is presented. For more details on this topic see references [8]-[11].

Dynasim incorporates Finite Element Method (FEM)-based and Static Catenary Equation-based models. FEM-based approaches are more robust in terms of modelling since each line is discretized in a number of finite elements (bar elements) and the full line dynamics is represented in model. Besides this, non-linear effects associated with the drag force, frictional forces and material and geometric behavior are automatically accounted for. Hydrodynamic loads acting on the lines are automatically computed for each finite element at each integration step. Catenary-based models are based on the static equilibrium of a catenary representing the mooring line. They are not so robust since they do not allow to take into account in the analysis the line dynamics and some nonlinear effects. Another point is that the hydrodynamic loading on the lines is computed by approximated methods when using a catenary-based approach. However, in computational terms, the catenary-based models are much faster than FEM-based models. Dynamic analyses using a catenary-based approach are identified as quasi-static analyses.

In Dynasim, mooring lines can be calculated by 4 different methods in the floater system dynamic analysis. These methods are:

1) Static Catenary Equation;
2) Catenary Characteristic Curve.
3) Explicit Finite Element Method (Explicit FEM);
4) Implicit Finite Element Method (Implicit FEM);

In the Static Catenary Equation method the Dynasim computes at each integration step the geometry and tension along the line by solving the standard static catenary equation, which is detailed, for instance, in Refs. [13] and [15]. Besides this, a simplified approach, where the mooring line, modeled as a bi-supported (fairlead to mudline) beam, discretized in small beam elements, is used to compute the drag and damping forces due to the current velocity. For more details, see reference [9].

The Catenary Characteristic Curve method is even more simplified than the Catenary Equation method. In this method, the catenary restoring forces curves are generated by the Dynasim for each line considering different positions of fairlead in the horizontal plane, before the beginning of the time domain simulation. During the simulation, the tensions along the line are estimated by interpolating the results previously obtained, according to the instantaneous position of the fairlead in the horizontal plane, as exposed in Figure 2-9. Only the drag and damping forces due to the current are considered, by the same manner as for the Catenary Equation method.

In the Explicit and Implicit FEM methods the mooring lines are divided in small finite elements, where the convergence (Explicit method) and precision (Explicit and Implicit methods) will depend on both the size of the elements of each line and the size of the time step.

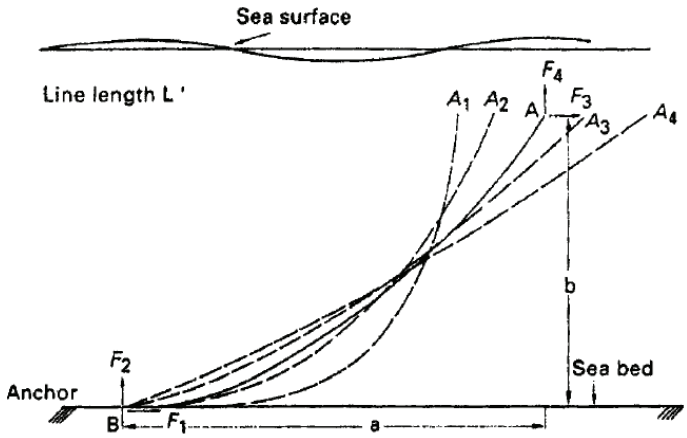

Figure 2-9 – Characteristic curves [16]

In this work, the Catenary Characteristic Curve approach is the first choice for the analyses performed. Explicit FEM approach is used in a final simulation, to extract all the non-linearities that could not be captured by the first method. The choice of these two methods was oriented according to the best cost benefit between precision of the results and computational time spent.

Another important observation is that the Dynasim [1] is able to consider the change of the axial stiffness in synthetic cables, such as polyesters ropes, during the short-term dynamic numerical simulations. The axial stiffness of these cables are related with the hysteresis grade of the synthetic fibers of these cables and can be expressed by the mean tension that the cable is submitted at each time step of the numerical simulation. According to Rossi [34], the axial stiffness of the polyester ropes can be approximately defined by:

$$EA_{DIN} = T_{MBL}\left(25\frac{T_{\mu}}{T_{MBL}} + 19\right) \tag{2.3.1}$$

where EA_{DIN} is the dynamic axial stiffness of the cable, T_{μ} is the mean tension of the line segment and T_{MBL} is the minimum specified cable break load tension.

This expression is important since it has an intrinsic relationship with the final stretched length of polyester ropes.

Finally, it is important to mention that Dynasim is able to discard the transient effects present in the beginning of the time-domain simulations. The *cutoff time* is the initial time period that is cut out of any response time-series obtained by the numerical simulation. This time interval shall be defined according to designers experience or after tests conducted before the analyses. Generally a *cutoff time* of 5,000s is enough for the most time-domain mooring analysis.

2.3.2 MOORING DESIGN METHODOLOGIES

In general terms there are two main methodologies used to design mooring systems concerning the Ultimate Limit State (ULS) design criteria: load-based and

response-based approaches. In the first approach it is assumed that the most critical structure response occurs simultaneously with the most severe environmental condition. So, the design is based on the extreme response occurring during extreme short-term environmental conditions. On the other hand, the response-based approach is based on the statistical treatment of the response considering its behavior in all possible environmental conditions that the structure will have to withstand during its lifetime.

2.3.2.1 LOAD-BASED METHODOLOGY

For the Brazilian offshore areas (classified as extra-tropical areas), the set of environmental conditions used in the load-based design (so-called design short-term methodology) is composed by 100-yr return period wind and wave and the 10-yr return period current and vice versa. All these data are based on a statistical treatment of the environmental parameters measured for the location where the platform will be installed. For waves, it is very common to express these extreme conditions with contour curves, as showed in Figure 2-10 – for instance see [17].

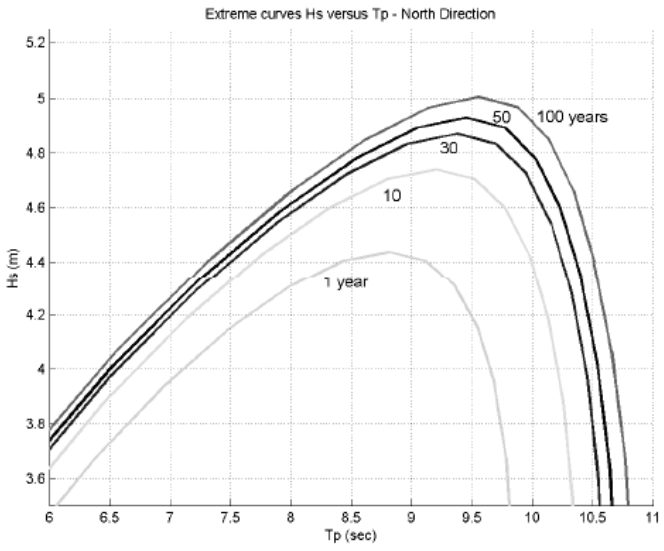

Figure 2-10 – Wave Environmental Contour Curves – N Direction

Companies as Petrobras, which spends a significant amount of capital in metocean area, are capable to generate the extreme conditions of wind, wave and current for 16 different geographic directions. Besides that, Petrobras can also estimate the change of current directions along the water depth, according to each current surface direction (see Figure 2-11).

Figure 2-11 – Example of current velocity and direction profile

It is not easy to define the proper incidence direction of the wave, wind and current in an extreme environmental event. Although design rules are not specific on the directions to be used in the combination of the environmental conditions; the Brazilian oil company Petrobras and the Classification Societies have established the arrangement presented in Figure 2-12 as a standard for design mooring systems of offshore units installed in Brazilian fields.

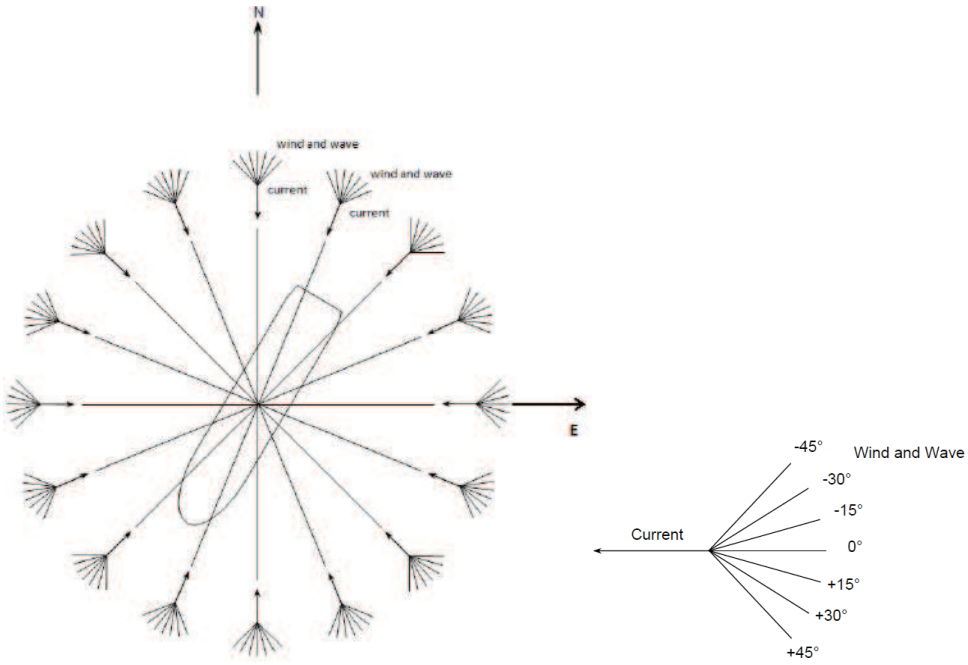

Figure 2-12 – Design environmental conditions used in Brazilian waters

For each environmental design condition a short-term stochastic dynamic numerical simulation using a simplified model for representing the mooring line (catenary-based model) is performed and a statistical analysis is made to compute the most probable value of the extreme tension at each line segment. This statistical treatment is based on the local peaks sample of simulated tension time history (see Figure 2-13) and is described in Chapter 3. The most critical design conditions are identified and for them new dynamic analysis, using FEM-based modelling for the mooring lines, are performed to identify the appropriate most probable short-term extreme tensions which are then used in the design check equations (safety factors). Similar design procedure shall be used for the Accidental Limit State (one line failed). For a better understanding about the load-based methodology, see the flow diagram exposed in Appendix C.

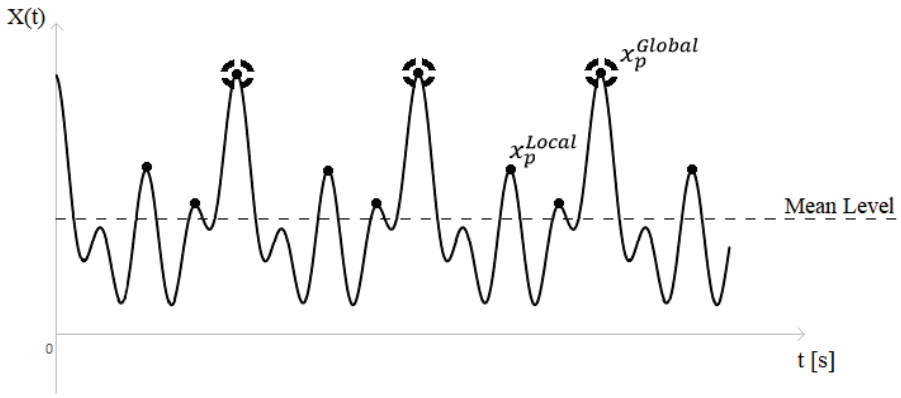

Figure 2-13 – Response global and local peaks.

This work will consider local peaks, with no correlation between them, since it is a conservative approach [26].

2.3.2.2 RESPONSE-BASED METHODOLOGY – PROPOSED METHODOLOGY

The response-based methodology, which is also known in literature as long-term analysis, based on time domain simulations, is the state-of-the-art method to design offshore structures. It can be used to predict the fatigue life of the structure as well as its design tensions. So, why such a good and powerful method is not the most used on design routine nowadays? The answer is, as always, the cost-benefit in relation to the other methods.

An accurate long-term procedure demands the integration of the short-term response over all short-term environmental conditions of the location where the floating unit will operate. The methodology requires the joint probability distributions of the environmental parameters, or a significant amount of simultaneous environmental data of wind, wind and current in order to be performed. The mathematical details of this approach are given in Chapter 3.

Generally, the long-term analysis is unfeasible to be used in the design routine because it requires a big power of computational processing in order to obtain the response within the limited design time.

In general, the two big problems related with the long-term analysis are: the number of short-term simulations (huge computer time demand) and the treatment of all data generated by the short-term realizations. In fact, even when simplifications are adopted, these two characteristics will be always a concern in this kind of analysis; especially when the focus is its applicability in the design routine.

In this dissertation a procedure for long-term analysis (response-based methodology) is proposed. Basically, the procedure follow these steps:

1) Obtain a large database of simultaneous short-term measurements of environmental parameters of wave, wind and current;

2) Define a discrete distribution of the floater draft T as one shown in Figure 2-14;

3) Perform dynamic numerical simulations for all short-term environmental conditions contained in the data base for each floater draft; these numerical simulations are performed using a catenary-based model for the system mooring lines and risers;

4) For each combination of short-term environmental condition-draft, establish the tension peaks distribution for each mooring line segment of interest in the analysis;

5) Obtain the long-term distribution of tension peaks for each mooring line segment of interest and the corresponding most probable extreme value for a given return period, say 100-yr;

6) Establish equivalent short-term conditions, for instance, by changing arbitrarily the values of a measured short-term environmental condition, in a specific draft, in order that the corresponding most probable short-term extreme tension in this condition is equal (or very close) to the extreme long-term value computed in the previous

step. Probably, there will be a proper equivalent short-term condition (environmental condition and draft) for each mooring line;

7) Perform the dynamic simulations of the floater system for those equivalent short-term environmental conditions using a FEM-based representation for the mooring lines;

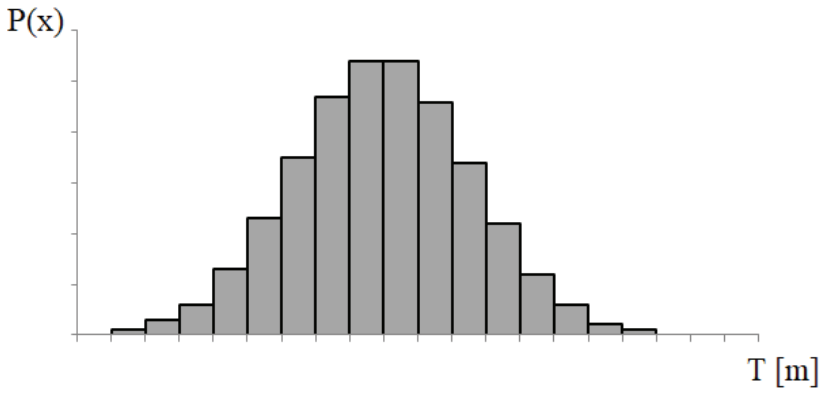

Figure 2-14 – Example of draft distribution of an FPSO platform

The case studies performed in this work are based on a 10-yr database of environmental conditions that were observed at Santos Basin (Brazil). The database contains a set of 29,218 of 3-hr environmental parameters, including the simultaneous environmental parameters (intensities and directions) of wind sea, swell, wind a superficial current velocity. Due to the limited information contained in the database, a triangular profile is adopted for modelling the current velocity through the water depth. Table 2-1 and Figure 2-15 illustrate just one of the 29,218 environmental conditions used in this work. All directions are measured clockwise with respect to North direction.

Table 2-1 – Environmental parameters of an observed short-term environmental condition.

	Definition Parameter	Value	Incidence Angle
Wind	Velocity	5.99 m/s	70.9°
Sea	Sig. Height / Peak Period	0.90m / 4.19s	80.0°
Swell	Sig. Height / Peak Period	1.33m / 9.66s	128.8°
Current	Velocity	0.13 m/s	190.6°

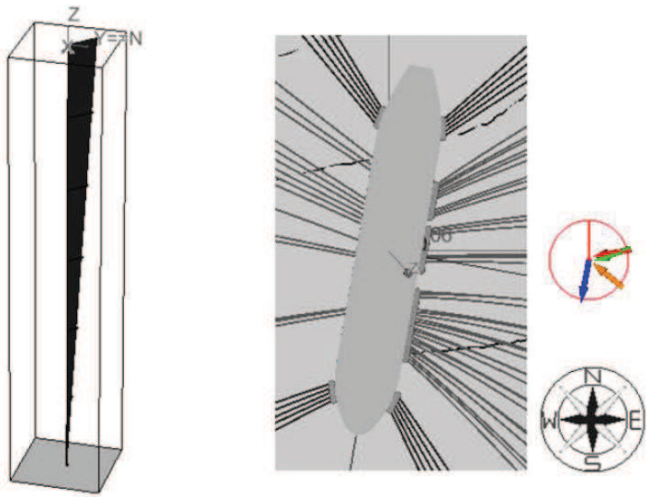

Figure 2-15 – Current profile and the directions of short-term environmental condition in the database

Due to the limited number of environmental conditions a procedure identified as Bootstrap – for more details, see Ref. [35] – is used to obtain a confidence interval for the estimated long-term tension (step 5 above). This procedure will be explained in the Chapter 3.3.

In order to avoid any misconception the following nomenclature will be used from now on in this dissertation:

- 100-yr most probable tension (or long-term tension) → Response obtained by the long-term formulation presented in Chapter 3.2;
- Upper bound of extreme response estimator (or centenary tension) → Response obtained after the Bootstrap procedure, according to the formulation presented in Chapter 3.3;
- Final design tension (or just design tension) → Response obtained after the numerical simulations with FEM modeled mooring lines (using the equivalent short-term conditions).

The mathematical background and development of the long-term mooring tension analysis is presented in Chapter 3, while the proposed long-term mooring analysis procedure is presented by a flowchart shown in Appendix D. In order to manage all short-term simulations and the corresponding huge number of files of the numerical simulations a computer system was also developed. This system is described in Chapter 4.

3 MOORING LINE TENSION STATISTICAL TREATMENT

The main goal of this work is to establish a numerical procedure for long-term analysis of tensions occurring in a mooring line of a floater system belonging to an offshore oil production unit. Initially, this chapter describes the short-term statistical analysis of this response parameter. In the sequence, the long-term analysis is described including a discrete approach based on the observed/measured simultaneous environmental parameters of wave, wind and current. Since the estimated long-term extreme response parameters are based on a discrete representation of the environmental data, there is some statistical uncertainty associated to them. Then, the next section describes the Bootstrap technique that has been used in this work in order to assess such uncertainty. Long-term analysis demands high computer power for running dynamic simulations and also for saving analyses intermediary results. So, a general overview of the computer system generated for this purpose is then described.

Since the long-term analysis is very computer demanding and costly, the mooring lines and risers are represented by quasi-static catenary equations in the numerical simulation of the floater system dynamics. For this reason, at the end, a response-based environmental conditions is used in more refined short-term simulations, using FEM, in an attempt to compensate the dynamic effects neglected by the quasi-static simulations.

3.1 SHORT-TERM DISTRIBUTION OF TENSION PEAKS

The tension time-series at a given point in a mooring line generated by means of a time-domain dynamic simulation of the floater and its lines (risers and mooring lines) for a given set of short-term environmental parameters of wave, wind and current and a specific floater draft can be seen as a single realization of the stochastic process representing this specific response. Then, the time domain stochastic process of line response (tension) for a given short-term condition can be defined by:

$$R_{\boldsymbol{Y}}(t|\boldsymbol{Y}=\boldsymbol{y}) = R_{PT}(K=k) + R_{D|\boldsymbol{Y}}(t|\boldsymbol{Y}=\boldsymbol{y}) \quad (3.1.1)$$

Where:

t = Time;

K = Floater draft (for FPSO-type floater the draft changes along time due to the amount of stored oil);

$\boldsymbol{Y}$ = Environmental parameters of a given short-term environmental condition including also a given floater draft $K = k$;

$\boldsymbol{y} = [V_W, \theta_W, H_{S1}, T_{P1}, \theta_1, H_{S2}, T_{P2}, \theta_2, V_C, \theta_C, k]$= Specific short-term condition – specific environmental condition (wind, sea wave, swell wave, current parameters and their directions "θ") and specific floater draft $K = k$;

$R_{\boldsymbol{Y}}(t|\boldsymbol{Y}=\boldsymbol{y})$ = Total short-term tension time-series, conditioned to the short-term condition $\boldsymbol{Y} = \boldsymbol{y}$;

$R_{PT}(K=k)$ = Line pre-tension conditioned to the draft condition $K = k$;

$R_{D|Y}(t|Y=y)$ = Dynamic short-term tension time-series, conditioned to the short-term condition $\boldsymbol{Y} = \boldsymbol{y}$;

Associated to the above process it is possible the corresponding sample of peaks:

$R_Y(r_P|Y=y)$ = Peaks sample of the total tension for a given short-term condition $\boldsymbol{Y} = \boldsymbol{y}$;

$R_{D|Y}(r_P|Y=y)$ = Peaks of the dynamic tension component for a given short-term condition $\boldsymbol{Y} = \boldsymbol{y}$.

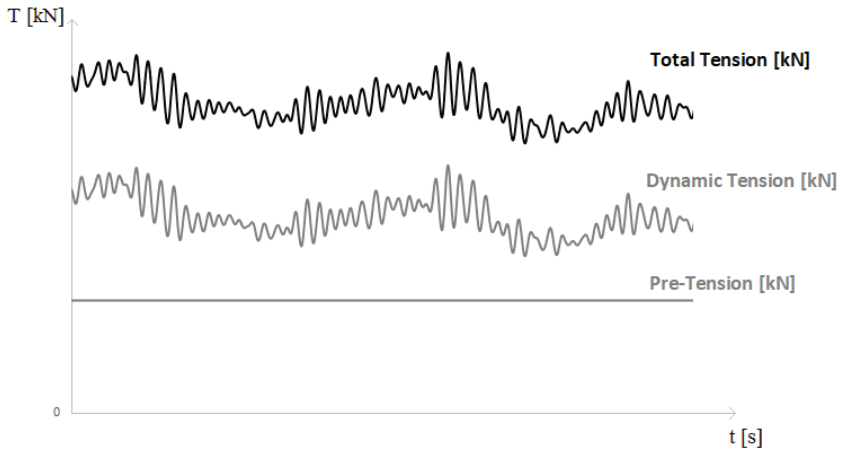

Figure 3-1 – Total Tension Components

Based on previous studies where the response stochastic process is assumed to be stationary and ergodic [26], an accurate and practical procedure to represent probability distribution associated to the peaks of the line tension process is the use of the three-parameter Weibull distribution (see also Appendix A). The modelling can be made considering the total tension process or only the dynamic tension process (total tension minus pre-tension). Although the result must be the equivalent, the preference to separate the signal lies on the reliability-based calibration of safety factors for mooring lines design. Due to the different origin of these two components (pre-tension and dynamic tension) it is common to establish different safety factors for both components. As this work does not focus on a reliability analysis, all analysis performed will be based on the peaks of the total tension. The associated probability density and cumulative distribution function for the peaks of the total tension are given, respectively, by:

$$f_{R_P|\boldsymbol{Y}}(r_P|\boldsymbol{y}) = \frac{\left(r_P - u_P^W(\boldsymbol{y})\right)^{\lambda_P^W(\boldsymbol{y})-1}}{\alpha_P^W(\boldsymbol{y})^{\lambda_P^W(\boldsymbol{y})}} \lambda_P^W(\boldsymbol{y}) e^{-\left(\frac{r_P - u_P^W(\boldsymbol{y})}{\alpha_P^W(\boldsymbol{y})}\right)^{\lambda_P^W(\boldsymbol{y})}} \quad for \quad r_P \geq u_p^W(\boldsymbol{y}) \tag{3.1.2}$$

And:

$$F_{R_P|\boldsymbol{Y}}(r_P|\boldsymbol{y}) = 1 - e^{-\left(\frac{r_P - u_P^W(\boldsymbol{y})}{\alpha_P^W(\boldsymbol{y})}\right)^{\lambda_P^W(\boldsymbol{y})}} \quad for \quad r_P \geq u_P^W(\boldsymbol{y}) \tag{3.1.3}$$

where $u_P^W(\boldsymbol{y})$, $\alpha_P^W(\boldsymbol{y})$ and $\lambda_P^W(\boldsymbol{y})$ are the location, scale and shape parameters of the Weibull distribution fitted to the peaks sample of the total tension time-series obtained by the floater simulation under the short-term condition $\boldsymbol{Y} = \boldsymbol{y}$. In this work, the fitting process employed was based on the method of moments using the mean, standard deviation and skewness coefficient of the peaks sample (see Appendix A).

In case one needs to work with the peaks of the dynamic tension component the only thing to do in order to obtain the corresponding probability distribution is to subtract the pre-tension from the location parameter defined above.

Another important aspect is that the extreme value distribution of the tension peaks within the short-term condition $\boldsymbol{Y} = \boldsymbol{y}$ can be established by means of the Order Statistics (see Appendix A). By assuming that the individual peaks belonging to the peaks sample are statistically independent ones, the cumulative distribution of the short-term largest tension peak is given by:

$$F_{R_P|\boldsymbol{Y}}^E(r_P|\boldsymbol{y}) = \left[F_{R_P|\boldsymbol{Y}}(r_P|\boldsymbol{y})\right]^{\nu_p(\boldsymbol{y})T_{st}} \tag{3.1.4}$$

and the corresponding probability density function is:

$$f_{R_P|\boldsymbol{Y}}^E(r_P|\boldsymbol{y}) = \nu_p(\boldsymbol{y})T_{st}\left[F_{R_P|\boldsymbol{Y}}(r_P|\boldsymbol{y})\right]^{(\nu_p(\boldsymbol{y})T_{st}-1)} f_{R_P|\boldsymbol{Y}}(r_P|\boldsymbol{y}) \tag{3.1.5}$$

where T_{st} is the short-term period duration (3-hr in the present work) and $\nu_p(\boldsymbol{y})$ is the rate of tension peaks given by:

$$\nu_p(\boldsymbol{y}) = \frac{N_p(\boldsymbol{y})}{T_{sim}} \tag{3.1.6}$$

where $N_p(\boldsymbol{y})$ is the number of peaks identified along the simulated tension time-series whose length (after cutting-out the transient period) is T_{Sim}.

By considering that the peaks distribution is modeled by the Weibull distribution, the most probable largest tension for the short-term condition $\boldsymbol{Y} = \boldsymbol{y}$ is given by (see the Type I Gumbel Asymptotic Distribution – Appendix A):

$$r_P^{MPV}(\boldsymbol{y}) = u_P^W(\boldsymbol{y}) + \alpha_P^W(\boldsymbol{y})\left[ln\left(\nu_p(\boldsymbol{y})T_{st}\right)\right]^{\frac{1}{\lambda_P^W(\boldsymbol{y})}} \tag{3.1.7}$$

3.2 LONG-TERM DISTRIBUTION OF TENSION PEAKS

There are many alternative ways to establish the long-term distribution of a response parameter due to the many short-term individual conditions that the marine structure is supposed to face in a long time period. There are methods based on the all short-term peaks distribution, on the extreme short-term peak distribution, etc., for instance, see Ref. [17] and [18]. Based on the all short-term peaks distribution, Battjes [36] showed that the long-term distribution of all response (line tension in the present case) peaks, can be expressed by:

$$F_{R_P}^{LT}(r_P) = \frac{1}{\nu_p^M}\int \nu_p(\boldsymbol{y})F_{R_P|\boldsymbol{Y}}(r_P|\boldsymbol{y})f_{\boldsymbol{Y}}(\boldsymbol{y})d\boldsymbol{y} \tag{3.2.1}$$

Supposing independence between the floater draft occurrence and the environmental condition parameters, Eq. (3.2.1) can be re-written by:

$$F_{R_P}^{LT}(r_P) = \frac{1}{\nu_p^M}\int\int \nu_p(k,\boldsymbol{c})F_{R_P|K,\boldsymbol{C}}(r_P|k,\boldsymbol{c})\, f_K(k)f_{\boldsymbol{C}}(\boldsymbol{c})dkd\boldsymbol{c} \tag{3.2.2}$$

where $\boldsymbol{C}$ is a vector containing the short-term environmental parameters of wave, wind and current, $\boldsymbol{c} = [V_W, \theta_W, H_{S1}, T_{P1}, \theta_1, H_{S2}, T_{P2}, \theta_2, V_C, \theta_C]$ is a specific realization of $\boldsymbol{C}$, $F_{R_P|K,\boldsymbol{C}}(r_P|k,\boldsymbol{c}) = F_{R_P|\boldsymbol{Y}}(r_P|\boldsymbol{y})$, $f_{\boldsymbol{C}}(\boldsymbol{c})$ is the joint probability distribution of the short-term environmental parameters, $f_K(k)$ is the floater draft probability density function, $\nu_p(k,\boldsymbol{c}) = \nu_p(\boldsymbol{y})$ and ν_p^M is long-term mean peaks rate given by:

$$\nu_p^M = \int\int \nu_p(k,\boldsymbol{c})\, f_K(k) f_{\boldsymbol{C}}(\boldsymbol{c}) dk d\boldsymbol{c} \tag{3.2.3}$$

Again assuming independence between response peaks, the most probable long-term extreme response for a return period of N_{yr} years, $r_{P_{Nyr}}^{MPV}$ is obtained by solving the following equation:

$$F_{R_P}^{LT}\left(r_{P_{Nyr}}^{MPV}\right) = 1 - \frac{1}{\bar{N}_p} \tag{3.2.4}$$

where $\bar{N}_p$ is the expected number of response peaks within long-term period of N_{yr} years, which is expressed by:

$$\bar{N}_p = N_{yr} N_{cond} T_{st} \nu_p^M \tag{3.2.5}$$

with T_{st} given in seconds and N_{cond} being the number of short-term environmental conditions for a period of 1-yr (it is equal to 2920 when T_{st} = 3-hr).

The solution of Eq. (3.2.4) is not straightforward, usually it is solved numerically by means of a zero-root finding algorithm. Schematically, Figure 3-2 shows some short-term response cumulative distribution, the long-term response cumulative distribution (in red) and the corresponding long-term most probable value.

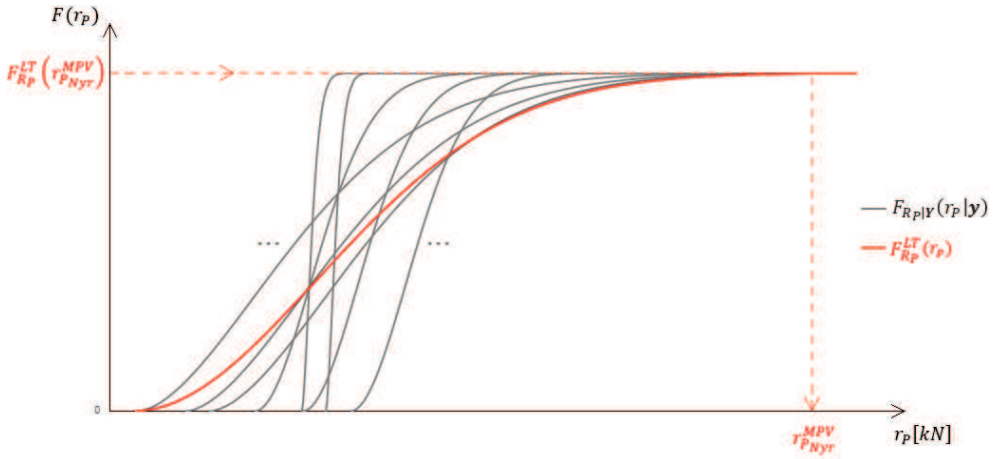

Figure 3-2 – Schematic of Long-Term Tension by Peak Distribution

3.2.1 DISCRETE CALCULATION OF THE LONG-TERM RESPONSE DISTRIBUTION

The solution of Eqs. (3.2.2) and (3.2.3) is a very challenging problem both involve n-fold numerical integration, where n is the number of environmental parameters (intensity and direction) of wave, wind and current (10 in case of considering sea and swell waves) plus 1 related to the floater draft. Another difficult point is that it is not very easy to establish the joint probability of the environmental parameters $f_{\boldsymbol{C}}(\boldsymbol{c})$**.** However, an alternative approach can be employed based on a discrete sample of simultaneously observed values of the environmental parameters and a given specific floater draft $K = k$. The basis for this approach can be explained using the estimator of the mean for a random variable X based on a sample $\boldsymbol{X} = \{x_1, \quad \cdots \quad , x_N\}$ which is given by:

$$\mu_X = \int_{-\infty}^{+\infty} x f_X(x) dx \approx m_X = \sum_{i=1}^{N} \frac{x_i}{N} \tag{3.2.6}$$

where μ_X is the "true" mean of X, m_X is the corresponding statistical estimator (the so-called sample mean), $f_X(x)$ is probability density function of X and N is the sample size.

Of course, the accuracy of m_X depends on the sample size N and the mean standard error is given by (for more details, see [35]):

$$s_{m_X} = \frac{\sigma_X}{\sqrt{N}} \tag{3.2.7}$$

where σ_X is the standard deviation of X, that is usually unknown and in practical applications can be represented by its corresponding sample estimator:

$$\sigma_X \approx s_X = \sqrt{\left(\sum_{i=1}^{N} \frac{(x_i - m_X)^2}{N}\right)} \tag{3.2.8}$$

Based on the same rational presented above, the long-term response distribution (Eq. 3.2.2), for the available database of simultaneous environmental conditions, can be approximately estimated by:

$$F_{R_P}^{LT}(r_P) \approx \tilde{F}_{R_P}^{LT}(r_P) = \frac{1}{\nu_p^M} \sum_{i=1}^{N_K} \sum_{j=1}^{N_C} \frac{\nu_p(k_i, \boldsymbol{c}_j) F_{R_{P|K,C}}\left(r_P \middle| k_i, \boldsymbol{c}_j\right)}{N_C} p_i \tag{3.2.9}$$

where N_K is the number of discrete floater drafts considered in the analysis, p_i $\left(\sum_{i=1}^{N_K} p_i = 1\right)$ is the relative frequency of occurrence of the ith floater draft (k_i), N_C is the total number of simultaneously observed environmental parameters of wave, wind and current, $\nu_p(k_i, \boldsymbol{c}_j)$ are $F_{R_{P|K,\boldsymbol{C}}}^{P}\left(r_P \middle| k_i, \boldsymbol{c}_j\right)$ the peak rate and short-term peaks distribution for the draft floater $K = k_i$ and the environmental parameters set $\boldsymbol{C} = \boldsymbol{c}_j$. The long-term mean rate of peaks can be obtained in a similar way, i.e.:

$$\nu_p^M \approx \tilde{\nu}_p^M = \sum_{i=1}^{N_K} \sum_{j=1}^{N_C} \frac{\nu_p(k_i, \boldsymbol{c}_j)}{N_C} p_i$$

(3.2.10)

An estimator for the most probable long-term extreme value can be obtained by using $\tilde{F}_{R_P}^{LT}(r_P)$ instead of $F_{R_P}^{LT}(r_P)$ in Eq. (3.2.4). Likewise the previous discussion related to the mean estimator, this estimator also presents a statistical uncertainty which is mainly dependent on the number of short-term environmental conditions N_C used (or available) in the estimation process. A standard error measure for this estimator is not easily obtained, so the so-called Bootstrap numerical procedure (for more details se, for instance, in Ref. [35]) can be used to get an approximate value for its standard error.

3.3 BOOTSTRAP ANALYSIS TO ESTIMATE THE UNCERTAINTY IN THE ESTIMATED LONG-TERM TENSION

Bootstrap technique relies on random sampling where a "new sample" is obtained by randomly taking each new sample component from the original one with replacement. For instance, in the case of the estimator for the mean of a random variable X based on a "original" sample $\boldsymbol{X} = \{x_1, \cdots, x_N\}$, the new samples $\boldsymbol{X}^* = \{x_1^*, \cdots, x_N^*\}$ is generated by randomly taken each sample component x_j^* from sample $\boldsymbol{X}$**.** This means that $\boldsymbol{X}^*$ may contain repeated values and, conversely, some components of $\boldsymbol{X}$ may not be in $\boldsymbol{X}^*$**.** Then, for each generated sample $\boldsymbol{X}_j^*, j = 1,2,\cdots, N_B$, with N_B being the number of Bootstrap (re)samples, a corresponding mean estimator m_{X_j} is obtained by Eq. (3.2.6). Then, the estimated mean value of X, i.e. m_X, is taken as the mean value of all m_{X_j} values and the corresponding standard error s_X is taken as the standard deviation of the sample containing all m_{X_j} values, to finally estimate a upper bound of a true mean confidence interval. The advantage of Bootstrap technique is that it can be applied for any statistic estimator. More details are given in [35].

In the present work, the Bootstrap technique can be applied to obtain a confidence interval for the long-term most probable extreme response value (most probable largest line tension – the centenary tension) by re-sampling N_C available simultaneous short-term environmental parameters sets from those originally simulated. In other words, each component in a specific Bootstrap $\boldsymbol{B}_i^*$ sample, $i = 1,2,..,N_C$, represented by a vector $\boldsymbol{c}_i$ containing a random generated set of environmental parameters $\boldsymbol{C} = \boldsymbol{c}_i$. The random generation must obey the frequency of occurrence for the floaters drafts and a uniform/equal probability of occurrence for each set of observed simultaneous environmental parameters of wave, wind, and current. In summary:

$$\boldsymbol{c}_i = \left[V_{W_i}, \theta_{W_i}, H_{S1_i}, T_{P1_i}, \theta_{1_i}, H_{S2_i}, T_{P2_i}, \theta_{2_i}, V_{C_i}, \theta_{C_i}\right] \tag{3.3.1}$$

Considering the N_C samples in the ith Bootstrap simulation an estimate of the long term most probable extreme value can be obtained by means of the Eq. (3.2.4). One very important aspect here is that it is not necessary to perform any new dynamic simulation of the structural system since the statistical parameters for the short-term peaks distribution have already been evaluated for any short-term condition $\boldsymbol{y}_i(\boldsymbol{c}_i, k_i)$. Then, for short, representing the long-term most probable value $r_{P_{Nyr}}^{MPV}$ simply as Z, after N_B Bootstrap analysis there will a set of N_B estimated values for Z, i.e.:

$$\boldsymbol{Z} = \left\{Z_1, Z_2, \dots, Z_{N_B}\right\} \tag{3.3.2}$$

Then the corresponding long-term extreme response estimator can be taken as the mean value of the sample $\boldsymbol{Z}$, i.e.:

$$\tilde{r}_{P_{Nyr}}^{MPV} = \sum_{j=1}^{N_B} \frac{Z_j}{N_B} \tag{3.3.3}$$

and its corresponding standard deviation is:

$$s_{\tilde{r}} = \sqrt{\sum_{j=1}^{N_B} \frac{\left(Z_j - \tilde{r}_{P_{Nyr}}^{MPV}\right)^2}{N_B}}$$

(3.3.4)

By assuming that the mean estimator can be modeled by a normal variable, the true mean with $(1-\alpha)100\%$ confidence interval is given by:

$$m_X - \kappa_\alpha s_X \leq \mu_X \leq m_X + \kappa_\alpha s_X$$

(3.3.5)

where $\kappa_\alpha = 1.282, 1.645 \; or \; 2.326$ for $\alpha = 0.10, 0.05 \; or \; 0.01$.

In that way, an upper bound for the extreme response estimator can be defined as:

$$\hat{r}_{P_{Nyr}}^{MPV} = \tilde{r}_{P_{Nyr}}^{MPV} + 2s_{\tilde{r}}$$

(3.3.6)

This upper bound corresponds to a confidence level of approximately 97.5% in which the true value of the extreme response estimator is equal or lower, based on the hypothesis that the estimator itself is described by a Normal distribution.

3.4 EQUIVALENT SHORT-TERM CONDITIONS

After finding the upper bound of the extreme response estimator, by applying the Bootstrap analysis, it will be necessary to define the equivalent short-term conditions that will induce, in each line, a short-term tension equal to the $\hat{r}_{P_{Nyr}}^{MPV}$ tension. These equivalent short-term conditions will be used in more refined final analyses, in an attempt to better

capture the dynamic effects neglected by the quasi-static analyses performed until this point of the work.

There is no restricted way to find these equivalent conditions. However, the proposal is to select the condition with the maximum short-term most probable extreme tension and change the wave, current and wind parameters until the short-term tension equals the mooring line $\hat{r}_{P_{Nyr}}^{MPV}$ tension. This procedure shall be performed by using quasi-static analyses.

Following the formulation exposed on Chapter 3.1 (Eq. 3.1.1), the stochastic process of line tension correspondent to the new condition can be defined by:

$$R_{\boldsymbol{Y}}(t|\boldsymbol{Y} = \boldsymbol{y_{new}}) = R_{\boldsymbol{Y}}(t|\boldsymbol{Y} = \boldsymbol{y} + \Delta\boldsymbol{y}) \tag{3.4.1}$$

where:

$$\boldsymbol{y} + \Delta\boldsymbol{y} = \begin{bmatrix} V_W + \Delta V_W, \theta_W, H_{S1} + \Delta H_{S1}, T_{P1}, \theta_1, \\ H_{S2} + \Delta H_{S2}, T_{P2}, \theta_2, V_C + \Delta V_C, \theta_C, k \end{bmatrix};$$

$R_{\boldsymbol{Y}}(t|\boldsymbol{Y} = \boldsymbol{y_{new}})$ = Total short-term tension time-series, conditioned on the new short-term condition $\boldsymbol{Y} = \boldsymbol{y_{new}} = \boldsymbol{y} + \Delta\boldsymbol{y}$.

The proposal is not change the waves peak periods, neither the environmental condition directions, because it would difficult the process of increasing the short-term tensions. In that way, a simple procedure that changes, at each step, the value of $\Delta V_W, \Delta H_{S1}, \Delta H_{S2}, \Delta V_C$ can be applied until the short-term tension equals the mooring line $\hat{r}_{P_{Nyr}}^{MPV}$ tension.

The final design tension of each mooring line can be estimated by running the short-term simulation with the equivalent conditions, using the Explicit FEM to evaluate the analyses on Dynasim. This final step is important to capture all the slender body effects such as stiffness, damping, inertia, wave and current loads neglected by the quasi-static analyses.

4 COMPUTER IMPLEMENTATION FOR LONG-TERM ANALYSIS

The long-term analysis procedure developed in this work involves many steps. For each of them a numerical computer module has been developed. The initial modules (first and second ones) are prepared to interact with Dynasim [1], which is the computer code used for the numerical simulations of the floater systems. The modules are prepared in order to divide, control and get the results of the short-term simulations using as many computers available as possible. Therefore, the following five numerical modules have been developed in Python [2]:

1 – Case Preparation;

2 – Short-Term Analysis;

3 – Long-Term Analysis;

4 – Bootstrap Analysis;

5 – Design Tension;

This chapter is dedicated to briefly explain each module and the main formulations inside each one of them. The separation of the code in five modules had the objective to control the errors during the implementation of the code, testing and checking the output of each module. At moment, the code is able to deal only with the tension time series.

Inside of some modules is necessary to find the root of some functions. For these cases, the Bisection root-finding method is used. The Newton-Raphson method was also tested but showed to be not trustful for a few situations. Although the Bisection method is slower than Newton-Raphson, it is also more reliable and, for this reason, was the chosen method. The Bisection method is a simple root-finding method that can be used for any continuous function.

4.1 CASE PREPARATION MODULE

One of the main ideas of this work was to enable the long-term procedure to be used in the design routine, i.e., without the necessity of investments in new expensive computers. Therefore, the proposed long-term procedure should be able to facilitate the use of any available computer and, thus, in order to reduce the risk of mistakes, a good numerical tool for the management of all analyses involved becomes necessary.

The Case Preparation Module will access the base design case file of the whole floating system prepared by Dynasim interface (including the data of hull, mooring system risers, etc. - the original file) and active, for all available drafts, the set of environmental conditions - from the available database of simultaneous environmental parameters - that the user want to run, saving the changes at the end. This module can also divide the initial set of environmental conditions in M other desired sub-sets of environmental conditions, to be used in the next modules.

Figure 4-1 exposes two examples of outputs of this module: in the first the original number of available simultaneous short-term environmental conditions were separated in blocks of 100 and 500 conditions; in the second the separation is in blocks of 500 and 250 conditions. Thus, the user is free to select different sets of environmental conditions.

Figure 4-1 – Module 1 –Two distinct outputs (data generation into folders)

This strategy aims at better exploring the use of different computers, with different kind of processing power, once the user can take each folder and run them in different machines. Inside of each folder exposed in Figure 4-1 it will contain the Dynasim files for running the corresponding short-term simulations for all indicated drafts selected for the long-term analysis. In this way, Module 1 just organizes and prepares the data for the next modules.

4.2 SHORT-TERM ANALYSIS MODULE

This module is responsible to read and process the time domain analyses outputs generated by the Dynasim (tension time series).

As already explained, the long-term analysis will be used to define equivalent short-term conditions to be performed in a more refined dynamic analysis. In that way, at present, this module is able only to read and process the outputs related with the top of each mooring line (fairlead tensions), although its architecture is prepared to do the same for the tension time series on the top of any line segment (chains, wire ropes, polyester ropes, etc.).

This module will be also responsible for processing the short-term statistics of the tension time series and deleting the large files generated by Dynasim for each short-term environmental condition. Considering that each time domain simulation output file generated by Dynasim can achieve more than 1GB, it is clear that this module must be capable to process the statistics of each tension time series, save just the main parameters and delete all Dynasim outputs. For each simulation the most important statistical parameters, as described in Chapter 3, of the tension time-series are stored: parameters of the 3P Weibull distribution fitted to the time-series peaks, peaks frequency rate, time-series mean value; most probable short-term (3-hr) extreme tension etc.

In order to keep the computer hard drive with enough space during the analyses, this module must run in parallel with the time domain analyses (Dynasim).

For each finished Dynasim analysis, this module operates through the following steps:

1. Read the top tension time series for each mooring line of the floating system;
2. For each top tension time series; compute its mean level, identify and store all local peaks above it (peaks sample) and computes the peaks frequency rate;
3. Compute the three parameters of Weibull model using the mean, standard deviation and skewness of the peaks sample;
4. Find the most probable (MPV) short-term extreme tension taking the Gumbel asymptotic distribution for the Weibull model;
5. Save all this computed parameters;
6. Delete the Dynasim output files.

In its current version, this module only identifies and works with the local peaks that are located above the mean level tension; although, for a future code revision, it is planned to work with the time-series global peaks, as suggested in [26].

The Short-Term Analysis Module follows the structure initiated by the Preparation Module (see Figure 4-2) and, in this way, each folder will also contain the files with the main parameters of short-term simulations stored in it. As mentioned before, this strategy aims to allow the use of different computers, networked or not, at any time.

SAIDA RESUMO ANALISE WEIBULL CURTO-PRAZO - SIMULAÇAO DE 7560os - LINHA 1

CALADO	CASOS	PROB. CASO	PROB. T	FORMA (PICOS)	ESCALA (PICOS)	LOCACAO (PICOS)	TRACOES EXTR. (GUMBEL)
1	1	3.4225477445e-05	1.5000000000e-01	1.7633625950e+00	8.7695443727e+00	1.6072923736e+03	1.6330513711e+03
1	2	3.4225477445e-05	1.5000000000e-01	1.6993605014e+00	9.5411946004e+00	1.6076795205e+03	1.6370016297e+03
1	3	3.4225477445e-05	1.5000000000e-01	1.7511504317e+00	1.0008237356e+01	1.6068361728e+03	1.6366166474e+03
1	4	3.4225477445e-05	1.5000000000e-01	1.7273102844e+00	1.0626122794e+01	1.6099028595e+03	1.6419689444e+03
1	5	3.4225477445e-05	1.5000000000e-01	1.7962057696e+00	1.0751560301e+01	1.6105174668e+03	1.6416422680e+03
1	6	3.4225477445e-05	1.5000000000e-01	1.7017026810e+00	1.0344892720e+01	1.6117770496e+03	1.6434536290e+03
1	7	3.4225477445e-05	1.5000000000e-01	1.7208749745e+00	1.1154972412e+01	1.6185144933e+03	1.6521463683e+03
1	8	3.4225477445e-05	1.5000000000e-01	1.8578584551e+00	1.2315490602e+01	1.6195807694e+03	1.6537885394e+03
1	9	3.4225477445e-05	1.5000000000e-01	1.9357952720e+00	1.0775798562e+01	1.6232226199e+03	1.6518905483e+03
1	10	3.4225477445e-05	1.5000000000e-01	1.7558357801e+00	1.3256901198e+01	1.6255012125e+03	1.6647253314e+03
1	11	3.4225477445e-05	1.5000000000e-01	1.7471698720e+00	1.3612227191e+01	1.6260563515e+03	1.6666425348e+03
1	12	3.4225477445e-05	1.5000000000e-01	1.7841482954e+00	1.3468560680e+01	1.6227379195e+03	1.6619999848e+03
1	13	3.4225477445e-05	1.5000000000e-01	1.7630100340e+00	1.2626163732e+01	1.6188733639e+03	1.6561660011e+03
1	14	3.4225477445e-05	1.5000000000e-01	1.7789423321e+00	1.2837555567e+01	1.6184502705e+03	1.6559032907e+03
1	15	3.4225477445e-05	1.5000000000e-01	1.7957559584e+00	1.1194874924e+01	1.6197369664e+03	1.6517710837e+03
1	16	3.4225477445e-05	1.5000000000e-01	1.7937829077e+00	1.1533223280e+01	1.6115820767e+03	1.6446014694e+03
1	17	3.4225477445e-05	1.5000000000e-01	1.8503750871e+00	1.1094150534e+01	1.6092579523e+03	1.6401108323e+03
1	18	3.4225477445e-05	1.5000000000e-01	1.7220559420e+00	1.1267173957e+01	1.6251286168e+03	1.6587436251e+03
1	19	3.4225477445e-05	1.5000000000e-01	1.7752279041e+00	1.3544928110e+01	1.6361114078e+03	1.6748985340e+03
1	20	3.4225477445e-05	1.5000000000e-01	1.7014565207e+00	1.2871995518e+01	1.6360572757e+03	1.6748696891e+03

Figure 4-2 – Module 2 – Short-Term outputs

4.3 LONG-TERM ANALYSIS MODULE

The Long-Term Analysis Module computes the long-term response (top tension). This module captures all short-term statistical results and computes the long-term cumulative distribution curve, performing the summation analytically (see Chapter 3.2.1), for the top tension of each line in the mooring system.

The main characteristics of this module are:

1. Read the outputs from the previous module and storage them into a tensor;
2. Read and storage the pre-tension of each mooring line;
3. Organize and save, for each line, the short-term outputs in a single folder;
4. Compute the long-term cumulative probability curve for the top tension of each mooring line and find out the corresponding 100-yr most probable value;
5. Save the long-term results;

To find the long-term responses, the short-term information must be correctly regrouped. Therefore, the Long-Term Analysis Module identifies the number of short-term conditions contained in the folders (see Figure 4-1), and organize all the information inside a 5-D tensor. As a quick explanation about this tensor, the five dimensions are:

1 – The number of columns contained in the previous module outputs;

2 – The total number of lines of the mooring system;

3 – The total number of short-term conditions;

4 – The total number of floater drafts;

5 – The total number of blocks (folders) of short-term conditions - see Figure 4-1.

In order to allow future reliability works, this module provides the long-term curves and responses for both total long-term tension and dynamic component of the long-term tension. The dynamic component of long-term tension will be obtained by subtracting the pre-tension acquired from the "zero condition" outputs. The "zero condition" is a short-term condition performed in Dynasim without any environmental condition acting on the system.

The mooring lines present different pre-tensions to each floater draft. In that way, the final pre-tension of each line will be called, from now on, by static tension and obtained by:

$$r_S = \int R_{PT}(k) f_K(k)\, dk \tag{4.3.1}$$

or:

$$r_S = \sum_{i=1}^{N_k} R_{PT}(k_i) p_i \tag{4.3.2}$$

where N_k is the number of discrete floater drafts considered in the analysis, p_i $\left(\sum_{i=1}^{N_k} p_i = 1\right)$ is the relative frequency of occurrence of the ith floater draft (k_i).

Moreover, as per Eq. (3.1.1), the dynamic parcel of long-term tension (and CDF curve) will be defined by:

$$r_{p_D} = r_p - r_S \tag{4.3.3}$$

$$F^{LT}_{R_{D|Y}}\left(r_{p_D}\right) = F^{LT}_{R_Y}(r_p) \tag{4.3.4}$$

Schematically, Figure 4-3 shows an output of long-term analysis module.

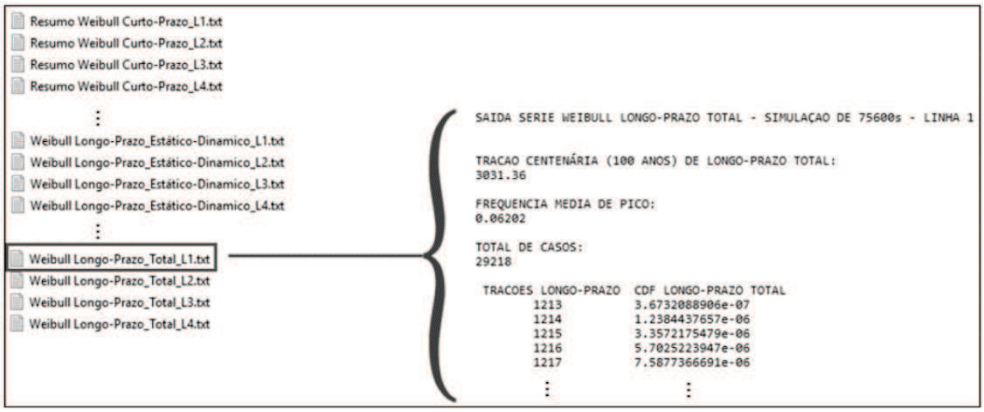

Figure 4-3 – Module 3 – Example of long-term analysis output

4.4 BOOTSTRAP ANALYSIS MODULE

The Bootstrap Analysis Module performs the Bootstrap technique in order to obtain an uncertainty estimator associated to the computed most probable long-term extreme tension. The module generates N_B re-samples of short-term conditions, estimates the most probable long-term (100-yr) extreme value for each of them and, finally, computes the corresponding confidence interval as described in Chapter 3.3. The main feature of the Bootstrap technique is that the short-term simulations do not need to be re-run again, i.e., it uses only the results already generated by the Module 3.

The main characteristics of this module are:

1. Read the short-term outputs organized by the previous module and storage them, again, in tensor format;
2. Generate the N_B samples by random sampling with replacement;

3. Compute the most probable 100-yr extreme tension and save in folders the results of each bootstrap sample (see Figure 4-4). The long-term CDF curve of each bootstrap sample is also possible to be obtained;
4. Save the N_B results;

Each new bootstrap sample of short-term conditions is generated using the Python random function, which consist of a uniform selection of a random element from the original sample of short-term conditions. For more details, see [12].

Figure 4-4 – Modulo 4 – N_B Outputs

4.5 DESIGN TENSION MODULE

This module identifies the upper bound of the 95% confidence interval for the most probable 100-yr extreme top tension estimator ($\hat{r}_{P_{Nyr}}^{MPV}$) of each mooring line, as exposed in Eq. (3.3.6). Then, for each mooring line, the worst most probable short-term extreme tension (centenary tension) and its respective short-term condition (environmental condition and draft), is used as the start point to define its corresponding equivalent short-term design condition (see Chapter 3.4). Figure 4-5 shows a partial output of this module.

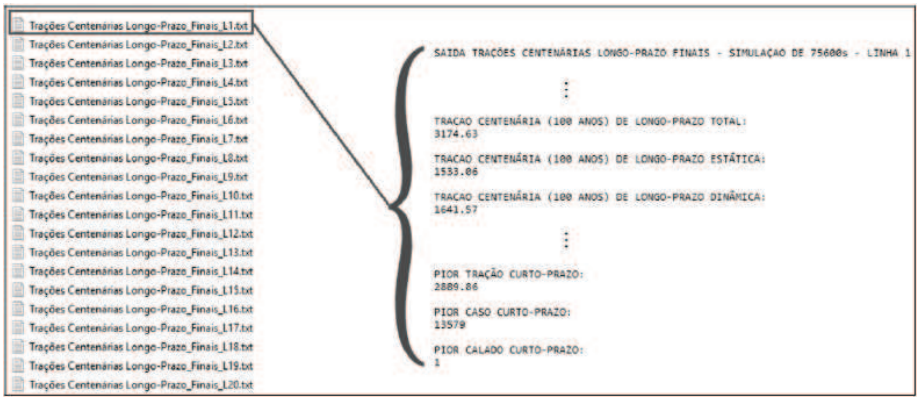

Figure 4-5 – Module 5 – Example of output

The definition of the equivalent short-term conditions is not automatic, although for future versions of the code this automation is planned.

5 CASE STUDIES

This chapter presents the application of the long-term methodology described in the previous chapters to the analysis of some case studies. In fact, three floating systems were considered in this work:

a) Spread-moored FPSO in a water depth of 2000m (see Figure 5-1);
b) Turret-moored FPSO in a water depth of 2230m (see Figure 5-2);
c) Semisubmersible platform in a water depth of 1800m (see Figure 5-3).

The main characteristics of each floater system studied are shown in Table 5-1. In the table, LOA is the Length Overall, B is the Breadth, D is the Depth and T_1, T_2, T_3 are the operational drafts of the floaters.

Table 5-1 – Platforms Main Characteristics

	FPSO Spread	FPSO Turret	Semi-Submersible
LOA [m]	326.19	266.00	94.32
B [m]	56.90	43.50	94.32
D [m]	28.60	23.00	55.00
T_1 [m]	11.32	8.55	-
T_2 [m]	15.90	-	34.00
T_3 [m]	20.45	11.83	-
Number of Mooring Lines	20	6	16

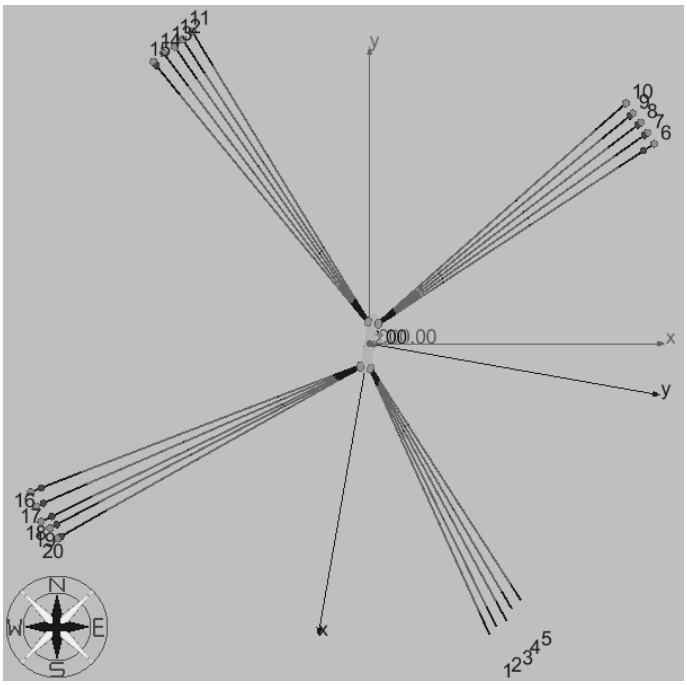

Figure 5-1 – FPSO Spread – 20 Mooring Lines (Upper View)

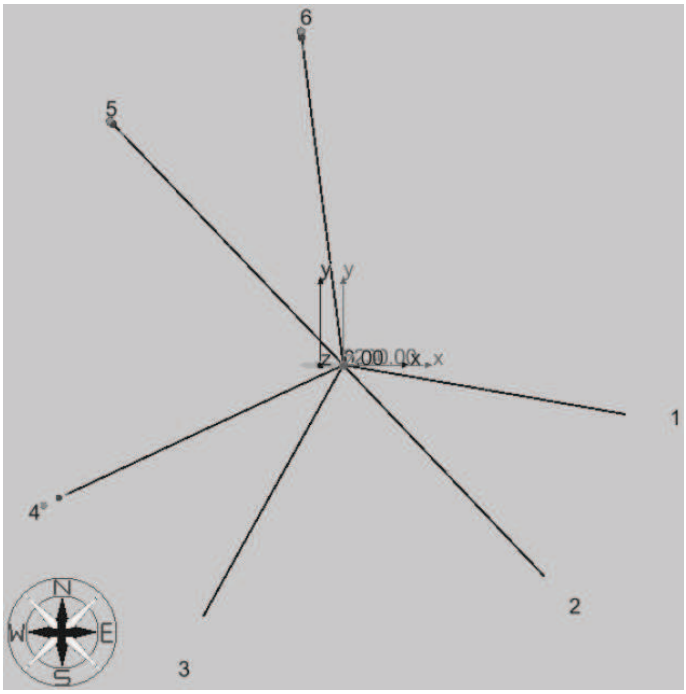

Figure 5-2 – FPSO Turret – 6 Mooring Lines (Upper View)

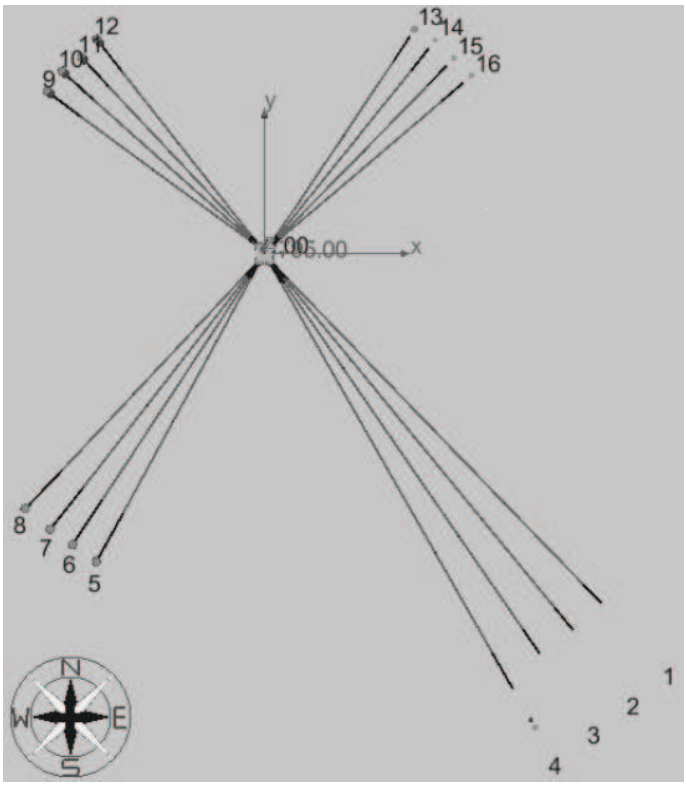

Figure 5-3 – Semi-Submersible – 16 Mooring Lines (Upper View)

For each floating system, the focus of the study is on the most probable 100-yr top tension in each mooring line considering the 10-yr database of simultaneous environmental parameters of wave, wind and current available for Santos Basin and the corresponding draft variation. As it does not store any oil, only a single one operational draft is assumed for the semisubmersible platform.

Based on some operational track of the FPSOs operated by PETROBRAS, the draft discrete probability distribution presented in Table 5-2 was adopted for the spread-moored FPSO analyzed in this work.

Table 5-2 – Spread-moored FPSO – Draft discrete probability of occurrence

Representative Draft	Draft Range	Draft (m)	Prob.
T_{MIN}	0% - 33.33%	11.32	15%
T_{MEAN}	33.33% - 66.67%	15.90	70%
T_{MAX}	66.67% - 100%	20.45	15%

The turret-moored FPSO used in this study is a Suezmax hull type, designed to perform TLDs (Long Duration Tests). For this reason, the change of drafts is small and

only two drafts were considered, i.e., the minimum and the maximum draft, with 50% of occurrence each (see Table 5-3).

Table 5-3 – Turret-moored FPSO – Draft discrete probability of occurrence

Representative Draft	Draft Range	Draft(m)	Prob.
T_{MIN}	0-50%	8.55	50%
T_{MAX}	50-100%	11.83	50%

5.1 INPUT PARAMETERS DEFINITIONS FOR TIME DOMAIN SIMULATIONS AND LONG-TERM EXTREME TENSION ESTIMATION

There are many parameters that should be properly set for a numerical time domain simulation in order to decrease the statistical uncertainty related to the results obtained, such as: sea spectrum discretization, wind representation, simulation length, etc. In the present work, wind-induced force was considered through a gust-wind model incorporated into Dynasim, using the NPD spectrum (Appendix B). Besides this, as the final long-term extreme top tension, the centenary tension, is taken as the upper bound of a Bootstrap-estimated confidence interval, it is appropriate to define, for instance, the minimum number of Bootstrap simulations in order to achieve a stable interval. Some details about this topic are described in what follows.

5.1.1 NUMERICAL SIMULATION PARAMETERS DEFINITION

As previously mentioned, some important aspects in a numerical simulation of a floating system are the sea spectrum discretization (the number of wave components) and the simulation length. In order to define these two parameters, some studies were initially performed for the spread-moored FPSO, since this is the most important floater system used in the Brazilian coast for producing oil. Only the full draft was considered in this initial study. The results obtained in this study were similar to those indicated in Refs. [13], [26], [27] and were extrapolated for the analysis of other case studies.

The analysis consisted in tests with fifteen different seeds in Dynasim for the worst short-term environmental conditions for each mooring line. For each seed a short-term numerical simulation was performed, a 3P-Weibull distribution was fitted to the top

tension sample of peaks and a corresponding short-term most probable extreme value was estimated based oh the asymptotic Gumbel distribution. Three different simulation lengths for the time domain analyses were tested: 3-hr, 6-hr and 12-hr. Besides this, five discretization for the wave spectrum were also tested: 64, 127, 316, 631 and 6031 wave components. The Figure 5-4 shows the coefficient of variation (CoV) of the fifteen estimates for the most probable short-term extreme value for each line and combination spectrum discretization x simulation length. The CoV is defined as:

$$CoV = \frac{s}{m} \tag{5.1.1}$$

where s is the standard deviation and m is the mean value of the fifteen estimates.

By observing the results, it is possible to see that the discretization with 631 and 6031 wave components (last two graphics) present results with very similar behavior, with low CoVs, mainly for the longer simulation lengths. Based on these results, a number of 1000 wave components was used in all other simulations performed. Although the fifteen estimates seems to be a small sample to define the simulation length, it indicates that longer simulations achieve lower CoVs and more variations of this parameter were considered in each study case as it will be described later.

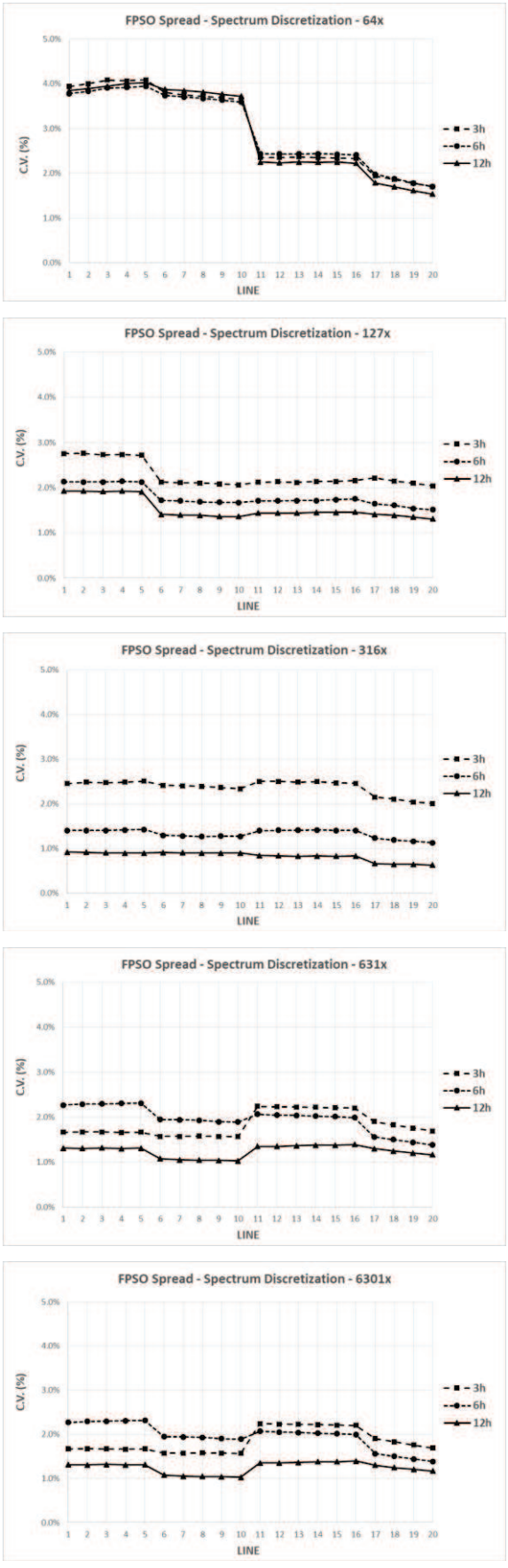

Figure 5-4 – Spread Moored FPSO – Spectrum discretization from 64 to 6301 wave components.

5.1.2 BOOTSTRAP NUMBER OF RE-SAMPLES

The minimum number (N_B) of random samples used in Bootstrap analysis was defined according to the statistic stabilization of the mean (long-term top tension response estimators – $\tilde{r}^{MPV}_{P_{100yr}}$) and standard deviation of the N_B long-term responses and, so, of the upper bound of the extreme top tension estimators ($\hat{r}^{MPV}_{P_{100yr}}$). The results obtained as function of the number of Bootstrap samples (N_B) are shown in Figure 5-5 to Figure 5-7, for the most loaded line of the three floater systems investigated, with short-term simulation lentghs of 15-hr. The standard deviation decay of the set of N_B upper bound response estimated values are also showed in these figures.

By observing the results, it is seen that a good choice for N_B is between 200 and 300. Then, $N_B = 200$ was adopted for the analysis performed in this work.

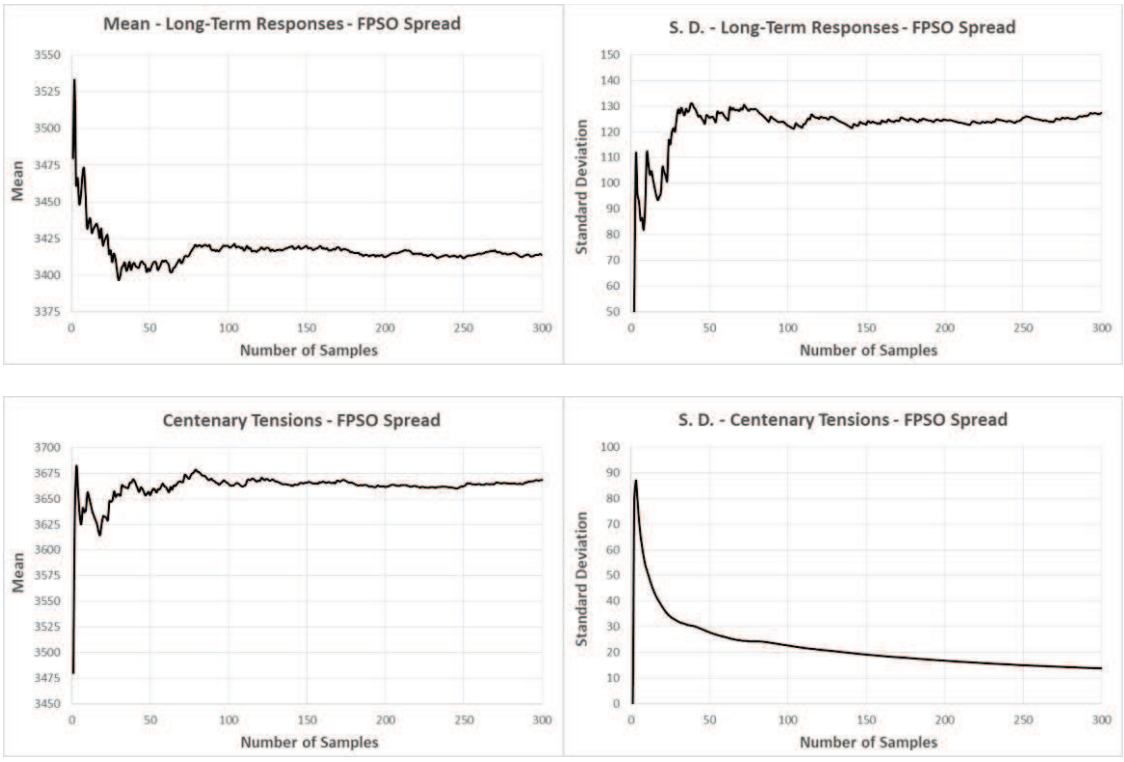

Figure 5-5 – Statistic stabilization of the Bootstrap samples– Spread-moored FPSO.

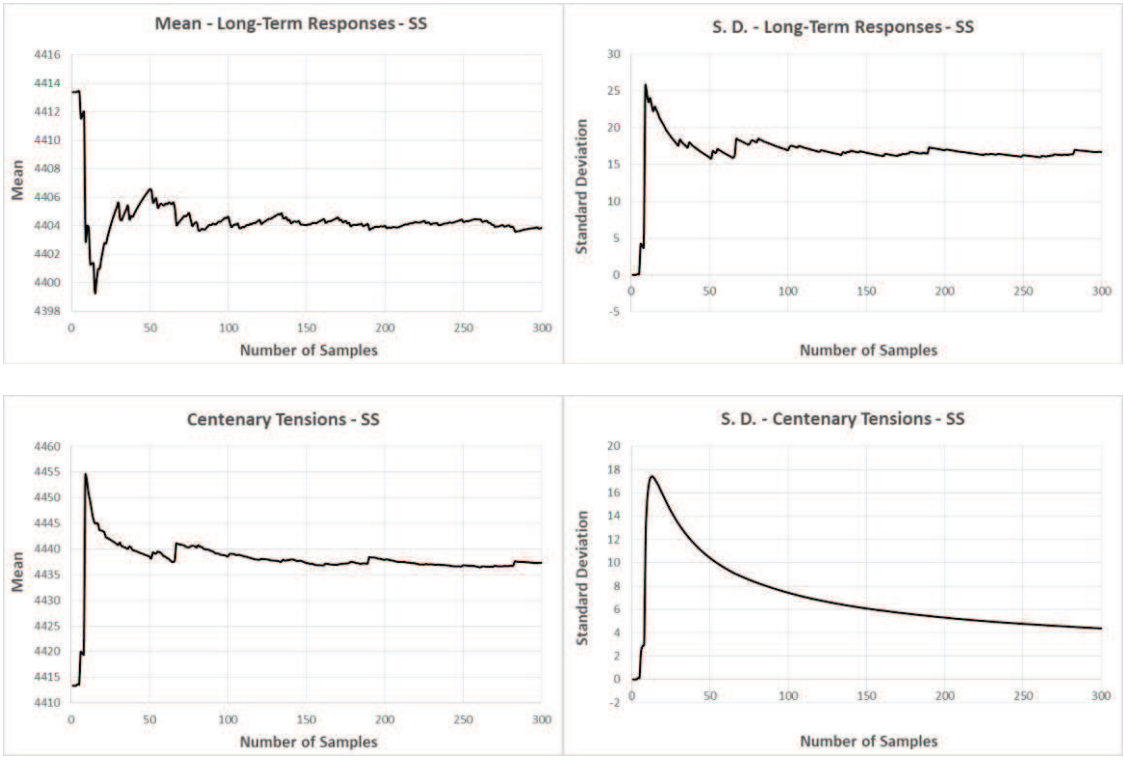

Figure 5-6 – Statistic stabilization of the Bootstrap samples – Semi-submersible platform.

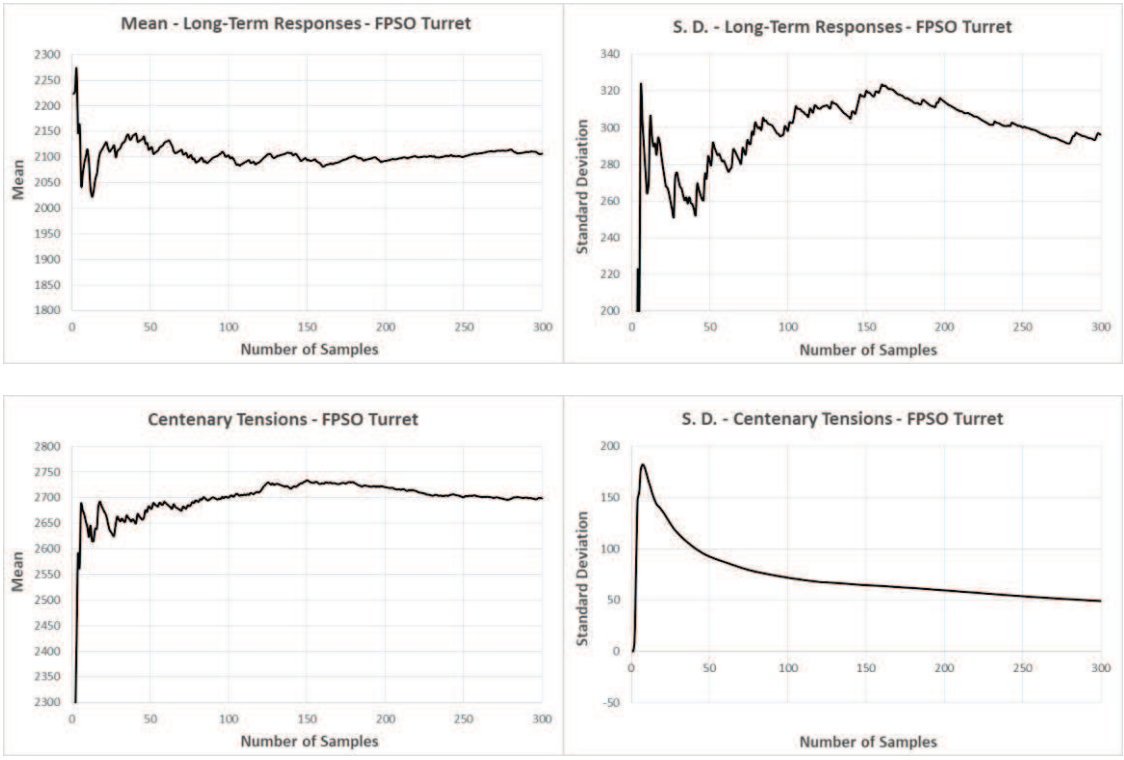

Figure 5-7 – Statistic stabilization of the Bootstrap samples – Turret-moored FPSO

5.2 ANALYSES RESULTS

As already mentioned in the previous chapters, all the results presented here are related to long-term analysis for 100-year return periods. These analyses are based on simultaneous environmental data of 3-hr sea-states along 10-year long environmental conditions database.

Only the tension at the top of fairleads are presented and for analyses considering the mooring system in its intact condition, i.e., damaged mooring system analyses are out of the scope of this work.

The long-term results were obtained according to the indication of API RP 2SK rule [4], which reads: "*The time domain simulation should be long enough to establish stable statistical peak values*." In this way, this dissertation also intends to indicate the minimum simulation length for the time domain analyses in order to achieve stable statistical results for the long-term analyses (see Chapter 5.2.2).

5.2.1 SHORT-TERM ANALYSES

One of the most important steps in the long-term analysis is the definition of the short-term distribution for the response peaks. In Ref. [26] it is shown that the three-parameter Weibull model, with the parameters being defined using the sample first three statistical moments (mean, standard deviation and skewness coefficient), is one of the most appropriate models for this short-term probability distribution. The Dynasim [1] contains a built-in routine for this purpose which is based on a Weibull-tail model, as described in Appendix A.

This chapter presents some 3-hr short-term extreme response analyses comparing these two aforementioned Weibull models. It is very important to say that the results do not intend to open a discussion of which kind of Weibull method must be used in the analyses, since only three cases were compared. The goal here is the verification and validation of the Short-term Analysis Module (see Chapter 4.2) developed in this work.

An important observation must be done here. The Dynasim version used in this work are not prepared to run the extreme analyses with a specific short-term period. The short-term period adopted in the code is equal to the simulation length. For example, if the numerical simulations are 30-hr long, the short-term extreme analyses will be refered

to a short-term period of also 30-hr, counting all peaks and informing the results related with a return-period of 30-hr. In other words, the short-term period and the simulation length are not disconnected in the version of the software used in this work. For this reason, only the 3-hr short-term simulations were evaluated.

It is also important to clarify that the Short-Term Analysis Module developed in this work considers the first and the last points of the tension time-series in the filter of maxima, in order to achieve a more conservative value for the extreme tension. As it will be shown in what follows, although the Dynasim discard these two points, the results are not influenced by this choice.

Table 5-4 to Table 5-6 present a summary of the comparison performed for the spread-moored FPSO, Semi-submersible platform and turret-moored FPSO, respectively. Figure 5-8 presents the cumulative distributions of the two Weibull models and the empirical one for the peaks of the mooring line of the spread-moored FPSO. Figure 5-9 presents a zoom of the upper-tail of these distributions. These figures also include an indication where the most probable short-term extreme value is located. Figure 5-10 and Figure 5-11 are the corresponding ones for the Semi-submersible platform and Figure 5-12 and Figure 5-13 are those associated to the turret-moored FPSO. Since the results obtained in all cases are similar, it is possible to see the computer implementation of the three-parameter Weibull model in the Short-term Analysis Module is correct and can be used in the long-term analysis.

Table 5-4 – Short-term extreme tension. Spread-moored FPSO – Line #11 – Mean draft + worst short-term environmental condition

Mooring Line	#11	**Draft**	T_{MEAN}
		Environmental Condition	19256
Dynasim (2-P Weibull-Tail)		**Short-Term Module (3-P Weibull)**	
Extreme Tension [kN]	3139	**Extreme Tension [kN]**	3091
% Non-Exceedance	99.828%	**% Non-Exceedance**	99.828%
N_Peaks	580	**N_Peaks**	580
Location (kN)	2279	**Location (3P) [kN]**	2264
Scale [kN]	199.0	**Scale (3P) [kN]**	219.0
Shape	1.264	**Shape (3P)**	1.393
Tension Difference (%)	-1.6%		

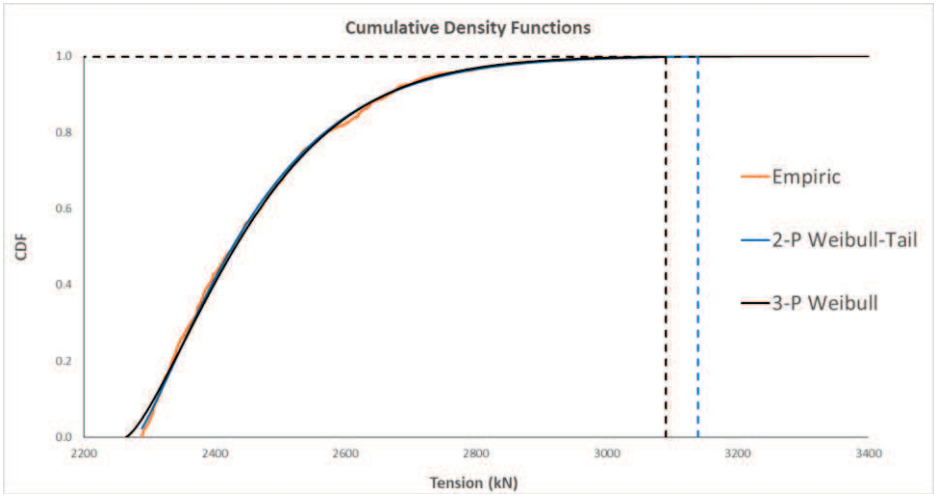

Figure 5-8 – Tension peaks CDF. Spread-moored FPSO– Line #11 – Mean draft + worst short-term environmental condition.

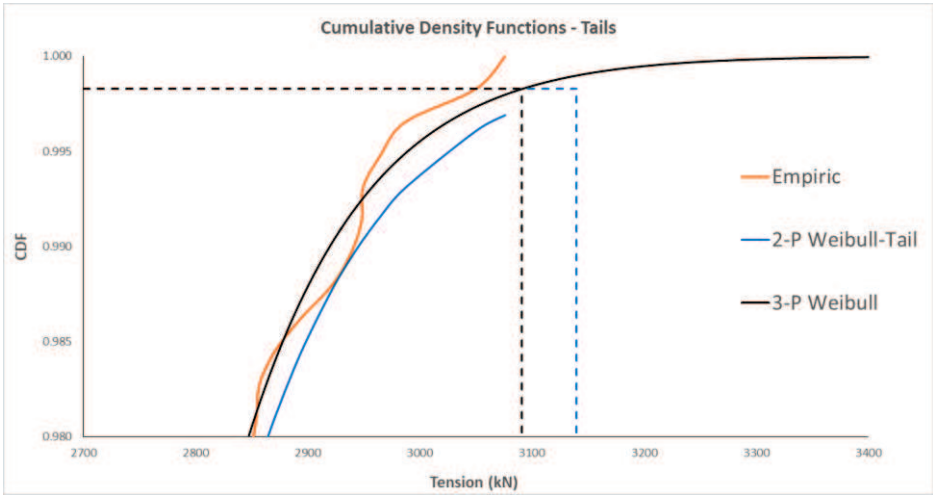

Figure 5-9 – Tension peaks CDF tail. Spread-moored FPSO – Line #11 – Mean draft + worst short-term environmental Condition.

Table 5-5 – Short-term extreme tension. Semi-submersible platform – Line #1 – Operational draft + worst short-term environmental condition

Line	#1	Draft	T_{OPER}
		Environmental Condition	4408
Dynasim (2-P Weibull-Tail)		Short-Term Module (3-P Weibull)	
Extreme Tension [kN]	4413	Extreme Tension [kN]	4413
% Non-Exceedance	99.903%	% Non-Exceedance	99.903%
N_Peaks	1027	N_Peaks	1028
Location [kN]	4407	Location (3P) [kN]	4407
Scale [kN]	1.923	Scale (3P) [kN]	2.063
Shape	1.647	Shape (3P)	1.794
Tension Difference (%)	0.0%		

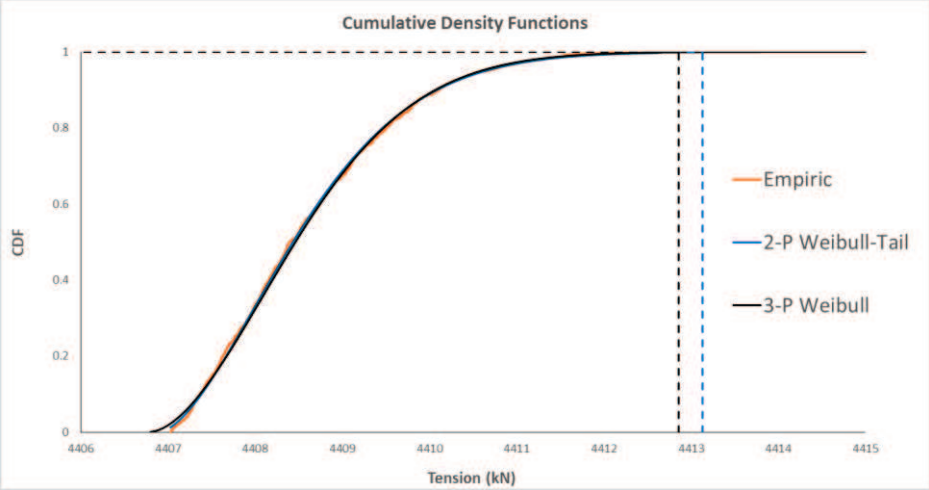

Figure 5-10 – Tension peaks CDF. Semi-submersible platform– Line #1 – Operational draft + worst short-term environmental condition.

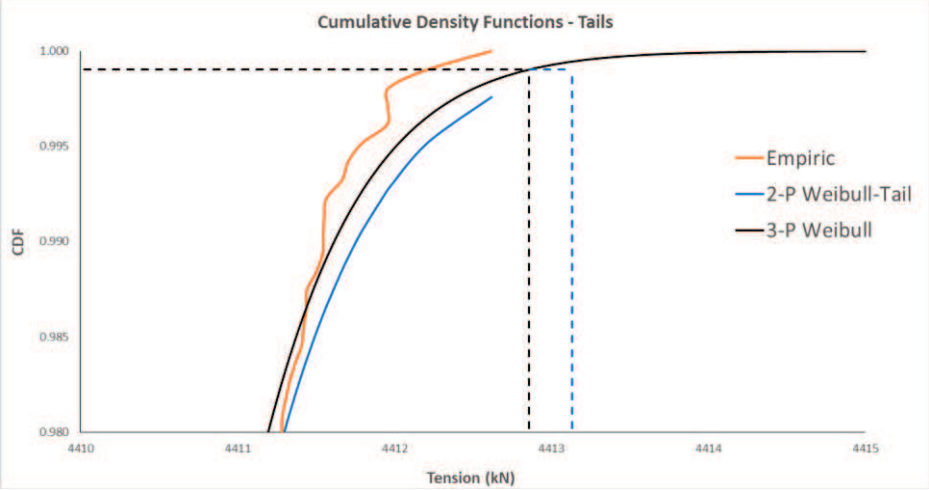

Figure 5-11 – Tension peaks CDF tail. Semi-submersible platform – Line #1 – Operational draft + worst short-term environmental condition.

Table 5-6 – Short-term extreme tension. Turret-moored FPSO– Line #2 – Full draft + worst short-term environmental condition

Line	#2	Draft	T_{MAX}
		Environmental Condition	4344
Dynasim (2-P Weibull-Tail)		Short-Term Module (3-P Weibull)	
Extreme Tension [kN]	2040	Extreme Tension [kN]	2145
% Non-Exceedance	99.765%	% Non-Exceedance	99.765%
N_Peaks	426	N_Peaks	426
Location [kN]	940.1	Location (3P) [kN]	944.2
Scale [kN]	127.2	Scale (3P) [kN]	117.0
Shape	0.835	Shape (3P)	0.773
Tension Difference (%)	4.9%		

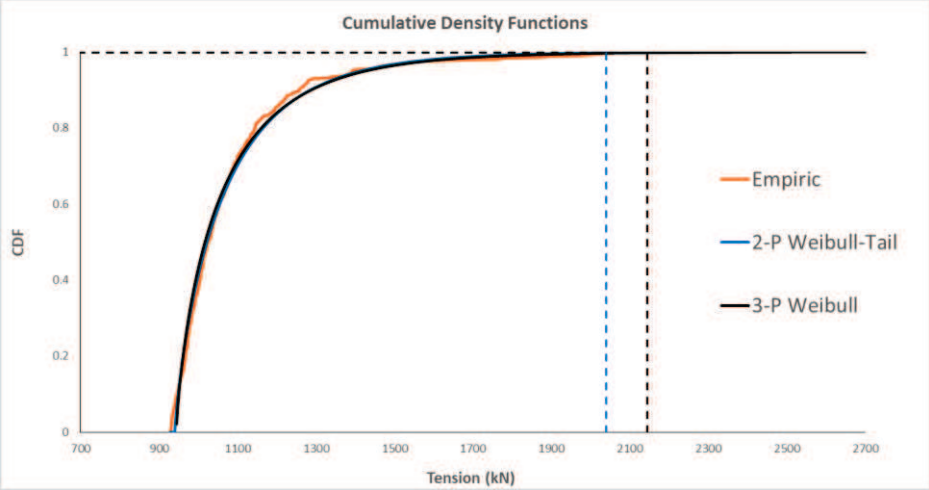

Figure 5-12 – Tension peaks CDF. Turret-moored FPSO. – Line #2 – Full draft + worst short-term environmental condition.

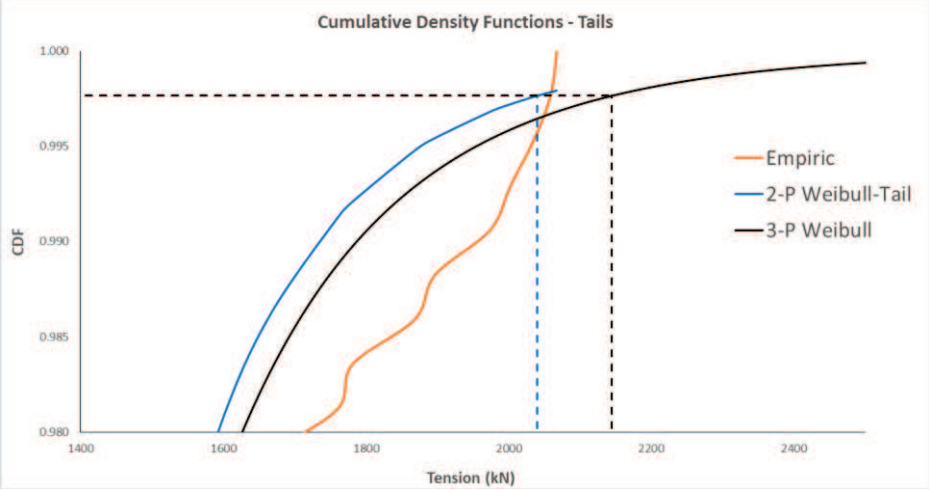

Figure 5-13 – Tension peaks CDF tail. Turret-moored FPSO – Line #2 – Full draft + worst short-term environmental condition.

5.2.2 LONG-TERM ANALYSES - RESPONSE-BASED METHODOLOGY

This section presents the results obtained for the long-term analyses performed in this work. Although each measured short-term is associated with a return-period of 3-hr duration, longer simulation lengths were used for the analyses of short-term conditions in order to identify a minimum simulation length to achieve a numerical stability for 100-yr most probable top tension of each line in the mooring system analyzed. The following simulation lengths were tested for the three floating systems investigated:

1) Spread-moored FPSO: 3-hr, 15-hr, 21-hr;
2) Semi-submersible platform: 3-hr, 15-hr;
3) Turret-moored FPSO: 3-hr, 15-hr, 30-hr;

Figure 5-14, Figure 5-15 and Figure 5-16 present the variation of the 100-yr most probable top tension for each mooring line as a function of the simulation length for the spread-moored FPSO, Semi-submersible platform and turret-moored FPSO, respectively. As it can be seen in these figures, a simulation length of 15-hr is enough to perform the short-term simulations for both FPSOs, while a 3-hr simulation length is enough for the Semi-submersible platform. In other words, the values of the 100-yr top tensions stabilize after these simulation lengths.

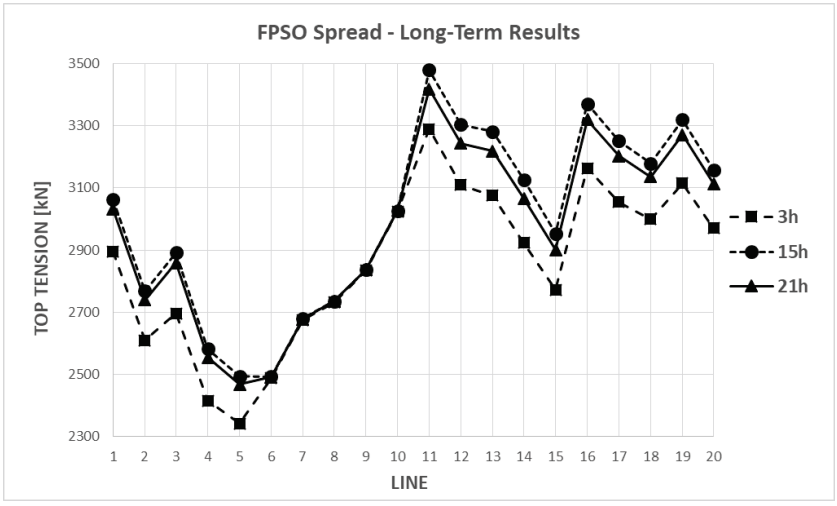

Figure 5-14 – Spread-moored FPSO: 100-yr most probable top tensions as function of the simulation length.

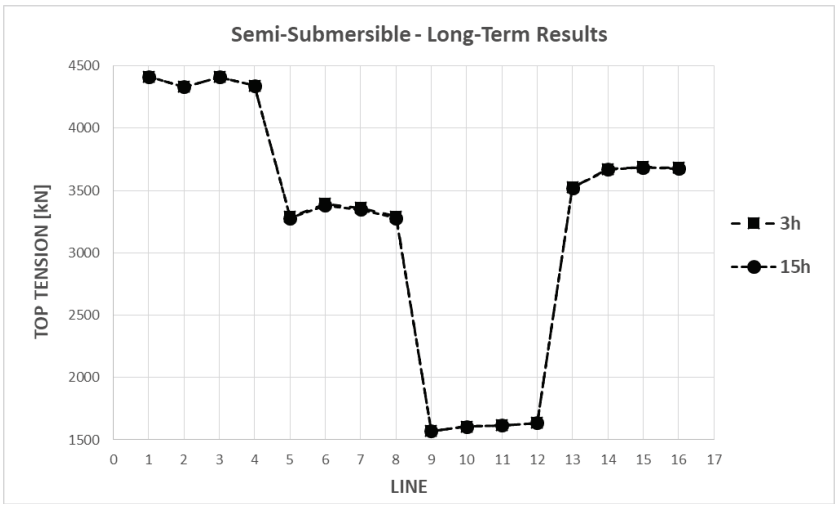

Figure 5-15 – Semi-submersible platform: 100-yr most probable top tensions as function of the simulation length.

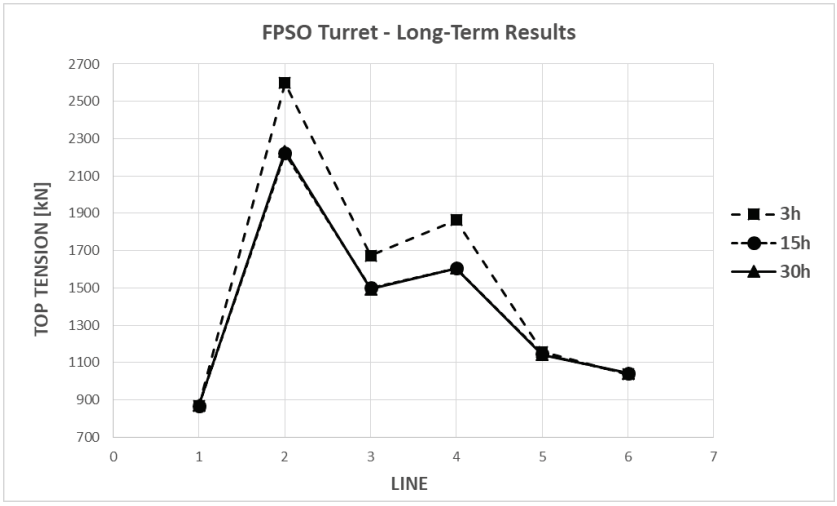

Figure 5-16 – Turret-moored FPSO: 100-yr most probable top tensions as function of the simulation length.

It is important to mention that the total number of short-term numerical simulations performed for each system and each simulation length is dependent on the number of drafts considered. Table 5-7 shows the total number short-term simulations for each system. This huge number simulations puts in evidence the need of a control system, as the one developed in this work, to perform a long-term analysis.

Table 5-7 – Total number of short-term simulations performed for the long-term analysis

Floating System	Drafts	Number of short-term simulations (for simulation length type)	Number of type of simulation lengths	Total number of short-term simulations
FPSO Spread	3	87,654	3	262,962
Semi-submersible	1	29,218	2	58,436
FPSO Turret	2	58,436	3	175,308

For sake of space saving, in what follows only the results associated to 15-hr simulation lengths will be presented. Table 5-8 to Table 5-10 present the long-term results for the 100-yr top tension in each line of the mooring system of the spread-moored FPSO, Semi-submersible platform and turret-moored FPSO, respectively. These tables also include the worst 3-hr most probable extreme top-tensions for each line and the difference between the long and short-term extreme values. Figure 5-17 and Figure 5-18 show the short-term and long-term cumulative probability distributions and the tail of these distributions, respectively, for the most loaded mooring line of the spread-moored FPSO. For this case, the 100-yr most probable top tension is 7.8% larger than the largest short-term extreme top tension among all short-term conditions and drafts considered. Figure 5-19 and Figure 5-20 present similar results for the Semi-submersible platform, while Figure 5-21 and Figure 5-22 present the corresponding ones for the Turret-moored FPSO. For the turret-moored FPSO the 100-yr most probable largest top tension is 15% larger than the largest short-term extreme top tension. The Semi-submersible platform presents an awkward result, i.e., the long and short-term extremes are almost the same. This explained by the fact that, for this floating system, the long-term response is dominated by a single extreme short-term environmental condition.

The semi-submersible platform has a very low dynamic behavior, with the largest currents dictating the short-term extremes. In fact, although the short-term curves are quite spread along the tension axis of long-term curve, as exposed by Figure 5-19, the severe short-term conditions, induced by higher currents velocities, can occur with smooth sea conditions, result in a narrow distribution of peak tensions, as exposed by Figure 5-19 and Figure 5-20, in which the most severe short-term condition presents a range of top peak tensions less than 15kN.

The results of 100-yr most probable top tensions associated to the other simulation lengths is presented in Appendix F.

Table 5-8 – Spread-moored FPSO. Extreme top tensions (simulation length of 15hr).

Spread-moored FPSO					
	Worst short-term condition			Long-Term Tension (kN)	Dif (%)
Line #	Environmental Condition	Draft	Extreme Tension (kN)		
1	13579	1	2896	3063	5.8%
2	12592	2	2597	2768	6.6%
3	12592	2	2693	2892	7.4%
4	12592	2	2416	2582	6.9%
5	12592	2	2344	2494	6.4%
6	25442	3	2489	2493	0.2%
7	25442	3	2676	2680	0.1%
8	25442	3	2733	2735	0.1%
9	25442	3	2832	2837	0.2%
10	25443	3	3025	3027	0.1%
11	**19256**	**2**	**3210**	**3480**	**8.4%**
12	19256	2	3042	3304	8.6%
13	19256	3	3015	3282	8.9%
14	19256	3	2883	3126	8.4%
15	19256	3	2748	2954	7.5%
16	19256	3	3140	3371	7.4%
17	19256	2	3035	3251	7.1%
18	19256	2	2988	3179	6.4%
19	19256	2	3101	3320	7.1%
20	19256	2	2959	3158	6.7%

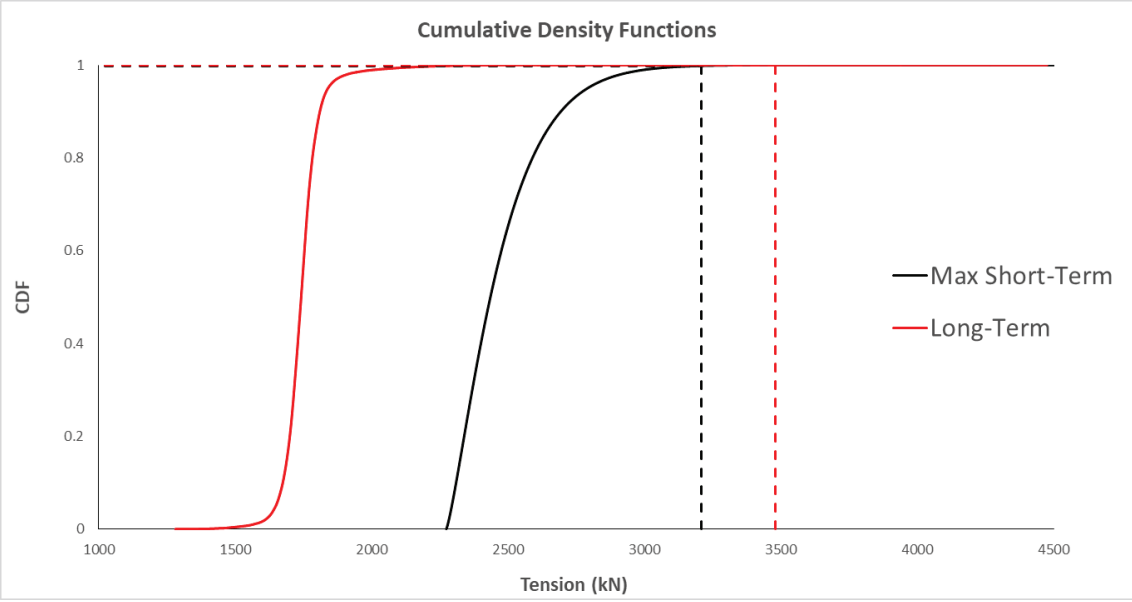

Figure 5-17 – Spread-moored FPSO - Line #11. Short-term and long-term top tension peaks cumulative probability distributions.

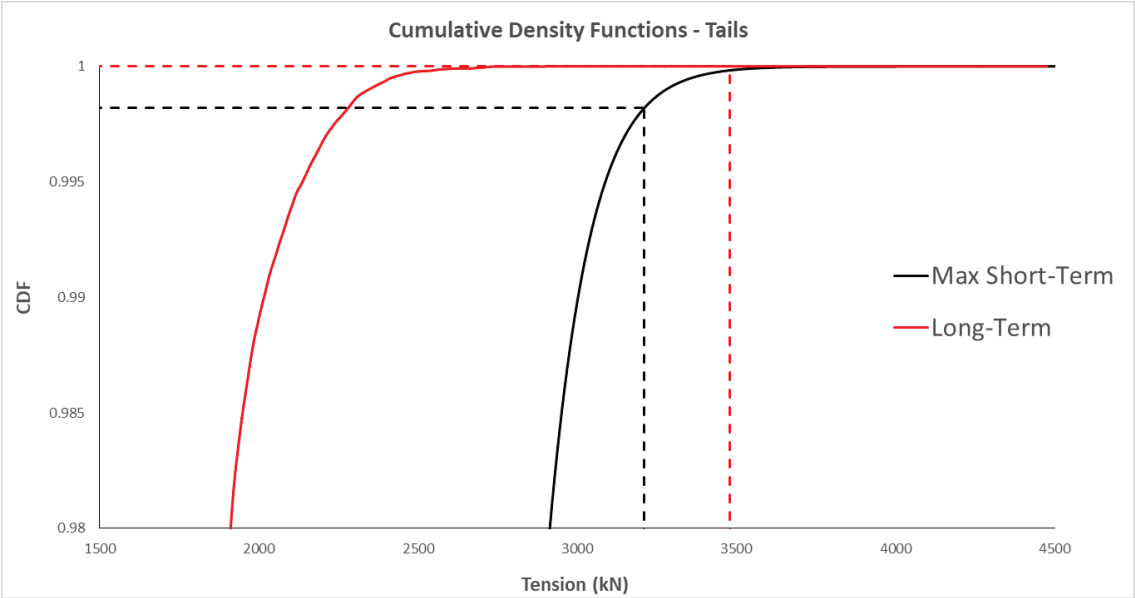

Figure 5-18 – Spread-moored FPSO - Line #11. Short-term and long-term top tension peaks cumulative probability distributions tails.

Table 5-9 – Semi-submersible platform. Extreme top tensions (simulation length of 15hr).

Semi-submersible platform					
	Worst short-term condition			Long-Term Tension (kN)	Dif (%)
Line #	Environmental Condition	Draft	Extreme Tension (kN)		
1	**4408**	**1**	**4412**	**4413**	**0.0%**
2	4408	1	4331	4332	0.0%
3	4408	1	4409	4410	0.0%
4	4407	1	4343	4344	0.0%
5	8123	1	3261	3278	0.5%
6	8123	1	3363	3382	0.6%
7	8123	1	3329	3348	0.6%
8	8123	1	3262	3281	0.6%
9	11920	1	1570	1571	0.1%
10	11920	1	1606	1606	0.0%
11	11920	1	1617	1617	0.0%
12	11920	1	1636	1636	0.0%
13	25443	1	3511	3523	0.3%
14	25443	1	3657	3669	0.3%
15	25443	1	3673	3685	0.3%
16	25442	1	3660	3675	0.4%

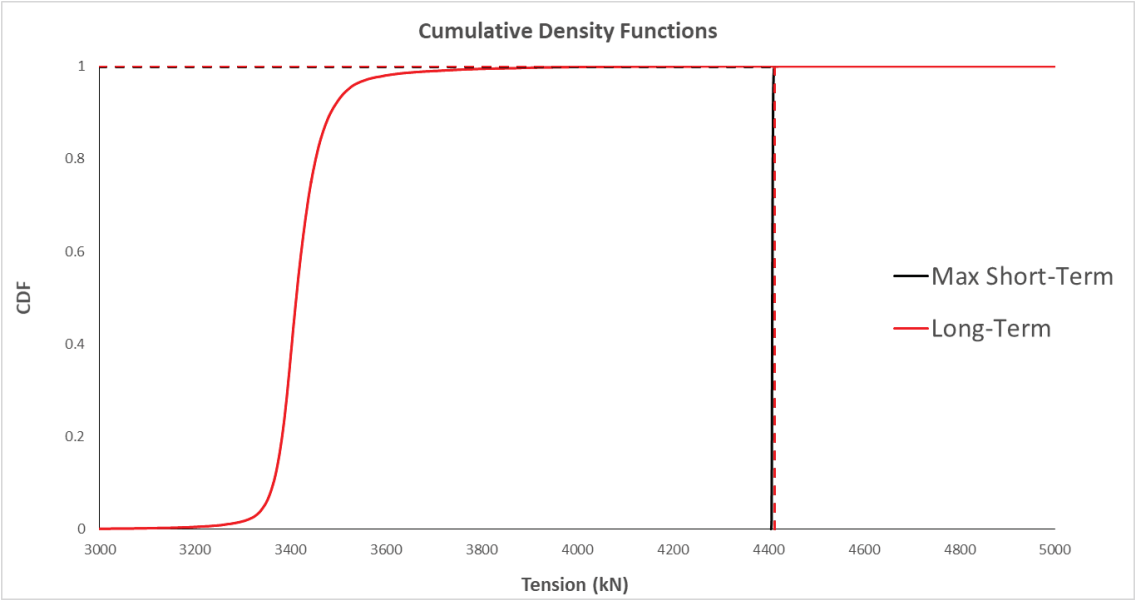

Figure 5-19 – Semi-submersible platform – Line #1. Short-term and long-term top tension peaks cumulative probability distributions.

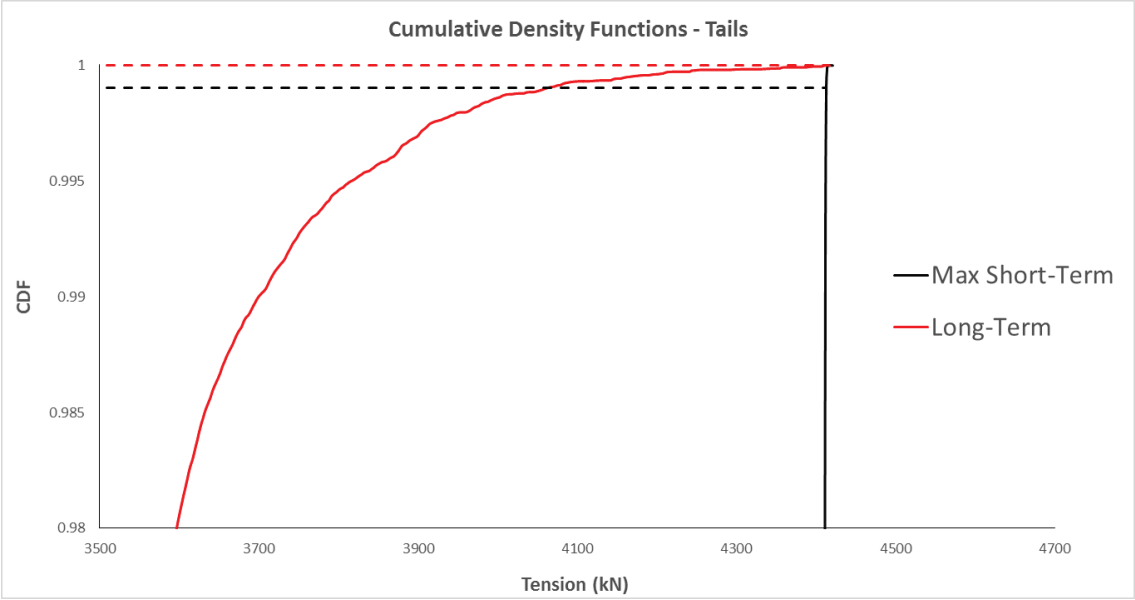

Figure 5-20 – Semi-Submersible – Line #1. Short-term and long-term top tension peaks cumulative probability distributions tails.

Table 5-10 – Turret-moored FPSO. Extreme top tensions (simulation length of 15hr).

Turret-moored FPSO					
	Worst short-term condition			Long-Term Tension (kN)	Dif (%)
Line #	Environmental Condition	Draft	Extreme Tension (kN)		
1	25442	1	865	869	0.5%
2	**4344**	**2**	**1888**	**2223**	**17.7%**
3	4344	2	1372	1500	9.3%
4	7978	2	1397	1605	14.9%
5	11920	2	1135	1145	0.9%
6	25443	1	1035	1042	0.7%

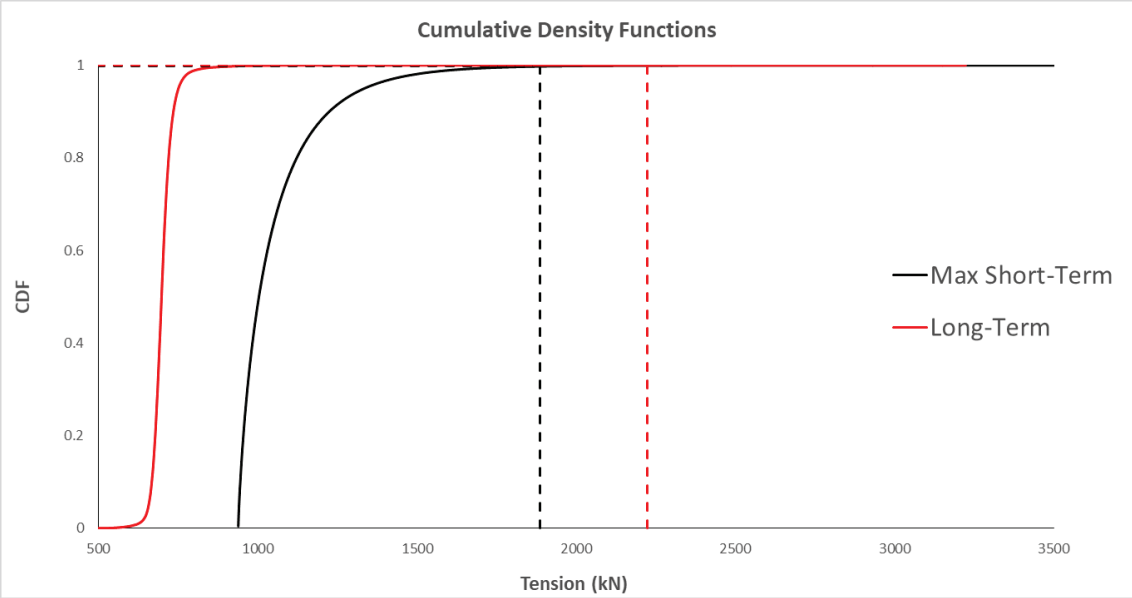

Figure 5-21 – Turret-moored FPSO – Line #2. Short-term and long-term top tension peaks cumulative probability distributions.

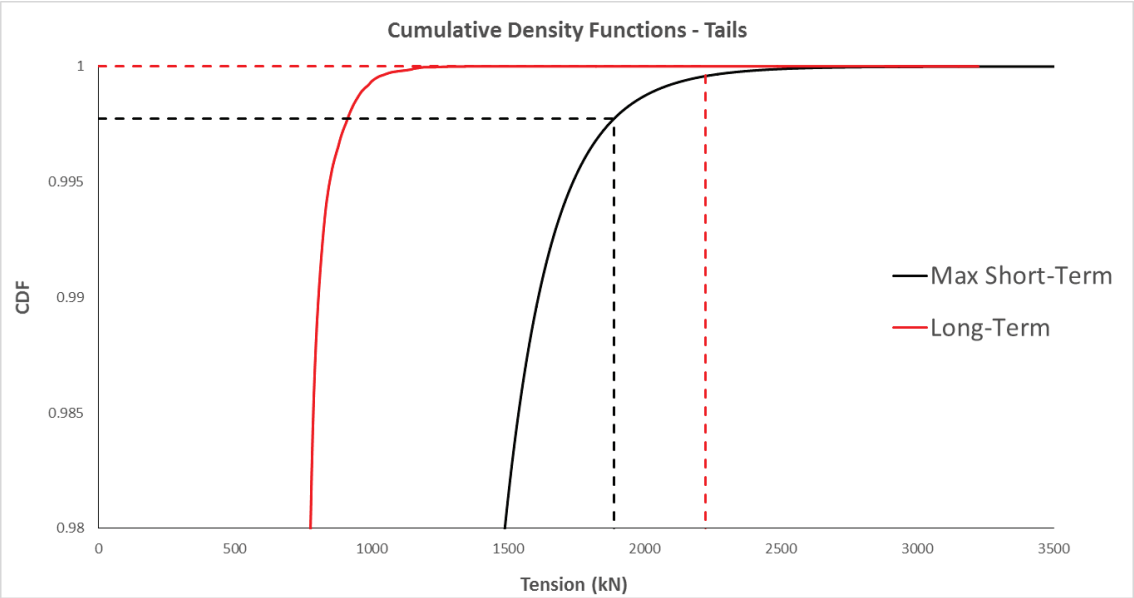

Figure 5-22 – Turret-moored FPSO – Line #2. Short-term and long-term top tension peaks cumulative probability distributions tails.

5.2.2.1 EQUIVALENT CONDITIONS AND DESIGN TENSIONS

After the calculation of the long-term (100-yr) top tensions, now it is time to carry out the Bootstrap analysis in order to find the upper bound of the 95% confidence interval of the extreme response estimator ($\hat{r}_{P_{Nyr}}^{MPV}$, also called by centenary tension, T_{100}). After this analysis, the equivalent short-term design conditions can be defined and, finally, find the 100-yr design tensions (T_{Dyn}) by running the Dynasim for these short-term conditions using a FEM-based discretization for the mooring lines. As in the previous section, the results presented are only for 15-hr simulation length.

Table 5-11 to Table 5-13 present a summary of the Bootstrap analysis, using $N_B = 200$ random re-samples, for the spread-moored FPSO, Semi-submersible plataform and turret-moored FPSO, respectively. The tables present the mean value of 100-yr most probable top tensions obtained from the N_B sample, the corresponding standard deviation and the upper-bound of the 95% confidence interval – see Eq. (3.3.6), which is identified as centenary tension T_{100}. Then this value is compared to the worst short-term extreme top tension and to estimated 100-yr most probable top tension computed in the previous section. As it can be seem in these tables, the statistical uncertainty is larger for the FPSO-based floating systems than for Semi-submersible platform. This, perhaps, can be explained not only by the magnitude of short-term conditions parameters, but also by the dynamic behaviors of these floating systems. Figure 5-23 to Figure 5-25 present the CDF

curve of the 29,218 short-term extreme responses of the critical mooring line (in the critical draft), of each platform. As shown in Figure 5-25 the FPSO Turret present a quite spread short-term extreme responses at the upper tail of this distribution for the mooring line number #2, which will affect the standard deviation of Bootstrap procedure.

The complete results, containing the other simulation lengths, are presented on Appendix G.

Table 5-11 – Spread-moored FPSO. Bootstrap Results. All lines (simulation length of 15hr).

Spread-moored FPSO							
Line #	**Short-Term Tension T_{Max} [kN]**	**Long-Term Tension T_{LT} [kN]**	**Bootstrap Mean Tension [kN]**	**Bootstrap Standard Deviation [kN]**	**Bootstrap Tension T_{100} [kN]**	$\frac{T_{100}-T_{Max}}{T_{Max}}$ (%)	$\frac{T_{100}-T_{LT}}{T_{LT}}$ (%)
L1	2896	3063	3021	96	3212	10.9%	4.9%
L2	2597	2768	2716	97	2910	12.0%	5.1%
L3	2693	2892	2794	157	3109	15.4%	7.5%
L4	2416	2582	2491	144	2778	15.0%	7.6%
L5	2344	2494	2401	141	2684	14.5%	7.6%
L6	2489	2493	2478	55	2589	4.0%	3.8%
L7	2676	2680	2659	65	2790	4.3%	4.1%
L8	2733	2735	2712	69	2851	4.3%	4.2%
L9	2832	2837	2811	77	2964	4.6%	4.5%
L10	3025	3027	2995	86	3168	4.7%	4.7%
L11	**3210**	**3480**	**3412**	**125**	**3662**	**14.1%**	**5.2%**
L12	3042	3304	3236	125	3486	14.6%	5.5%
L13	3015	3282	3212	129	3470	15.1%	5.7%
L14	2883	3126	3059	123	3305	14.7%	5.7%
L15	2748	2954	2894	109	3112	13.2%	5.4%
L16	3140	3371	3324	96	3516	12.0%	4.3%
L17	3035	3251	3207	90	3387	11.6%	4.2%
L18	2988	3179	3140	80	3300	10.4%	3.8%
L19	3101	3320	3275	91	3456	11.4%	4.1%
L20	2959	3158	3118	83	3283	11.0%	3.9%

Table 5-12 – Semi-submersible platform. Bootstrap Results. All lines (simulation length of 15hr).

Semi-submersible platform							
Line #	**Short-Term Tension T_{Max} [kN]**	**Long-Term Tension T_{LT} [kN]**	**Bootstrap Mean Tension [kN]**	**Bootstrap Standard Deviation [kN]**	**Bootstrap Tension T_{100} [kN]**	**$\frac{T_{100}-T_{Max}}{T_{Max}}$ (%)**	**$\frac{T_{100}-T_{LT}}{T_{LT}}$ (%)**
L1	**4412**	**4413**	**4404**	**17**	**4438**	**0.6%**	**0.6%**
L2	4331	4332	4320	18	4355	0.6%	0.5%
L3	4409	4410	4398	19	4436	0.6%	0.6%
L4	4343	4344	4334	23	4379	0.8%	0.8%
L5	3261	3278	3227	77	3382	3.7%	3.2%
L6	3363	3382	3325	86	3497	4.0%	3.4%
L7	3329	3348	3303	70	3444	3.5%	2.9%
L8	3262	3281	3260	40	3339	2.4%	1.8%
L9	1570	1571	1569	3	1574	0.3%	0.2%
L10	1606	1606	1597	11	1619	0.8%	0.8%
L11	1617	1617	1602	18	1638	1.3%	1.3%
L12	1636	1636	1621	18	1658	1.4%	1.3%
L13	3511	3523	3486	81	3648	3.9%	3.6%
L14	3657	3669	3628	94	3815	4.3%	4.0%
L15	3673	3685	3643	101	3846	4.7%	4.4%
L16	3660	3675	3631	107	3845	5.1%	4.6%

Table 5-13 – Turret-moored FPSO. Bootstrap Results. All lines (simulation length of 15hr).

Turret-moored FPSO							
Line #	**Short-Term Tension T_{Max} [kN]**	**Long-Term Tension T_{LT} [kN]**	**Bootstrap Mean Tension [kN]**	**Bootstrap Standard Deviation [kN]**	**Bootstrap Tension T_{100} [kN]**	**$\frac{T_{100}-T_{Max}}{T_{Max}}$ (%)**	**$\frac{T_{100}-T_{LT}}{T_{LT}}$ (%)**
L1	865	869	857	30	917	6.0%	5.4%
L2	**1888**	**2223**	**2044**	**320**	**2683**	**42.2%**	**20.7%**
L3	1372	1500	1471	68	1606	17.1%	7.1%
L4	1397	1605	1594	44	1682	20.4%	4.8%
L5	1135	1145	1126	30	1186	4.5%	3.6%
L6	1035	1042	1025	32	1090	5.3%	4.6%

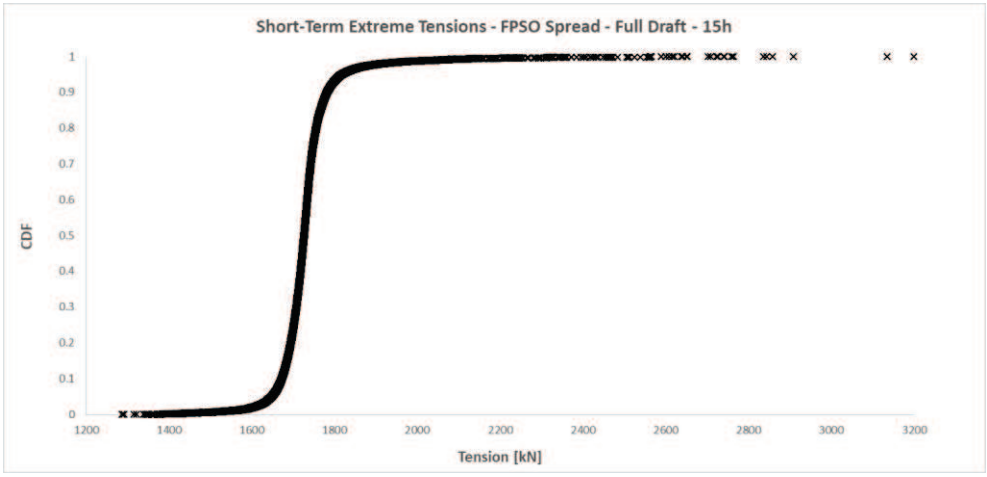

Figure 5-23 – FPSO Spread – Line #11 – Empiric CDF curve of extreme short-term top tensions

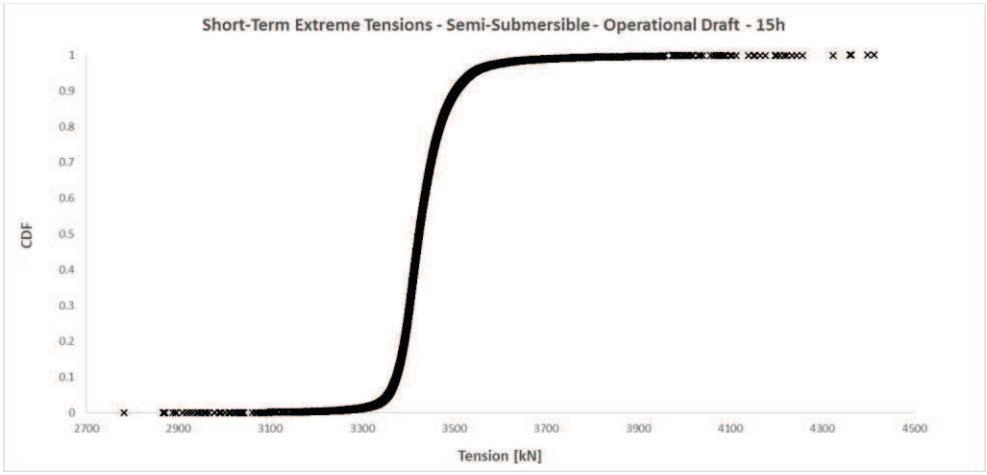

Figure 5-24 – Semi-Submersible – Line #1 – Empiric CDF curve of extreme short-term top tensions

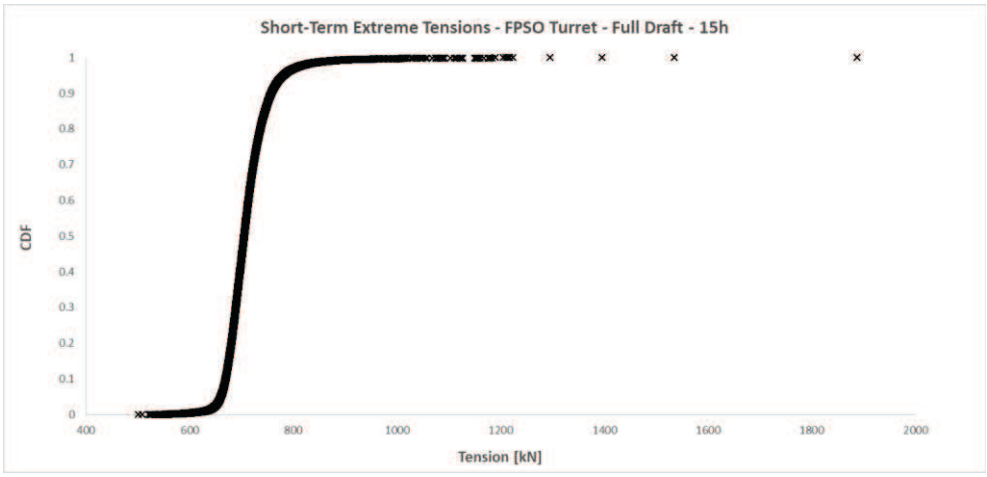

Figure 5-25 – FPSO Turret – Line #2 – Empiric CDF curve of extreme short-term top tensions

After defining the upper bound of the 95% confidence interval of 100-yr most probable top tension for each line (the centenary tension T_{100}) of each floating system, the corresponding short-term equivalent design conditions were defined (see Chapter 3.4). A short-term design environmental condition is one whose corresponding most probable extreme value is equal or very close to the centenary tension T_{100}. For each line, this condition was defined by adjusting the corresponding individual short-term environmental condition with the largest most probable short-term top tension. Table 5-14 to Table 5-16 present the equivalent short-term environmental conditions (see Chapter 3.4) for the mooring lines of the spread-moored FPSO, Semi-submersible platform and turret-moored FPSO, respectively.

The final step of the whole methodology was to run the Dynasim with the mooring lines modelled with finite elements for each equivalent short-term design condition defined previously. Basically, the discretization of each mooring line was made with truss elements of 10m. Table 5-17 to Table 5-19 show the final design tensions obtained for the top of each mooring line of the three floating systems investigated in this work. Regarding the most loaded mooring line in each floating system, it is possible to say, as already expected, that only the FPSO-based floating systems have presented some dynamic amplification in their mooring lines for the severe equivalent short-term conditions. However, it is not a general trend when one looks at all mooring lines.

Table 5-14 – Spread-moored FPSO. All Lines. Equivalent short-term design conditions – 15hr

Spread-moored FPSO - Equivalent short-term design conditions													
Line #	T_{Target} [kN]	Draft [m]	Original short-term conditions					Equivalent short-term conditions					$\frac{T_{Eq}-T_{Targ}}{T_{Targ}}$
			V_C [m/s]	V_W [m/s]	Hs_1 [m]	Hs_2 [m]	$T_{Original}$ (T_{Max}) [kN]	V_C [m/s]	V_W [m/s]	Hs_1 [m]	Hs_2 [m]	T_{Eq} [kN]	
L1	3212	T_1	1.02	13.33	2.77	0.61	2896	1.12	14.73	3.05	0.68	3216	0.10%
L2	2910	T_2	0.07	18.28	0.86	4.81	2597	0.07	19.75	0.95	5.18	2916	0.20%
L3	3109	T_2	0.07	18.28	0.86	4.81	2693	0.07	19.73	0.93	5.23	3103	-0.20%
L4	2778	T_2	0.07	18.28	0.86	4.81	2416	0.07	19.85	0.93	5.21	2773	-0.20%
L5	2684	T_2	0.07	18.28	0.86	4.81	2344	0.07	19.54	0.94	5.24	2686	0.10%
L6	2589	T_3	1.25	10.60	2.24	0.73	2489	1.29	11.00	2.32	0.78	2589	0.00%
L7	2790	T_3	1.25	10.60	2.24	0.73	2676	1.29	11.00	2.32	0.76	2792	0.10%
L8	2851	T_3	1.25	10.60	2.24	0.73	2733	1.29	11.05	2.33	0.76	2852	0.00%
L9	2964	T_3	1.25	10.60	2.24	0.73	2832	1.29	11.18	2.38	0.79	2964	0.00%
L10	3168	T_3	1.26	10.52	2.24	0.79	3025	1.30	11.25	2.43	0.83	3169	0.00%
L11	**3662**	**T_2**	**0.24**	**13.62**	**0.00**	**5.43**	**3210**	**0.26**	**15.61**	**0.00**	**6.01**	**3662**	**0.00%**
L12	3486	T_2	0.24	13.62	0.00	5.43	3042	0.26	15.81	0.00	5.99	3488	0.10%
L13	3470	T_3	0.24	13.62	0.00	5.43	3015	0.26	16.46	0.00	5.94	3478	0.20%
L14	3305	T_3	0.24	13.62	0.00	5.43	2883	0.26	15.64	0.00	5.94	3313	0.20%
L15	3112	T_3	0.24	13.62	0.00	5.43	2748	0.26	15.39	0.00	5.92	3120	0.30%
L16	3516	T_3	0.24	13.62	0.00	5.43	3140	0.27	16.79	0.00	5.91	3523	0.20%
L17	3387	T_2	0.24	13.62	0.00	5.43	3035	0.27	15.10	0.00	5.89	3391	0.10%
L18	3300	T_2	0.24	13.62	0.00	5.43	2988	0.27	15.10	0.00	5.89	3303	0.10%
L19	3456	T_2	0.24	13.62	0.00	5.43	3101	0.27	15.10	0.00	5.89	3455	0.00%
L20	3283	T_2	0.24	13.62	0.00	5.43	2959	0.27	15.10	0.00	5.89	3285	0.10%

Table 5-15 – Semi-submersible platform. All Lines. Equivalent short-term design conditions – 15hr

Semi-submersible platform - Equivalent short-term design conditions													
Line #	T_{Target} [kN]	Draft [m]	Original Short-Term Conditions					Equivalent Short-Term Conditions					$\frac{T_{Eq}-T_{Targ}}{T_{Targ}}$
			V_C [m/s]	V_W [m/s]	Hs_1 [m]	Hs_2 [m]	$T_{Original\ (T_{Max})}$ [kN]	V_C [m/s]	V_W [m/s]	Hs_1 [m]	Hs_2 [m]	T_{Eq} [kN]	
L1	**4438**	**T_1**	**1.13**	**6.03**	**0.85**	**1.01**	**4412**	**1.14**	**6.35**	**1.05**	**1.22**	**4438**	**0.00%**
L2	4355	T_1	1.13	6.03	0.85	1.01	4331	1.14	6.35	1.05	1.22	4356	0.00%
L3	4436	T_1	1.13	6.03	0.85	1.01	4409	1.14	6.43	1.12	1.32	4436	0.00%
L4	4379	T_1	1.13	6.03	0.85	1.01	4343	1.15	6.14	0.88	1.04	4379	0.00%
L5	3382	T_1	1.10	12.14	3.29	1.51	3261	1.16	13.50	3.90	1.95	3380	0.00%
L6	3497	T_1	1.10	12.14	3.29	1.51	3363	1.17	13.75	3.95	2.00	3505	0.20%
L7	3444	T_1	1.10	12.14	3.29	1.51	3329	1.16	13.50	3.90	1.95	3446	0.10%
L8	3339	T_1	1.10	12.14	3.29	1.51	3262	1.15	13.00	3.52	1.65	3347	0.20%
L9	1574	T_1	1.03	8.92	1.86	0.92	1570	1.04	9.04	1.89	0.93	1575	0.00%
L10	1619	T_1	1.03	8.92	1.86	0.92	1606	1.06	9.24	1.95	0.96	1621	0.10%
L11	1638	T_1	1.03	8.92	1.86	0.92	1617	1.07	9.48	2.05	1.02	1639	0.10%
L12	1658	T_1	1.03	8.92	1.86	0.92	1636	1.07	9.48	2.05	1.02	1657	-0.10%
L13	3648	T_1	1.26	10.52	2.24	0.79	3511	1.31	10.75	2.30	0.81	3644	-0.10%
L14	3815	T_1	1.26	10.52	2.24	0.79	3657	1.31	11.00	2.45	0.95	3814	0.00%
L15	3846	T_1	1.26	10.52	2.24	0.79	3673	1.31	11.15	2.55	1.05	3847	0.00%
L16	3845	T_1	1.26	10.52	2.24	0.79	3660	1.31	11.15	2.55	1.05	3840	-0.10%

Table 5-16 – Turret-moored FPSO. All Lines. Equivalent short-term design conditions – 15hr

Turret-moored FPSO - Equivalent short-term design conditions													
Line #	T_{Target} [kN]	Draft [m]	Original Short-Term Conditions					Equivalent Short-Term Conditions					$\frac{T_{Eq}-T_{Targ}}{T_{Targ}}$
			V_C [m/s]	V_W [m/s]	Hs_1 [m]	Hs_2 [m]	$T_{Original\ (T_{Max})}$ [kN]	V_C [m/s]	V_W [m/s]	Hs_1 [m]	Hs_2 [m]	T_{Eq} [kN]	
L1	917	T_1	1.25	10.60	2.24	0.73	865	1.35	11.80	2.70	1.15	916	-0.10%
L2	**2683**	**T_2**	**0.83**	**14.61**	**0.00**	**6.83**	**1888**	**1.01**	**17.76**	**0.00**	**8.36**	**2683**	**0.00%**
L3	1606	T_2	0.83	14.61	0.00	6.83	1372	0.92	15.93	0.00	7.45	1609	0.20%
L4	1682	T_2	0.21	13.87	0.00	6.61	1397	0.25	15.68	0.00	7.45	1683	0.10%
L5	1186	T_2	1.03	8.92	1.86	0.92	1135	1.10	9.83	2.38	1.36	1182	-0.30%
L6	1090	T_1	1.26	10.52	2.24	0.79	1035	1.34	11.62	2.70	1.28	1087	-0.30%

Table 5-17 – Spread-moored FPSO. All lines. Final design top tension (simulation length of 15hr).

Spread-moored FPSO - Final design top tension			
Line #	Equivalent short-Term conditions		$\frac{T_{Dyn} - T_{QS}}{T_{QS}}$ (%)
	Quasi-static tension (T_{QS}) [kN]	Dynamic tension (T_{Dyn}) [kN]	
L1	3216	3397	5.6%
L2	2916	3121	7.0%
L3	3103	3345	7.8%
L4	2773	2938	6.0%
L5	2686	2895	7.8%
L6	2589	2618	1.1%
L7	2792	2829	1.3%
L8	2852	2890	1.3%
L9	2964	3018	1.8%
L10	3169	3262	2.9%
L11	**3662**	**4467**	**22.0%**
L12	3488	3841	10.1%
L13	3478	3473	-0.1%
L14	3313	3308	-0.1%
L15	3120	3288	5.4%
L16	3523	3608	2.4%
L17	3391	3611	6.5%
L18	3303	3546	7.3%
L19	3455	3737	8.2%
L20	3285	3922	19.4%

Table 5-18 – Semi-submersible platform. All lines. Final design top tension (simulation length of 15hr).

Semi-submersible platform. Final design top tension			
Line #	Equivalent short-term conditions		$\frac{T_{Dyn} - T_{QS}}{T_{QS}}$ (%)
	Quasi-static tension (T_{QS}) [kN]	Dynamic tension (T_{Dyn}) [kN]	
L1	**4438**	**4410**	**-0.6%**
L2	4356	4300	-1.3%
L3	4436	4415	-0.5%
L4	4379	4329	-1.1%
L5	3380	3377	-0.1%
L6	3505	3501	-0.1%
L7	3446	3437	-0.3%
L8	3347	3340	-0.2%
L9	1575	1607	2.0%
L10	1621	1650	1.8%
L11	1639	1669	1.8%
L12	1657	1685	1.7%
L13	3644	3616	-0.8%
L14	3814	3789	-0.7%
L15	3847	3825	-0.6%
L16	3840	3822	-0.5%

Table 5-19 – Turret-moored FPSO. All lines. Final design top tension (simulation length of 15hr).

Turret-moored FPSO - Final design top tension			
Line #	Equivalent short-term conditions		$\frac{T_{Dyn} - T_{QS}}{T_{QS}}$ (%)
	Quasi-static tension (T_{QS}) [kN]	Dynamic tension (T_{Dyn}) [kN]	
L1	916	1119	22.1%
L2	**2683**	**2580**	**-3.8%**
L3	1609	1886	17.2%
L4	1683	1861	10.6%
L5	1182	1216	2.8%
L6	1087	1226	12.8%

6 CONCLUSION AND FUTURE WORK

This work presented the development of methodology for long-term response analysis of tensions in the mooring lines of an offshore floating system. Essentially, it is based on the short-term numerical simulations for set of 10-yr long short-term environmental data of 3-hr sea-states, observed (or inferred) in the location where the floating is (or will be) installed (will operate). Each short-term environmental condition is composed of the simultaneously observed environmental parameters of wave, wind and current. The wave data can be represented by the sea and swell components. The analysis take into account the unit draft variation in the long-term. The long-term response distribution is a draft-weighted average of all short-term response peaks distribution, modelled in the present work by the three parameters Weibull distribution.

Due to the large number of environmental conditions to be analyzed, the initial analysis is based on the catenary equation modelling for each line and each riser connected to the floater. The Bootstrap approach is employed in order to take into account the statistical uncertainty associated to the estimated long-term most probable extreme response due to the limited number of short-term environmental conditions.

Once the upper bound of the long-term extreme tensions (the centenary tensions) have been evaluated, an equivalent short-term design environmental condition is defined for each line of the mooring system. This equivalent short-term environmental condition is any set of environmental condition whose short-term most probable extreme response is equal (or very close) to the long-term most probable extreme value. The equivalent short-term design environmental conditions can be obtained by making small changes around the parameters of an analyzed condition that resulted in a large most probable short-term extreme value. Then, this equivalent short-term environmetal conditions are applied in a numerical model where the lines are discretized by finite elements, i.e., a more accurate model, but very time-consuming. The short-term extreme responses estimated from the results of this last model are taken as final design values.

One very important aspect is that the methodology requires some *control system* in order to manage, verify and get the results of all short-term simulations. This *control system* was developed in Phyton and, among other features, it allows the use of many computers for running the short-term simulations.

The methodology has been used in the long-term analysis of the mooring system of three floating systems: a spread-moored FPSO, a turret-moored FPSO and a Semi-submersible platform. Some aspects related to the systems modelling were observed and are recommended in future analyses:

- as also indicated in Ref. [26], the wave spectrum shall be well discretized, the use of at least 1000 wave components is recommended;
- a minimum time duration of 15-hr for each short-term simulation is indicated for FPSOs in order to obtain stable short-term statistical parameters of the response;
- a minimum number of 200 random re-samples shall be used in the Bootstrap procedure.

Other aspects observed during the analyses which are related to the computer system used to perform the long-term analysis using the Dynasim code are:

- although the Python code (Short-Term Analysis Module) is able to erase the Dynasim files after reading, it is recommended a minimum of 1TB free space on the hard disk (a buffer) in order to avoid any type of problem related with the short-term simulations when using the parallel processing tool available on Dynasim in association with only one Short-Term Analysis Module process;
- the long-term analyses of spread moored systems showed to be the most time consuming ones. Considering the short-term simulation with a time duration of 15hr, three drafts, with the spectrum discretized by more than 1000 wave components, using four computers Intel Core i7, 32G RAM, the long-term analysis took about 1 month to be finished;

Concerning the results of long-term analyses themselves, it was observed that the FPSO mooring systems presented the larger dynamic amplifications. The Semi-submersible platform presents a quasi-static behavior and the wave-loading in not very important for its response. The largest responses are dominated by the short-term environmental conditions with largest current velocities.

A very important step has been done for the use of long-term analysis in the design of mooring systems. In computer terms, the methodology presented in this work can be used without any significant difficult. However, some future studies are still necessary in order to recommend its daily use, among others:

- the use of larger environmental data base in order to identify the minimum number of environmental conditions to be employed in the long-term analysis;
- using the database of environmental conditions, compare the obtained long-term extreme results with those obtained with the standard design long-term methodology based on the extreme environmental conditions;
- perform a long-term analysis using a FEM-based model for the lines (fully-coupled model) since the beginning of the process;

Other improvements in the developed methodology can be also implemented:

- create a central interface, user-friendly, for the code, making it easy for other users to use;
- implement the possibility of using global tension peaks instead of local peaks and compare the results obtained by these two methodologies;

As the last one but not the least suggestion for future work is the use of this methodology in the reliability analysis studies in order to obtain a calibrated design methodology for design moored floating systems in Brazilian waters.

REFERENCES

[1] TPN-DYNASIM. *Dynamic Simulation*. Version 5.5.9. Petrobras/PUC-RJ/USP/UFAL/UFRJ, Abr. 2018.

[2] PYTHON. *Python Software Foundation*. Python Language, version 3.6. Disponível em: <https://www.anaconda.com/distribution/>. Acesso em 10 Out. 2017.

[3] POSMOOR. *Position Mooring*. Mobile Offshore Units. Det Norske Veritas, Norway, 1989.

[4] API RP 2SK. *Recommended Practice for Design and Analysis of Stationkeeping Systems for Floating Structures*. American Petroleum Institute, USA, 2005.

[5] INTERNATIONAL STANDARD ISO 19901-7. *Petroleum and natural gas industries – Specific requirements for offshore structures – Part 7: Stationkeeping systems for floating offshore structures and mobile offshore units*. International Organization for Standardization, 2013.

[6] OFFSHORE STANDARD DNV-OS-E301. *Position Mooring*. Det Norske Veritas, Jul. 2015.

[7] INTERNATIONAL STANDARD ISO 19904-1. *Petroleum and natural gas industries – Floating offshore structures – Part 1: Monohulls, semi-submersibles and spars*. International Organization for Standardization, 2006.

[8] DYNASIM. *Manual do Usuário*. Versão 5.2.3 Petrobras/PUC-RJ/USP/UFAL/UFRJ, Dez. 2014.

[9] DYNASIM. *Manual Teórico*. Petrobras/PUC-RJ/USP/UFAL/UFRJ.

[10] DYNASIM. *Manual da Linguagem PDL*. Petrobras/PUC-RJ, Jun 2015.

[11] DOOLINES. *Manual Teórico do DOOLINES*. Versão 1.1. Laboratório de Computação Científica e Visualização – LCCV. Universidade Federal de Alagoas. Maceió, Alagoas, Jan. 2014.

[12] PYTHON 3.7.4RC1 DOCUMENTATION. The Python Standard Library. Disponível em: <https://docs.python.org/3/library/random.html>. Acesso em: 03 abr. 2019.

[13] FALTINSEN, O. M., 1990, *Sea loads on Ships and Offshore Structures.* 1 ed. United Kingdom, Cambridge University Press.

[14] OCHI, M. K., 1998, *Ocean Waves: The Stochastic Approach*. 1 ed. United Kingdom, Cambridge University Press.

[15] CHAKRABARTI, S. K., 2005, *Handbook of Offshore Engineering Volume II*. 1 ed. Plainfield, Illinois, USA, Elsevier.

[16] CHAKRABARTI, S. K., 2005, *Handbook of Offshore Engineering Volume I*. 1 ed. Plainfield, Illinois, USA, Elsevier.

[17] NAESS, A., MOAN, T., 2013, *Stochastic Dynamics of Marine Structures*. United Kingdom, Cambridge University Press.

[18] SAGRILO, L. V. S., NAESS, A., DORIA, A. S., 2011, "On the long-term response of marine structures", *Applied Ocean Research*, v. 33, pp. 208–214.

[19] HØRTE, T., LIE, H., MATHISEN, J., "Calibration of an Ultimate Limit State of Mooring Lines". *Offshore Mechanics and Artic Engineering*, OMAE98-1457, Lisbon, Portugal, 1998.

[20] MATHISEN, J., HØRTE, T., LIE, H., *et al,* "Calibration of a Progressive Collapse Limit State for Mooring Lines". *Offshore Mechanics and Artic Engineering*, OMAE98-1458, Lisbon, Portugal, 1998.

[21] MATHISEN, J., HØRTE, T., "Calibration of a Fatigue Limit State of Mooring Lines". *International Conference on Computational Methods in Marine Engineering*, N-1322, Høvik, Norway, 2005.

[22] HØRTE, T., OKKENHAUG, S., PAULSHUS, Ø., "Mooring System Calibration of the Intact Condition, Ultimate Limit State (ULS)". *Offshore Mechanics and Artic Engineering.* OMAE2017-61529, Trondheim, Norway, 2017.

[23] HØRTE, T., OKKENHAUG, S., PAULSHUS, Ø., "Mooring System Calibration of the Damaged Condition, Accidental Limit State (ALS)")". *Offshore Mechanics and Artic Engineering.* OMAE2017-61533, Trondheim, Norway, 2017.

[24] VÁZQUEZ-HERNÁNDEZ, A. O., ELLWANGER, G. B., SAGRILO, L. V. S., 2011, "Long-Term response analysis of FPSO mooring systems", *Applied Ocean Research*, v. 33, pp. 375–383.

[25] VÁZQUEZ-HERNÁNDEZ, A. O., ELLWANGER, G. B., SAGRILO, L. V. S., 2006, "Reliability-based Comparative study for mooring lines design criteria". *Applied Ocean Research*, v. 28, pp. 398–406.

[26] SIMÃO, M. L., 2019, *Extreme Value Estimation of Mooring Lines Top Tension*. M. Sc. dissertation, COPPE/UFRJ, Rio de Janeiro, RJ, Brasil;

[27] JOURNEÉ, J. M. J., MASSIE, W. W., 2001, *Offshore Hydromechanics*. 1 ed. Delft University of Technology.

[28] LEVY, L. A. P., 1989, *Análise de Movimentos de Corpos Flutuantes no Domínio do Tempo*. Dissertação de M. Sc., COPPE/UFRJ, Rio de Janeiro, RJ, Brasil.

[29] OBOKATA, J., 1987, "On the Basic Design of Single Point Mooring Systems, 1st report: Applications of the Dynamic Stability Analysis to the Primary Planning of the System". *Journal of the Society of Naval Architects of Japan*, v. 161, p. 183.

[30] CUMMINS, W. E., 1962, *The Impulse Response Function and Ship Motions*. Research and Development Report, Department of the Navy. David Taylor Model Basin, Hydromechanics Laboratory.

[31] ARANHA, J. A. P., 1994, "A Formula for 'Wave Damping' in the Drift of a Floating Body". *Journal of Fluid Mechanics*, v. 275, pp. 147 – 155.

[32] ARANHA, J. A. P., 2001, "Low Frequency Wave Force Spectrum Influenced by Wave-Current Interaction". *Applied Ocean Research*, v. 23, pp. 147-157.

[33] ARANHA, J. A. P., FERNANDES, A.C., 1995, "On The Second Order Low Frequency Force Spectrum". *Applied Ocean Research*, v. 17, pp. 311-313.

[34] ROSSI, R.R., 2002, *Cabos de Poliéster para Ancoragem de Plataformas Oceânicas em águas Ultraprofundas*. Dissertação de M. Sc., COPPE/UFRJ, Rio de Janeiro, RJ, Brasil.

[35] EFRON, B., TIBSHIRANI, R., 1993, *An Introduction to the Bootstrap*. 1 ed. New York, USA, Chapman & Hall.

[36] BATTJES, J. A., 1970, *Long-Term Wave Height Distribution at Seven Stations around the British Isles*. Report no. A44, Godalming: National Institute of Oceanography.

[37] BURY, K. V., 1975, *Statistical Models in Applied Science*. 1 ed. New York, USA, John Wiley & Sons.

[38] ANG, A. H. S., TANG, W. H., 1984, *Probability Concepts in Engineering Planning and Design*. 1 ed. New York, USA, John Wiley & Sons.

APPENDIX A – STATISTICAL DISTRIBUTION

A random variable X can be represented by its corresponding probability distribution which, in turn, can be expressed by either its probability density function (PDF) $f_X(x)$ or its cumulative probability function (CDF) $F_X(x)$. These two are related by

$$f_X(x) = \frac{dF(x)}{dx} \tag{A.1}$$

and

$$F_X(x) = \int_{-\infty}^{x} f_X(x)dx \tag{A.2}$$

Some important characteristic parameters of a random variable, such as the first four statistical moments, mean (μ), standard deviation (σ), skewness (γ) and kurtosis (κ) coeffients are, respectively, obtained by:

$$\mu = \int_{-\infty}^{\infty} x f_X(x)dx \tag{A.3}$$

$$\sigma = \sqrt{\int_{-\infty}^{\infty} (x-\mu)^2 f_X(x)dx} \tag{A.4}$$

$$\gamma = \frac{\int_{-\infty}^{\infty} (x-\mu)^3 f_X(x)dx}{\sigma^3} \tag{A.5}$$

$$\kappa = \frac{\int_{-\infty}^{\infty} (x-\mu)^4 f_X(x)dx}{\sigma^4} \tag{A.6}$$

In what follows some important probability distributions used in engineering are described.

A.1 GAUSS, RICE AND RAYLEIGH DISTRIBUTIONS

These three probability distributions (Gauss, Rice and Rayleigh) are connected to a Gaussian random process $X(t)$ with known mean value μ and spectral density $S(\omega)$. Just to remember that the standard deviation of this process corresponds to square root of zero-order moment (m_o) of this function. The n-order moment of $S(\omega)$ is defined as:

$$m_n = \int_0^\infty \omega^n S(\omega) d\omega \tag{A.7}$$

A.1.1 GAUSS DISTRITUTION

The Gauss probability density function (PDF) is given by:

$$f_X(x) = \frac{1}{\sigma\sqrt{2\pi}} e^{-\frac{1}{2}\left(\frac{x-\mu}{\sigma}\right)^2} \tag{A.8}$$

where μ is the mean and σ of the random variable X (in case of a Gaussian random process $\sigma = \sqrt{m_0}$). There is no analytical solution for its corresponding CDF, however, it is defined as:

$$F_X(x) = \Phi\left(\frac{x-\mu}{\sigma}\right) \tag{A.9}$$

where $\Phi(.)$ is the CDF of a standard Gaussian random variable ($\mu = 0$ and $\sigma = 1$) which is tabulated in almost every book on probability and statistics.

A.1.2 RICE AND RAYLEIGH DISTRITUTIONS

The peaks X_p of a Gaussian random process $X(t)$ is given theoretically by the Rice distribution whose PDF is:

$$f_{X_p}(x_p) = \frac{\varepsilon}{\sqrt{2\pi}\sqrt{m_0}} e^{-\frac{1}{2}\left[\frac{x_p}{\sqrt{m_0}\varepsilon}\right]^2} + \frac{x_p}{m_0}\sqrt{1-\varepsilon^2}\, e^{-\frac{1}{2}\left(\frac{x_p}{\sqrt{m_0}}\right)^2} \Phi\left[\frac{x_p}{\sqrt{m_0}\varepsilon}\sqrt{1-\varepsilon^2}\right] \tag{A.10}$$

where ε is the spectrum bandwidth-related parameter given by:

$$\varepsilon = \sqrt{1 - \frac{m_2^2}{m_0 m_4}} \tag{A.11}$$

When $\varepsilon \to 1$ the process is broad band and the Rice distribution converges to the Gaussian one. However, when $\varepsilon \to 0$ the process is narrow band and the Rice distribution becomes the Rayleigh distribution, whose PDF is given by:

$$f_{X_p}(x_p) = \frac{x_p}{m_0} e^{-\frac{1}{2}\left(\frac{x_p}{\sqrt{m_0}}\right)^2} \tag{A.12}$$

The CDF for the Rice distribution can only be obtained numerically, except when it becomes a Rayleigh distribution. For this situation:

$$F_{X_p}(x_p) = 1 - e^{-\frac{1}{2}\left(\frac{x_p}{\sqrt{m_0}}\right)^2}$$

(A.13)

A.2 WEIBULL DISTRIBUTION

A.2.1 THREE-PARAMETER WEIBULL MODEL

The PDF and CDF of random variable X with a 3-Parameter Weibull distribution are defined, respectively, by:

$$f_X(x) = \frac{(x-u)^{\lambda-1}}{\alpha^{\lambda}}\lambda e^{-\left(\frac{x-u}{\alpha}\right)^{\lambda}} \qquad for \quad x \geq u$$

(A.14)

$$F_X(x) = 1 - e^{-\left(\frac{x-u}{\alpha}\right)^{\lambda}} \qquad for \quad x \geq u$$

(A.15)

where u, α and λ are the so-called, respectively, location, scale and shape parameters of the distribution. The relationships of these parameters with the first four statistical moments of X are [37]:

$$\mu = u + \alpha\Gamma\left(1 + \frac{1}{\lambda}\right) \tag{A.16}$$

$$\sigma = \alpha\sqrt{\Gamma\left(1 + \frac{2}{\lambda}\right) - \Gamma^2\left(1 + \frac{1}{\lambda}\right)} \tag{A.17}$$

$$\gamma = \frac{\Gamma\left(1 + \frac{3}{\lambda}\right) - 3\Gamma\left(1 + \frac{1}{\lambda}\right)\Gamma\left(1 + \frac{2}{\lambda}\right) + 2\Gamma^3\left(1 + \frac{1}{\lambda}\right)}{\left[\Gamma\left(1 + \frac{2}{\lambda}\right) - \Gamma^2\left(1 + \frac{1}{\lambda}\right)\right]^{\frac{3}{2}}}$$

(A.18)

$$\kappa = \frac{\Gamma\left(1+\frac{4}{\lambda}\right) - 4\Gamma\left(1+\frac{1}{\lambda}\right)\Gamma\left(1+\frac{3}{\lambda}\right) + 6\Gamma^2\left(1+\frac{1}{\lambda}\right)\Gamma\left(1+\frac{2}{\lambda}\right) - 3\Gamma^4\left(1+\frac{1}{\lambda}\right)}{\left[\Gamma\left(1+\frac{2}{\lambda}\right) - \Gamma^2\left(1+\frac{1}{\lambda}\right)\right]^2}$$

(A.19)

where $\Gamma(.)$ = Gamma function;

An important observation is that the Rayleigh distribution (mentioned before) is a specific case of a Weibull distribution, with $= 0$, $\lambda = 2$ and $\alpha = \sqrt{2m_0}$.

A.2.2 TWO-PARAMETER WEIBULL MODEL

The 2-Parameter Weibull distribution is the same of Eq. (A.14) and Eq. (A.15), with the location parameter being equal to zero. Then, the corresponding PDF and CDF are:

$$f_X(x) = \frac{x^{\lambda-1}}{\alpha^\lambda}\lambda e^{-\left(\frac{x}{\alpha}\right)^\lambda}$$

(A.20)

$$F_X(x) = 1 - e^{-\left(\frac{x}{\alpha}\right)^\lambda}$$

(A.21)

This model has one advantage when used in the probability distribution fitting process. Through some mathematical transformation it can be linearized as:

$$\ln\{-\ln[1 - F_X(x)]\} = \lambda \ln x - \lambda \ln \alpha$$

(A.22)

If a sample $\boldsymbol{X} = [x_1, x_2, \dots, x_N]$ and the corresponding empirical CDF values $\boldsymbol{p} = \left[\frac{1}{N+1}, \frac{2}{N+1}, \dots, \frac{N}{N+1}\right]$ are available, the two parameters of the Weibull model the best fits the data can be obtained through linear regression analysis. The advantage of this procedure is that the fitting can be directed for some part of the data, i.e., the distribution can be fitted for only some part of the sample. In extreme analysis is the upper tail that is important. A procedure largely used in the short-term simulations of marine structures is the so-called Weibull-tail fitting. This procedure is implemented in Dynasim [1] and consists in obtain the two parameters of Weibull distribution for six sets of that, i.e., above 60%, 65%, 70%, 80%, 85%, 90% percentiles of the empirical cumulative distribution. The final model parameters λ and α are taken as the corresponding mean values of the six fittings.

A.2.3 GUMBEL OR TYPE I PROBABILITY DISTRIBUTION

The PDF and CDF of a random variable X with a Gumbel probability distribution are, respectively, given by:

$$f_X(x) = \alpha e^{-\alpha(x-u)-e^{-\alpha(x-u)}} \tag{A.23}$$

$$F_X(x) = e^{-e^{-\alpha(x-u)}} \tag{A.24}$$

where α and u are, respectively, the scale and location parameters of the distribution. These parameters are related to the mean μ and standard deviation σ of X by:

$$\alpha = \frac{\pi}{\sigma\sqrt{6}} \tag{A.25}$$

$$u = \mu - \frac{0.5722}{\alpha} \tag{A.26}$$

It is important to point out that the parameter u is the most probable value of this distribution, i.e., at the point $x = u$ is the position where the CDF $F_X(x)$ reaches its maximum value.

A.3 PROBABILITY DISTRIBUTION OF EXTREME VALUES

Structures should be designed to withstand extreme maximum loads, as the storage capacity of a dam must be designed to guarantee the water supply for a city during extreme minimum levels of the river where it is installed. Extreme values have their own population and are usually related to a given return period. For instance, the largest level in some point of a river in period of one year varies along various years of observation. If a sample of largest yearly-observed values is available, the 1-yr extreme level probability distribution is obtained by fitting a probability model to this data sample. However, if for some reason, the 100-yr extreme is required it is very likely that a large sample of 100-yr maxima will be not available. For this latter case, other approaches must be followed in order to obtain the extreme distribution and one of them is the so-called Order Statistics, described in what follows. For convenience, only maximum extreme value statistics will be commented.

A.3.1 ORDER STATISTICS

Assume that, for instance, in the return period of interest the random variable $\boldsymbol{X}$ is observed N times. Then, a single sample of this random variable in such period given by:

$$\boldsymbol{X} = \{X_1, X_2, \dots, X_N\} \tag{A.27}$$

where X_i means the i[th] observation of the random variable, that is also a random variable. However, the probably distribution of each observation is governed by the probability of $\boldsymbol{X}$ itself, or in other words:

$$F_{X_1}(x) \cong F_{X_2}(x) \cong \cdots \cong F_{X_N}(x) = F_{\boldsymbol{X}}(x) \tag{A.28}$$

Defining the sample of maximum value of $\boldsymbol{X}$ in N observations as:

$$\boldsymbol{X}_E = max\{X_1, X_2, \ldots, X_N\} \tag{A.29}$$

it is possible to identify that if a given value x_e belongs to the maximum sample, then:

$$P(\boldsymbol{X}_E \leq x_e) = P(X_1 \leq x_e \cap X_2 \leq x_e \cap \ldots \cap X_N \leq x_e) \tag{A.30}$$

By Assuming that the observations X_i are statistically independent, then Eq. (A.30) becomes:

$$P(\boldsymbol{X}_E \leq x_e) = P(X_1 \leq x_e) \cdot P(X_2 \leq x_e) \cdot \ldots \cdot P(X_N \leq x_e) \tag{A.31}$$

or

$$P(\boldsymbol{X}_E \leq x_e) = \prod_{i=1}^{N} P(X_i \leq x_e) \tag{A.32}$$

Generalizing the expression, for any value of x_e, since $P(X_i \leq x_e)$ is the $F_{X_i}(x_e)$ itself, $P(\boldsymbol{X}_E \leq x_e)$ is the cumulative probability distribution of the extreme value at $\boldsymbol{X}_E = x_e$ and using Eq. (A.28), results:

$$F_{\boldsymbol{X}_E}(x) = [F_{\boldsymbol{X}}(x)]^N \tag{A.33}$$

Consequently, the probability density function of the extreme value is given by:

$$f_{\boldsymbol{X}_E}(x) = \frac{F_{\boldsymbol{X}_E}(x)}{dx} = N[F_{\boldsymbol{X}}(x)]^{N-1} f_{\boldsymbol{X}}(x) \tag{A.34}$$

In this context the ordinary probability distribution of **X**, i.e., $F_{\boldsymbol{X}}(x)$ (or $f_{\boldsymbol{X}}(x)$) is identified as initial or parent distribution. Once this distribution is known, the extreme value distribution can be derived for any N or any other return period of interest. This procedure is schematically shown in Figure A-1. Usually, the most probable value of the extreme distribution is the most wanted result.

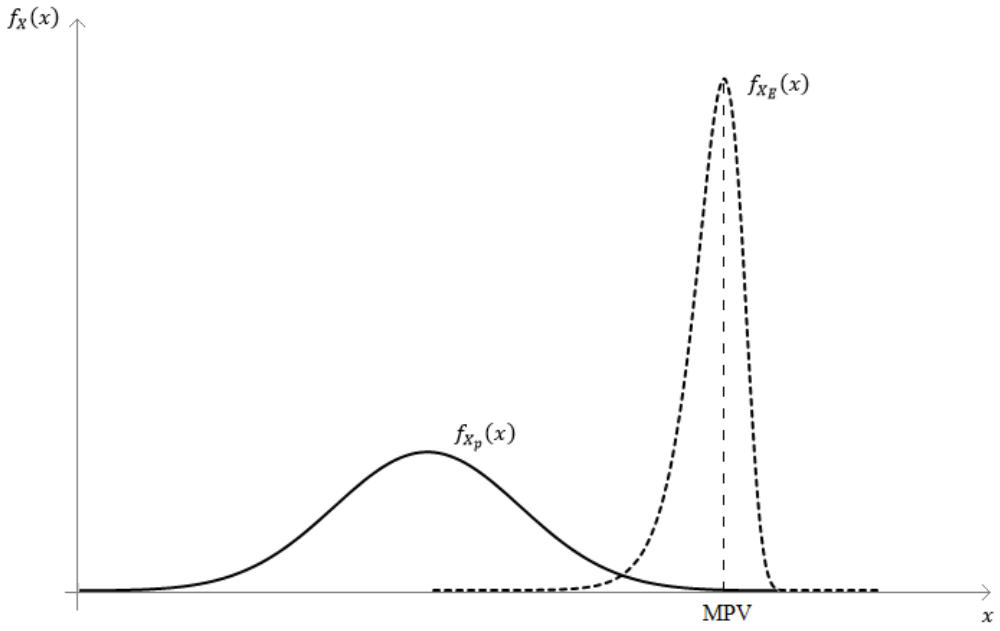

Figure A-1 – Initial and extreme maximum distribution with the corresponding most probable value.

A.3.2 ASYMPTOTIC EXTREME VALUE DISTRIBUTION

The approach described before leads to the "exact" extreme value distribution, for any value of N. However, when $N \to \infty$, the extreme distribution tend to converge to asymptotic functions, which are of three types:

1 – Gumbel Asymptotic Distribution (Type I);

2 – Fréchet Asymptotic Distribution (Type II);

3 – Weibull Asymptotic Distribution (Type II);

The domain of attraction of these three distributions depend on the tail behavior of the initial distribution in the direction of maximum value. Most of practical distributions used in offshore engineering, such as: Weibull and Normal, have the Gumbel distribution as its asymptotic form. This is because these distributions have an exponential decay in the direction of maximum extreme. This behavior is identified by the following expression:

$$\frac{f_X(x)}{1 - F_X(x)} = -\frac{f'_X(x)}{f_X(x)} \tag{A.35}$$

where $f_X(x)$ and $F_X(x)$ are PDF and CDF, respectively, of the initial random variable X.

The Gumbel distribution, as described previously in this Appendix, has two parameters, α and u. It can be shown [38] that this parameters can be derived by the two following expressions:

$$F_X(u) = 1 - \frac{1}{N} \tag{A.36}$$

$$\alpha = N f_X(u) \tag{A.37}$$

that applied to a Weibull model as the initial distribution result in:

$$\alpha = \frac{\lambda_w}{\alpha_w}(\ln N)^{\frac{\lambda_w - 1}{\lambda_w}} \tag{A.38}$$

$$u = u_w + \alpha_w(\ln N)^{\frac{1}{\lambda_w}} \tag{A.39}$$

with u_w, α_w and λ_w being the parameters of the 3-P Weibull distribution and N is the number of repetitions of the variable X in the return period considered. When using the 2-P Weibull tail distribution, u_w can be replaced by the mean μ of peaks sample.

APPENDIX B – WIND AND WAVE SPECTRUMS

JONSWAP sea spectrum, adjusted for Santos/Campos Basins is:

$$S(\omega) = \alpha \frac{g^2}{\omega^5} e^{-1.25\left(\frac{\omega_p}{\omega}\right)^4} \gamma^{e^{-\frac{(\omega-\omega_p)^2}{2\sigma^2\omega_p^2}}} \tag{B.1}$$

where: $\gamma = 6.4T_p^{-0.491}$ → Peak parameter or peak enhancement factor;

$\alpha = 0.3125\frac{H_S^2}{T_p^4}[1 - 0.287ln(\gamma)]$ → Form parameter or Phillips constant;

$\sigma = \begin{cases} \sigma_a = 0.07, \ for\ \omega \leq \omega_p \\ \sigma_b = 0.09, \ for\ \omega > \omega_p \end{cases}$ → Shape parameter or peak width;

g = Gravity acceleration;

ω = Wave frequency (rad/s);

ω_p = Peak frequency (rad/s);

H_S = Wave significant height;

T_p = Wave peak period ($T_p = 2\pi/\omega_P$);

NPD wind spectrum is:

$$S(\omega) = \frac{320\left(\frac{U_{10}}{10}\right)^2}{2\pi(1 + \widetilde{\omega}^{0.468})^{3.561}} \tag{B.2}$$

where $\widetilde{\omega} = 172\frac{\omega}{2\pi}\left(\frac{U_{10}}{10}\right)^{-0.75}$

ω = Wind frequency (rad/s);

U_{10} = Hourly wind velocity at 10m above sea level

APPENDIX C – LOAD-BASED METHODOLOGY

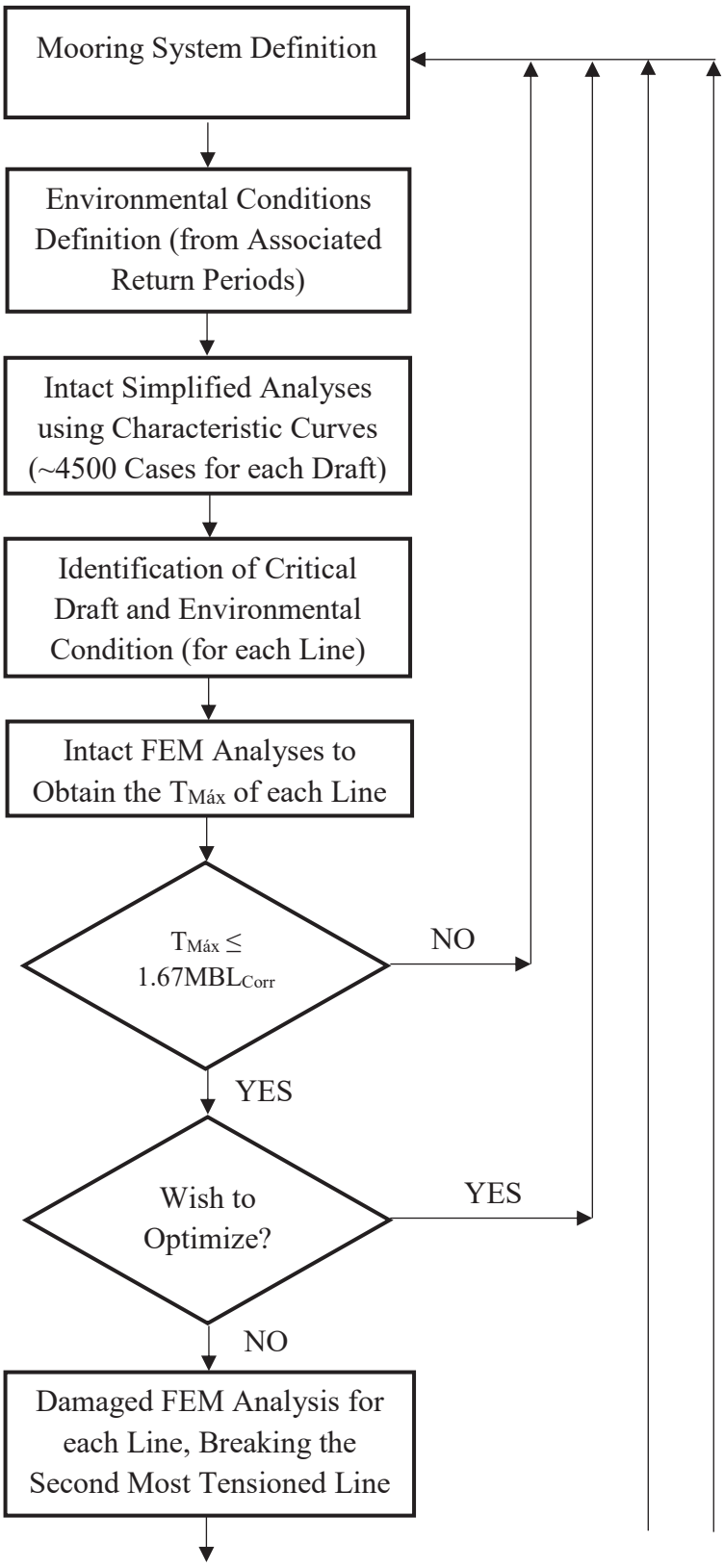

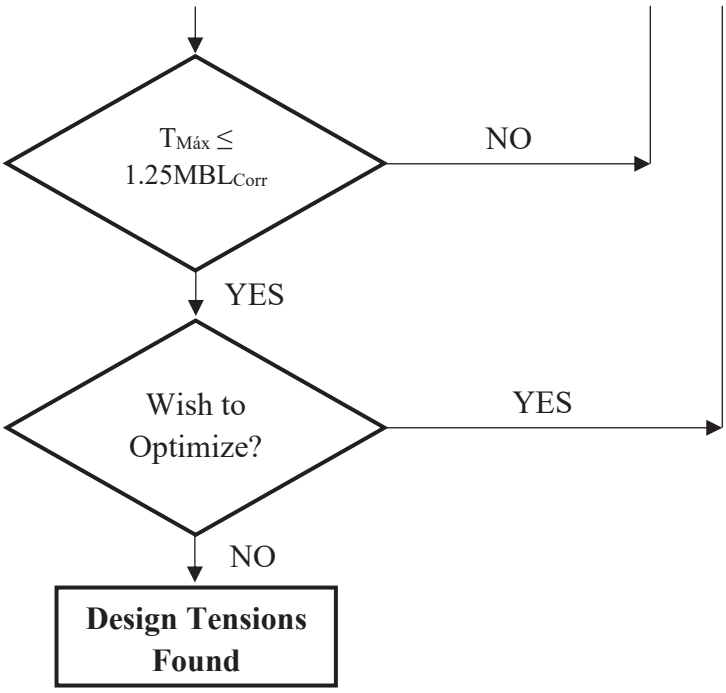

Important Considerations:

1) The procedure above is specific for the determination of Design Tensions. For other responses, such as Design Offsets, the procedure will be different;

2) The Damaged Condition Analysis could follow the same sequence of the Intact Condition Analysis, running at first all the environmental conditions for each line (with second line broken), using the characteristic curves (catenary equation) to represent the mooring lines and then use the FEM to find the final tensions. However, such procedure can lead to 2 or 3 times more processing time and the mooring design could be responsible to delay the platform project. Besides that, it has been found that the use of the worst cases of Intact Analysis to run the Damaged Analyses result in design tensions very close to those of a broader analysis.

APPENDIX D – RESPONSE-BASED METHODOLOGY

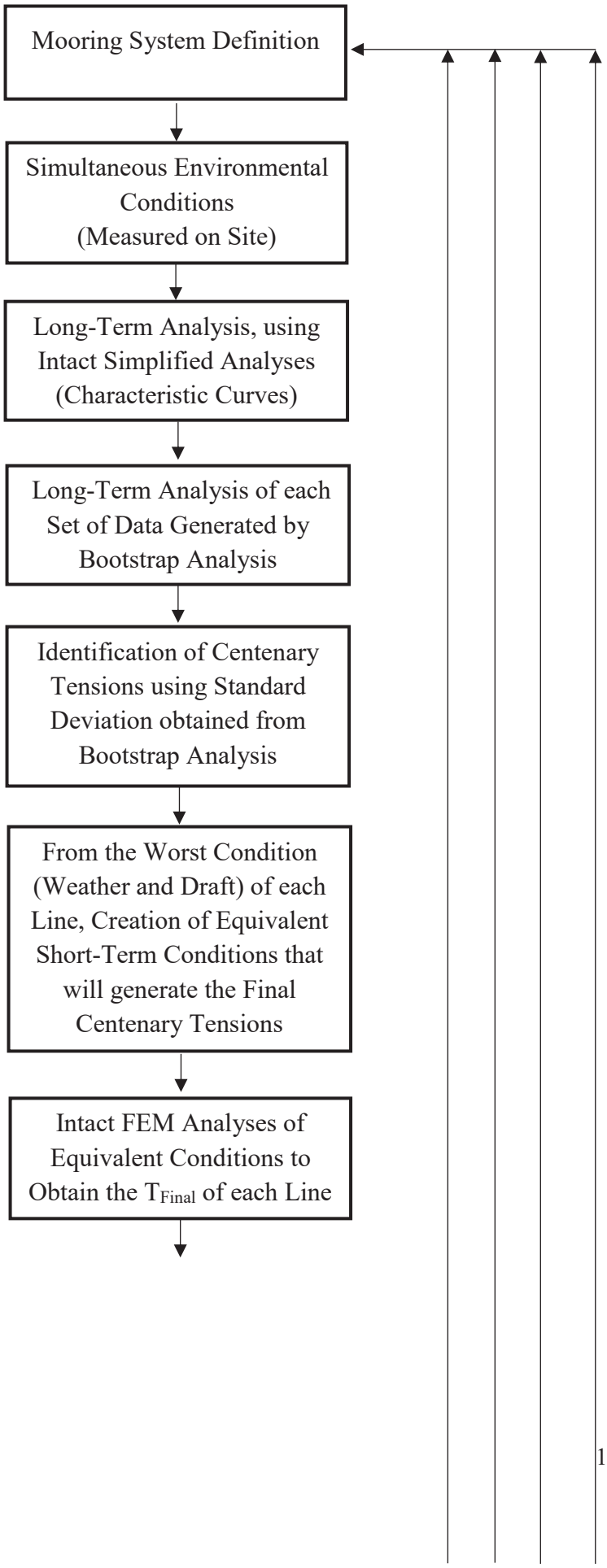

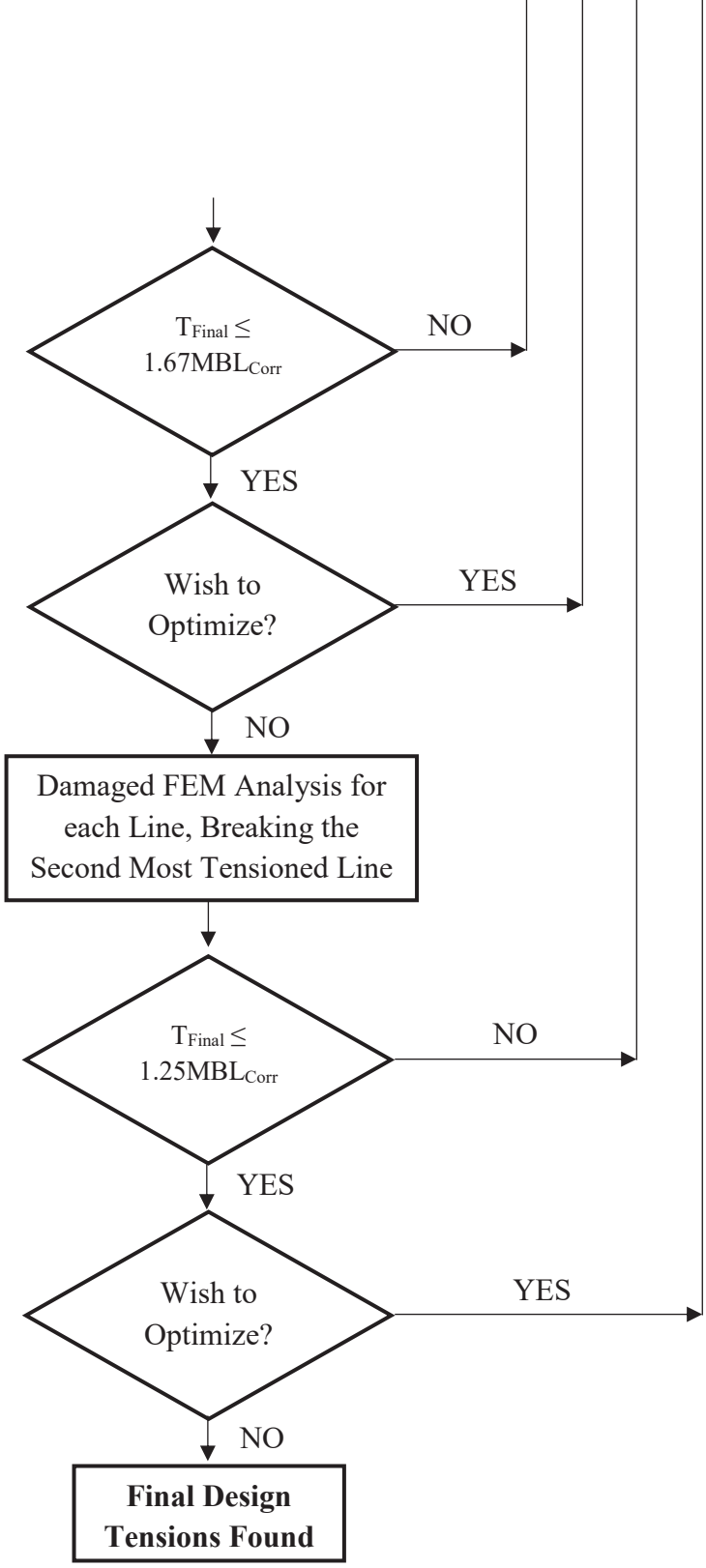

Important Consideration: The Long-Term analysis could also be done for each broken line in order to obtain the Damaged Long-Term Tension. However, this procedure would result in a need of a higher processing power and it would be not feasible for the everyday design routine. Besides that, a discussion of return period to be used on the Damaged Long-Term analysis should be raised due to the low exposure time of the platform operating with one or more lines broken.

APPENDIX E – CONVENTIONAL ANALYSIS RESULTS

The results presented here are related with the environmental conditions used on a conventional design short-term methodology (load-based methodology). The intention is not to compare these results with those obtained from the proposed long-term analysis. The tables and figures show that the Short-Term Analysis Module (see Chapter 4.2) provide reliable results - comparing with the reference (Dynasim).

For the FPSOs, only the full draft results are presented. Only the tension at the top of fairleads are presented and only the intact analyses were conducted.

Table E-1 – Short-term extreme tension. Spread-moored FPSO – Full draft + worst environmental condition. Load-based methodology

Spread-moored FPSO. Full draft – Conventional load-based methodology						
Line #	**Conventional Environmental Condition**	**Current, Wind, Waves**	**Draft**	**2-P Weibull Short-Term Tension (kN)**	**3-P Weibull Short-Term Tension (kN)**	**Dif (%)**
1	**3956**	10,100,100	3	5907	5961	0.9%
2	**3956**	10,100,100	3	5673	5731	1.0%
3	**3956**	10,100,100	3	5978	6031	0.9%
4	**3956**	10,100,100	3	5709	5765	1.0%
5	**3956**	10,100,100	3	5703	5760	1.0%
6	**3799**	10,100,100	3	6062	5960	-1.7%
7	**3799**	10,100,100	3	6230	6127	-1.7%
8	**3799**	10,100,100	3	6096	5993	-1.7%
9	**3799**	10,100,100	3	6036	5934	-1.7%
10	**3799**	10,100,100	3	6084	5984	-1.7%
11	**3046**	10,100,100	3	5924	5927	0.0%
12	**3046**	10,100,100	3	5846	5852	0.1%
13	**3046**	10,100,100	3	5920	5920	0.0%
14	**3046**	10,100,100	3	5846	5852	0.1%
15	**3046**	10,100,100	3	5698	5707	0.2%
16	**2850**	**10,100,100**	**3**	**6456**	**6463**	**0.1%**
17	**2850**	10,100,100	3	6230	6237	0.1%
18	**2850**	10,100,100	3	5975	5983	0.1%
19	**2850**	10,100,100	3	6198	6211	0.2%
20	**2850**	10,100,100	3	5906	5915	0.2%

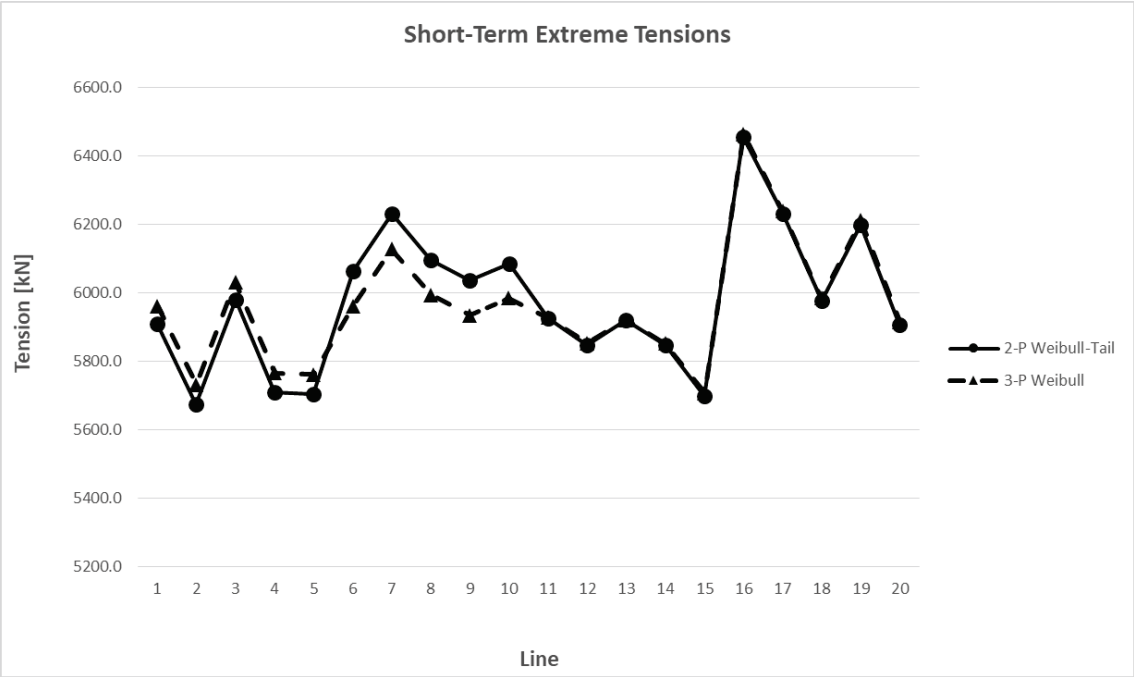

Figure E-1 – Short-term extreme tension. Spread-moored FPSO – Full draft + worst environmental condition. Load-based methodology

Table E-2 – Short-term extreme tension. Semi-submersible platform – Operational draft + worst environmental condition. Load-based methodology

Semi-submersible platform. Operational draft – Conventional load-based methodology						
Line #	**Conventional Environmental Condition**	**Current, Wind, Waves**	**Draft**	**2-P Weibull Short-Term Tension (kN)**	**3-P Weibull Short-Term Tension (kN)**	**Dif (%)**
1	**1667**	**100, 10, 10**	**1**	**5186**	**5176**	**-0.2%**
2	**1667**	100, 10, 10	1	5023	5013	-0.2%
3	**1667**	100, 10, 10	1	5022	5011	-0.2%
4	**1667**	100, 10, 10	1	4867	4855	-0.3%
5	**1667**	100, 10, 10	1	2331	2329	-0.1%
6	**962**	100, 10, 10	1	2289	2288	0.0%
7	**962**	100, 10, 10	1	2367	2367	0.0%
8	**962**	100, 10, 10	1	2478	2479	0.0%
9	**962**	100, 10, 10	1	2173	2163	-0.5%
10	**962**	100, 10, 10	1	2212	2203	-0.4%
11	**962**	100, 10, 10	1	2280	2271	-0.4%
12	**962**	100, 10, 10	1	2194	2188	-0.3%
13	**1251**	100, 10, 10	1	3583	3574	-0.2%
14	**1251**	100, 10, 10	1	3728	3719	-0.3%
15	**1251**	100, 10, 10	1	3740	3729	-0.3%
16	**1495**	100, 10, 10	1	3721	3715	-0.2%

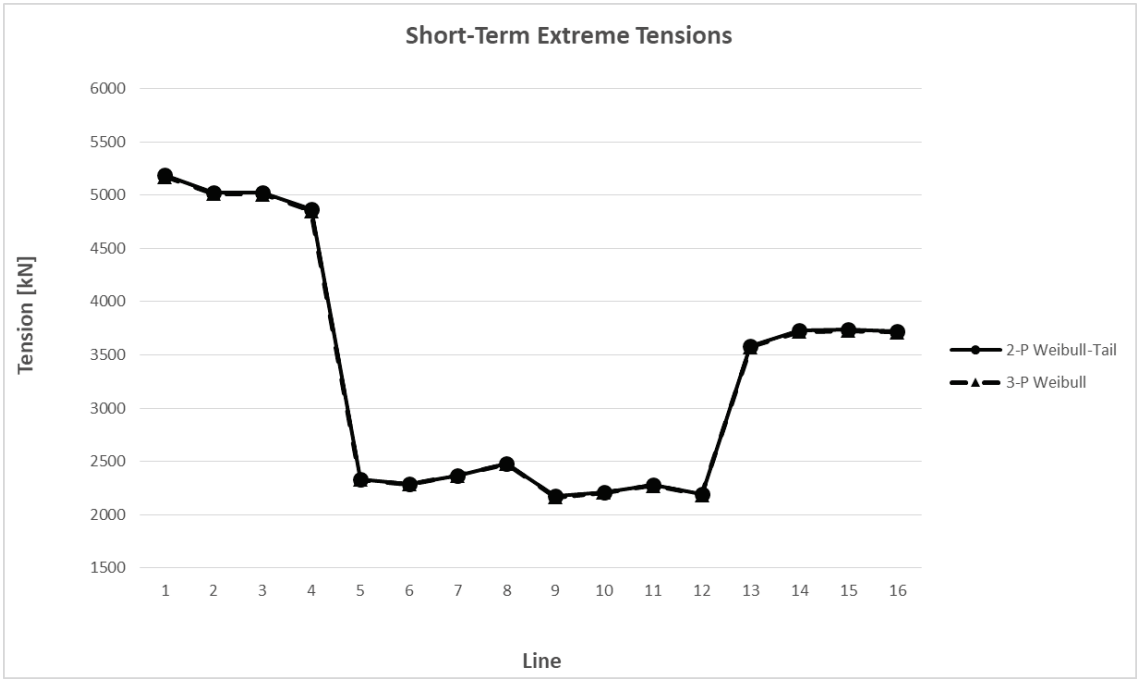

Figure E-2 – Short-term extreme tension. Semi-submersible platform – Operational draft + worst environmental condition. Load-based methodology

Table E-3 – Short-term extreme tension. Turret-moored FPSO – Full draft + worst environmental condition. Load-based methodology

Turret-moored FPSO. Full Draft – Conventional load-based methodology						
Line #	**Conventional Environmental Condition**	**Current, Wind, Waves**	**Draft**	**2-P Weibull Short-Term Tension (kN)**	**3-P Weibull Short-Term Tension (kN)**	**Dif (%)**
1	**3783**	10,100,100	2	1994	1919	-3.9%
2	**4072**	10,100,100	2	2905	2918	0.5%
3	**2607**	10,100,100	2	3407	3378	-0.9%
4	**2786**	**10,100,100**	**2**	**3874**	**3823**	**-1.3%**
5	**3116**	10,100,100	2	2112	2070	-2.0%
6	**3429**	10,100,100	2	2402	2318	-3.6%

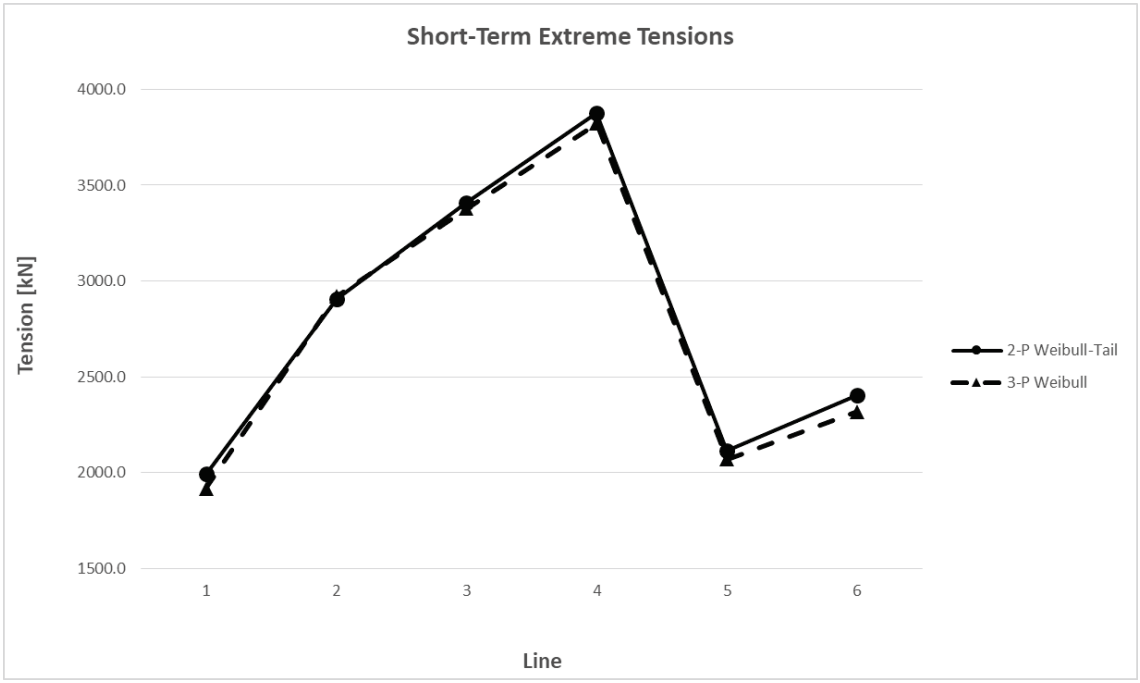

Figure E-3 – Short-term extreme tension. . Turret-moored FPSO – Full draft + worst environmental condition. Load-based methodology

APPENDIX F – LONG-TERM RESULTS

The results presented here are related with the 10-yr database of environmental conditions that were observed at Santos Basin (Brazil).

The results below were obtained by the Long-Term Analysis Module (see Chapter 4.3). Therefore, the results are the original ones, obtained by the long-term analysis, i.e, the Bootstrap procedure was not used here.

Only the tension at the top of fairleads are presented and only the intact analyses were conducted.

Table F-1 – Spread-moored FPSO. Extreme top tensions (simulation length of 3hr).

Spread-moored FPSO					
	Worst short-term condition			Long-Term Tension (kN)	Dif (%)
Line #	Environmental Condition	Draft	Extreme Tension (kN)		
1	13579	1	2871	2894	0.8%
2	13579	1	2574	2610	1.4%
3	20316	3	2592	2696	4.0%
4	20316	3	2320	2416	4.1%
5	12592	2	2236	2342	4.7%
6	25442	3	2487	2488	0.0%
7	25442	3	2674	2675	0.0%
8	25442	3	2730	2732	0.1%
9	25443	3	2830	2834	0.1%
10	25443	3	3022	3024	0.1%
11	**19256**	**2**	**3091**	**3290**	**6.4%**
12	19256	2	2923	3110	6.4%
13	19256	2	2888	3076	6.5%
14	19256	2	2752	2923	6.2%
15	19256	2	2627	2772	5.5%
16	19256	2	2998	3164	5.5%
17	19256	1	2904	3055	5.2%
18	19256	1	2871	3000	4.5%
19	19256	1	2974	3115	4.7%
20	19256	1	2848	2970	4.3%

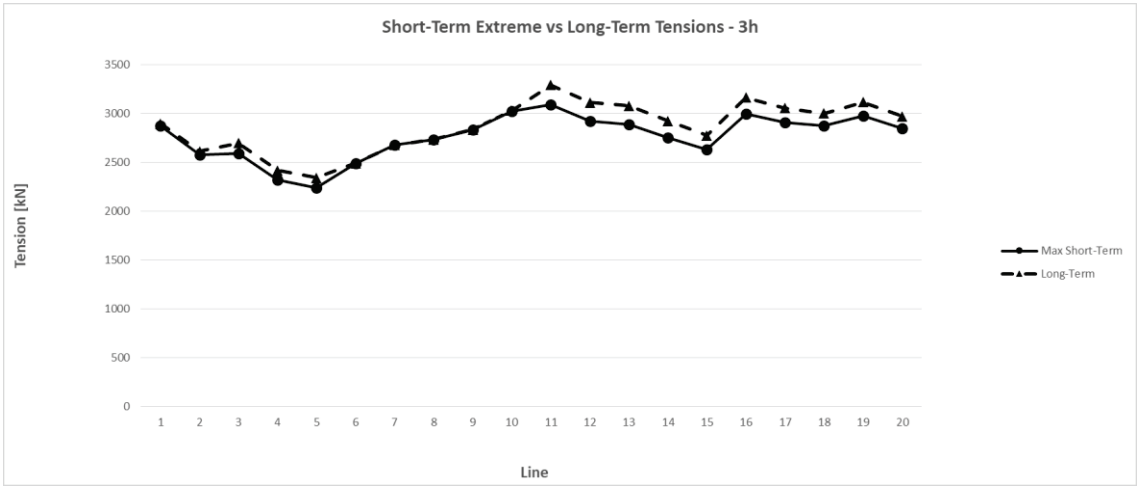

Figure F-1 – Spread-moored FPSO. Extreme top tensions (simulation length of 3hr).

Table F-2 – Spread-moored FPSO. Extreme top tensions (simulation length of 15hr).

Spread-moored FPSO					
	Worst short-term condition			Long-Term Tension (kN)	Dif (%)
Line #	Environmental Condition	Draft	Extreme Tension (kN)		
1	13579	1	2896	3063	5.8%
2	12592	2	2597	2768	6.6%
3	12592	2	2693	2892	7.4%
4	12592	2	2416	2582	6.9%
5	12592	2	2344	2494	6.4%
6	25442	3	2489	2493	0.2%
7	25442	3	2676	2680	0.1%
8	25442	3	2733	2735	0.1%
9	25442	3	2832	2837	0.2%
10	25443	3	3025	3027	0.1%
11	**19256**	**2**	**3210**	**3480**	**8.4%**
12	19256	2	3042	3304	8.6%
13	19256	3	3015	3282	8.9%
14	19256	3	2883	3126	8.4%
15	19256	3	2748	2954	7.5%
16	19256	3	3140	3371	7.4%
17	19256	2	3035	3251	7.1%
18	19256	2	2988	3179	6.4%
19	19256	2	3101	3320	7.1%
20	19256	2	2959	3158	6.7%

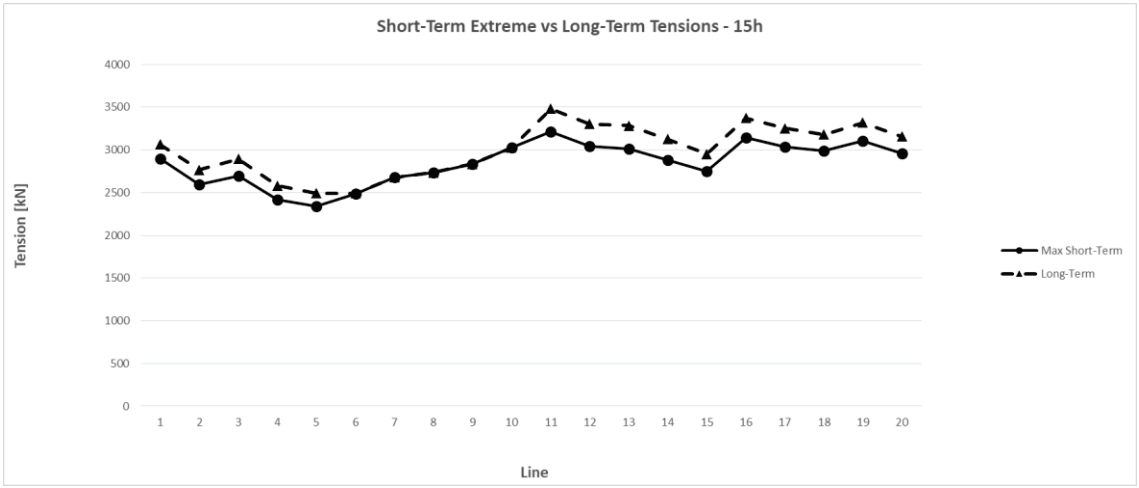

Figure F-2 – Spread-moored FPSO. Extreme top tensions (simulation length of 15hr).

Table F-3 – Spread-moored FPSO. Extreme top tensions (simulation length of 21hr).

Spread-moored FPSO					
	Worst short-term condition			Long-Term Tension (kN)	Dif (%)
Line #	Environmental Condition	Draft	Extreme Tension (kN)		
1	13579	1	2890	3031	4.9%
2	13579	1	2589	2740	5.8%
3	12592	2	2671	2859	7.0%
4	12592	2	2397	2554	6.5%
5	12592	2	2326	2468	6.1%
6	25442	3	2488	2491	0.1%
7	25442	3	2675	2678	0.1%
8	25442	3	2732	2735	0.1%
9	25442	3	2833	2837	0.1%
10	25443	3	3026	3028	0.1%
11	**19256**	**2**	**3161**	**3418**	**8.1%**
12	19256	2	2995	3243	8.3%
13	19256	2	2965	3219	8.6%
14	19256	3	2835	3066	8.1%
15	19256	3	2707	2901	7.2%
16	19256	2	3103	3320	7.0%
17	19256	2	3001	3203	6.7%
18	19256	2	2957	3136	6.1%
19	19256	2	3066	3271	6.7%
20	19256	2	2926	3114	6.4%

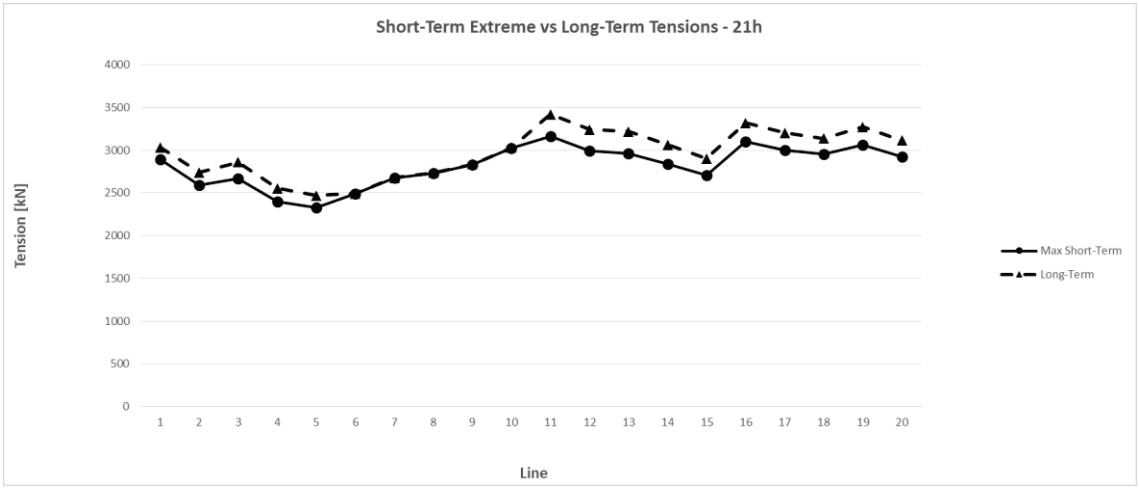

Figure F-3 – Spread-moored FPSO. Extreme top tensions (simulation length of 21hr).

Table F-4 – Semi-Submersible platform. Extreme top tensions (simulation length of 3hr).

Semi-submersible platform					
	Worst short-term condition			Long-Term Tension (kN)	Dif (%)
Line #	Environmental Condition	Draft	Extreme Tension (kN)		
1	**4408**	**1**	**4413**	**4414**	**0.0%**
2	4408	1	4331	4332	0.0%
3	4408	1	4409	4410	0.0%
4	4407	1	4343	4344	0.0%
5	8123	1	3268	3289	0.6%
6	8123	1	3371	3394	0.7%
7	8123	1	3336	3360	0.7%
8	8123	1	3270	3293	0.7%
9	11920	1	1570	1571	0.1%
10	11920	1	1606	1606	0.0%
11	11920	1	1617	1617	0.0%
12	11920	1	1636	1636	0.0%
13	25443	1	3514	3526	0.3%
14	25443	1	3660	3672	0.3%
15	25443	1	3676	3690	0.4%
16	25442	1	3665	3682	0.5%

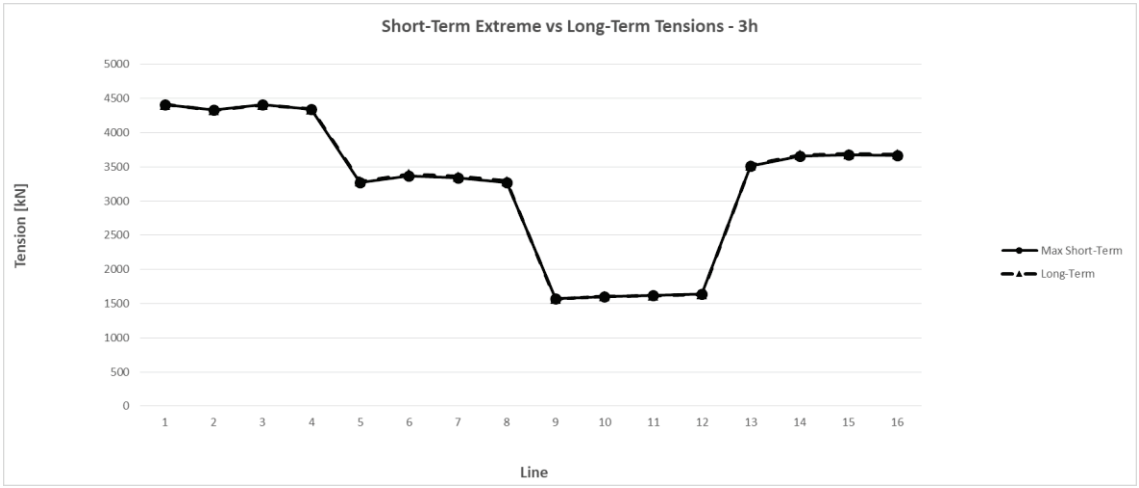

Figure F-4 – Semi-Submersible platform. Extreme top tensions (simulation length of 3hr).

Table F-5 – Semi-Submersible platform. Extreme top tensions (simulation length of 15hr).

Semi-submersible platform					
	Worst short-term condition			Long-Term Tension (kN)	Dif (%)
Line #	Environmental Condition	Draft	Extreme Tension (kN)		
1	**4408**	**1**	**4412**	**4413**	**0.0%**
2	4408	1	4331	4332	0.0%
3	4408	1	4409	4410	0.0%
4	4407	1	4343	4344	0.0%
5	8123	1	3261	3278	0.5%
6	8123	1	3363	3382	0.6%
7	8123	1	3329	3348	0.6%
8	8123	1	3262	3281	0.6%
9	11920	1	1570	1571	0.1%
10	11920	1	1606	1606	0.0%
11	11920	1	1617	1617	0.0%
12	11920	1	1636	1636	0.0%
13	25443	1	3511	3523	0.3%
14	25443	1	3657	3669	0.3%
15	25443	1	3673	3685	0.3%
16	25442	1	3660	3675	0.4%

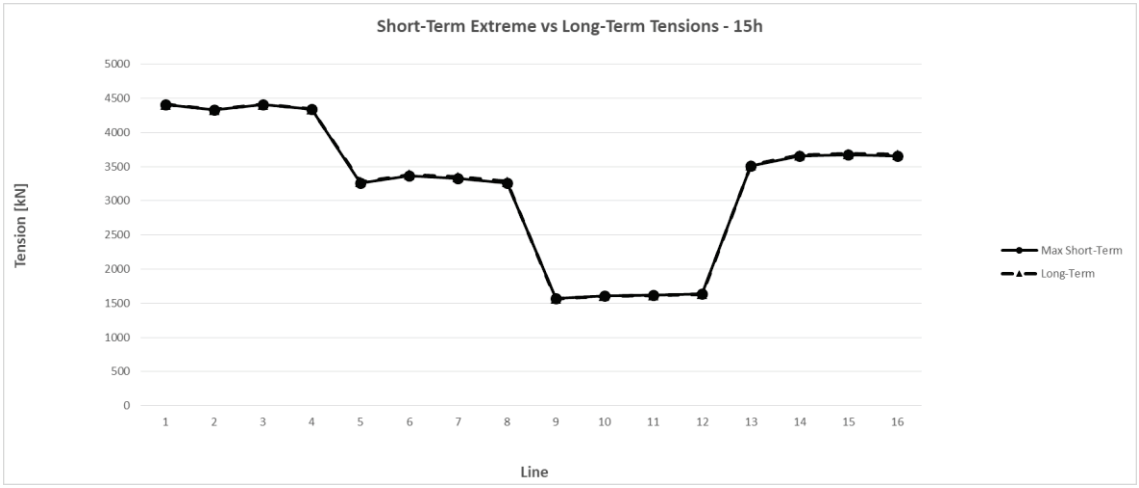

Figure F-5 – Semi-Submersible platform. Extreme top tensions (simulation length of 15hr).

Table F-6 – Turret-moored FPSO. Extreme top tensions (simulation length of 3hr).

Turret-moored FPSO					
	Worst short-term condition			Long-Term Tension (kN)	Dif (%)
Line #	Environmental Condition	Draft	Extreme Tension (kN)		
1	25442	1	863	866	0.3%
2	**4344**	**2**	**2145**	**2598**	**21.1%**
3	4344	2	1482	1674	13.0%
4	7076	2	1532	1863	21.6%
5	11920	2	1142	1156	1.2%
6	25443	1	1032	1037	0.5%

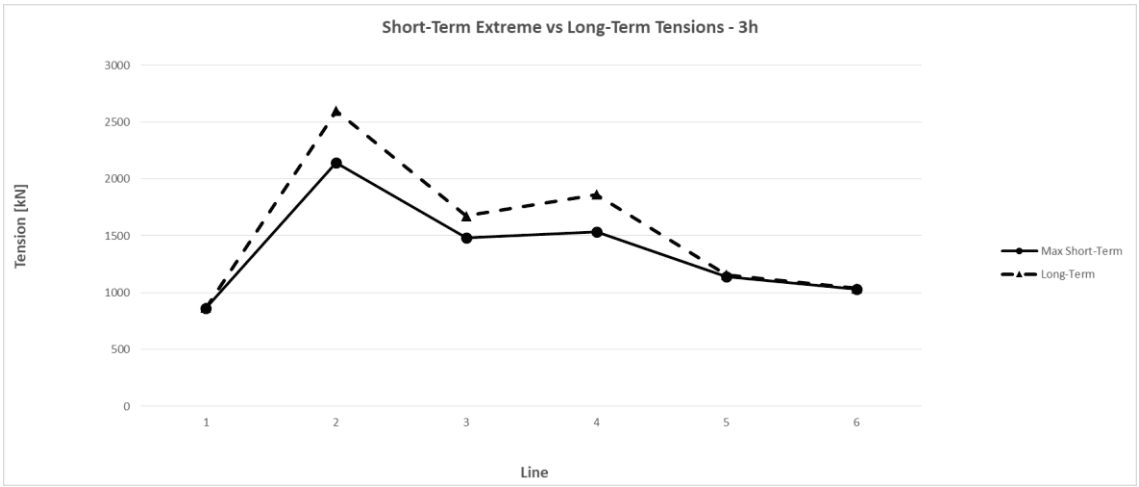

Figure F-6 – Turret-moored FPSO. Extreme top tensions (simulation length of 3hr).

Table F-7 – Turret-moored FPSO. Extreme top tensions (simulation length of 15hr).

Turret-moored FPSO					
	Worst short-term condition			Long-Term Tension (kN)	Dif (%)
Line #	Environmental Condition	Draft	Extreme Tension (kN)		
1	25442	1	865	869	0.5%
2	**4344**	**2**	**1888**	**2223**	**17.7%**
3	4344	2	1372	1500	9.3%
4	7978	2	1397	1605	14.9%
5	11920	2	1135	1145	0.9%
6	25443	1	1035	1042	0.7%

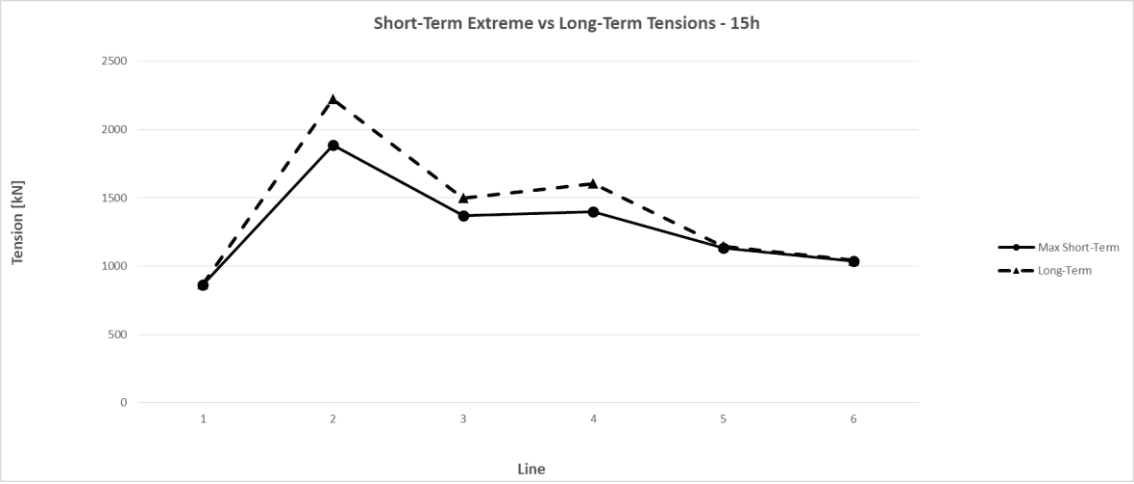

Figure F-7 – Turret-moored FPSO. Extreme top tensions (simulation length of 15hr).

Table F-8 – Turret-moored FPSO. Extreme top tensions (simulation length of 30hr).

Turret-moored FPSO					
	Worst short-term condition			Long-Term Tension (kN)	Dif (%)
Line #	Environmental Condition	Draft	Extreme Tension (kN)		
1	25442	1	865	870	0.6%
2	**4344**	**2**	**1894**	**2233**	**17.9%**
3	4344	2	1366	1494	9.4%
4	7978	2	1401	1606	14.6%
5	11920	2	1133	1142	0.8%
6	25443	1	1036	1043	0.7%

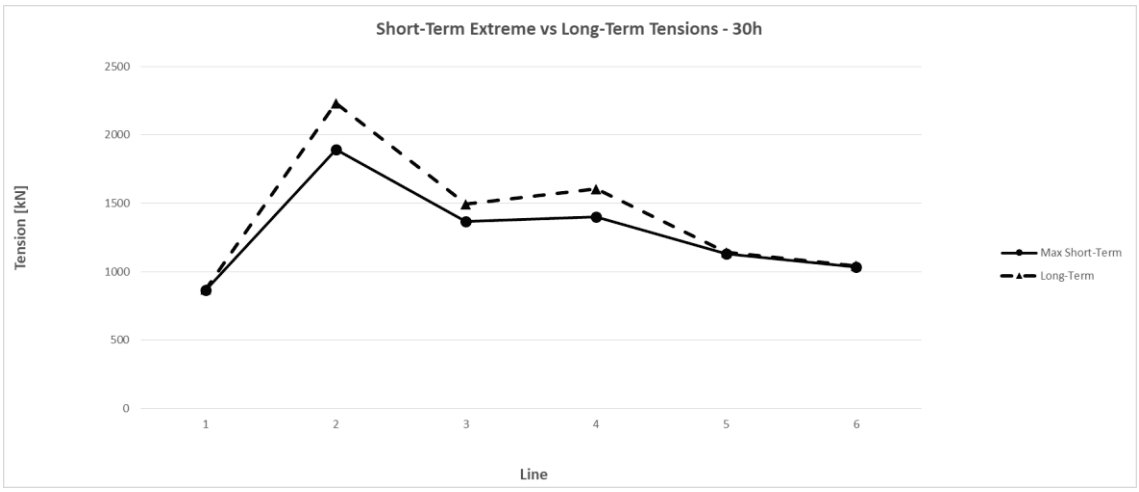

Figure F-8 – Turret-moored FPSO. Extreme top tensions (simulation length of 30hr).

APPENDIX G – CENTENARY TENSIONS

The centenary tensions (T_{100}) presented below were obtained by the Design Tension Module (see Chapter 4.5), after the application of the Bootstrap procedure. By this appendix is also possible to see the stabilization of the responses, indicating the minimum (or the ideal) time duration of short-term simulations.

The responses stabilization can be identified by the last three columns of tables with duration of time domain simulations bigger than 3hr. In this work, the responses were classified as stables when difference between them to the previous responses (those with lower duration of time domain simulation) were smaller than 2%. Although the results show stabilization for Semi-Submersible for simulations of 3hr, the centenary tensions (T_{100}) of this platform were also obtained by short-term simulation with 15hr of duration.

In order to simplify the tables, the differences are presented by the formulation:

$$\frac{T_i}{T_j} \tag{G.1}$$

But, actually, the real formulation on tables is:

$$\frac{T_i - T_j}{T_j} \tag{G.2}$$

Only the tension at the top of fairleads are presented and only the intact analyses were conducted.

Table G-1 – Spread-moored FPSO. Bootstrap Results. All lines (simulation length of 3hr).

Spread-moored FPSO							
Line #	**Short-Term Tension T_{Max} [kN]**	**Long-Term Tension T_{LT} [kN]**	**Bootstrap Mean Tension [kN]**	**Bootstrap Standard Deviation [kN]**	**Bootstrap Tension T_{100} [kN]**	$\frac{T_{100}}{T_{Max}}$	$\frac{T_{100}}{T_{LT}}$
L1	2871	2894	2885	30	2946	2.6%	1.8%
L2	2574	2610	2607	31	2670	3.7%	2.3%
L3	2592	2696	2664	75	2813	8.5%	4.3%
L4	2320	2416	2381	72	2525	8.9%	4.5%
L5	2236	2342	2299	79	2457	9.9%	4.9%
L6	2487	2488	2470	49	2569	3.3%	3.2%
L7	2674	2675	2655	62	2779	3.9%	3.9%
L8	2730	2732	2713	65	2843	4.1%	4.0%
L9	2830	2834	2815	68	2951	4.3%	4.1%
L10	3022	3024	3003	73	3149	4.2%	4.1%
L11	**3091**	**3290**	**3242**	**105**	**3452**	**11.7%**	**4.9%**
L12	2923	3110	3064	102	3269	11.8%	5.1%
L13	2888	3076	3029	105	3238	12.1%	5.2%
L14	2752	2923	2879	97	3074	11.7%	5.1%
L15	2627	2772	2734	84	2902	10.5%	4.7%
L16	2998	3164	3134	71	3276	9.3%	3.5%
L17	2904	3055	3028	66	3159	8.8%	3.4%
L18	2871	3000	2976	57	3090	7.6%	3.0%
L19	2974	3115	3088	65	3218	8.2%	3.3%
L20	2848	2970	2945	58	3062	7.5%	3.1%

Table G-2 – Spread-moored FPSO. Bootstrap Results. All lines (simulation length of 15hr).

Spread-moored FPSO										
Line #	**Short-Term Tension T_{Max} [kN]**	**Long-Term Tension T_{LT} [kN]**	**Bootstp Mean Tension [kN]**	**Bootstp $S.D.$ [kN]**	**Bootstp Tension T_{100} [kN]**	$\frac{T_{100}}{T_{Max}}$	$\frac{T_{100}}{T_{LT}}$	$\frac{T_{15hr}}{T_{3hr}}$ (T_{LT})	$\frac{T_{15hr}}{T_{3hr}}$ (T_{100})	$\frac{T_{15hr}}{T_{3hr}}$ (T_{Max})
L1	2896	3063	3021	96	3212	10.9%	4.9%	5.9%	9.0%	0.9%
L2	2597	2768	2716	97	2910	12.0%	5.1%	6.1%	9.0%	0.9%
L3	2693	2892	2794	157	3109	15.4%	7.5%	7.3%	10.5%	3.9%
L4	2416	2582	2491	144	2778	15.0%	7.6%	6.9%	10.0%	4.1%
L5	2344	2494	2401	141	2684	14.5%	7.6%	6.5%	9.3%	4.8%
L6	2489	2493	2478	55	2589	4.0%	3.8%	0.2%	0.8%	0.1%
L7	2676	2680	2659	65	2790	4.3%	4.1%	0.2%	0.4%	0.1%
L8	2733	2735	2712	69	2851	4.3%	4.2%	0.1%	0.3%	0.1%
L9	2832	2837	2811	77	2964	4.6%	4.5%	0.1%	0.4%	0.1%
L10	3025	3027	2995	86	3168	4.7%	4.7%	0.1%	0.6%	0.1%
L11	**3210**	**3480**	**3412**	**125**	**3662**	**14.1%**	**5.2%**	**5.8%**	**6.1%**	**3.9%**
L12	3042	3304	3236	125	3486	14.6%	5.5%	6.2%	6.7%	4.1%
L13	3015	3282	3212	129	3470	15.1%	5.7%	6.7%	7.2%	4.4%
L14	2883	3126	3059	123	3305	14.7%	5.7%	6.9%	7.5%	4.7%
L15	2748	2954	2894	109	3112	13.2%	5.4%	6.5%	7.2%	4.6%
L16	3140	3371	3324	96	3516	12.0%	4.3%	6.6%	7.3%	4.7%
L17	3035	3251	3207	90	3387	11.6%	4.2%	6.4%	7.2%	4.5%
L18	2988	3179	3140	80	3300	10.4%	3.8%	6.0%	6.8%	4.1%
L19	3101	3320	3275	91	3456	11.4%	4.1%	6.6%	7.4%	4.3%
L20	2959	3158	3118	83	3283	11.0%	3.9%	6.4%	7.2%	3.9%

Table G-3 – Spread-moored FPSO. Bootstrap Results. All lines (simulation length of 21hr).

Spread-moored FPSO										
Line #	**Short-Term Tension T_{Max} [kN]**	**Long-Term Tension T_{LT} [kN]**	**Bootstp Mean Tension [kN]**	**Bootstp S. D. [kN]**	**Bootstp Tension T_{100} [kN]**	$\frac{T_{100}}{T_{Max}}$	$\frac{T_{100}}{T_{LT}}$	$\frac{T_{21hr}}{T_{15hr}}$ (T_{LT})	$\frac{T_{21hr}}{T_{15hr}}$ (T_{100})	$\frac{T_{21hr}}{T_{15hr}}$ (T_{Max})
L1	2890	3031	3000	87	3175	9.9%	4.7%	-1.0%	-1.2%	-0.2%
L2	2589	2740	2703	87	2877	11.1%	5.0%	-1.0%	-1.1%	-0.3%
L3	2671	2859	2784	143	3070	14.9%	7.4%	-1.1%	-1.2%	-0.8%
L4	2397	2554	2483	130	2743	14.5%	7.4%	-1.1%	-1.3%	-0.8%
L5	2326	2468	2395	130	2654	14.1%	7.5%	-1.1%	-1.1%	-0.8%
L6	2488	2491	2474	45	2565	3.1%	3.0%	-0.1%	-0.9%	0.0%
L7	2675	2678	2656	55	2767	3.4%	3.3%	-0.1%	-0.8%	0.0%
L8	2732	2735	2710	63	2836	3.8%	3.7%	0.0%	-0.5%	0.0%
L9	2833	2837	2809	74	2957	4.4%	4.2%	0.0%	-0.2%	0.0%
L10	3026	3028	2995	85	3165	4.6%	4.5%	0.0%	-0.1%	0.0%
L11	**3161**	**3418**	**3376**	**113**	**3603**	**14.0%**	**5.4%**	**-1.8%**	**-1.6%**	**-1.5%**
L12	2995	3243	3201	113	3427	14.4%	5.7%	-1.9%	-1.7%	-1.6%
L13	2965	3219	3175	117	3410	15.0%	5.9%	-1.9%	-1.7%	-1.6%
L14	2835	3066	3023	112	3248	14.6%	5.9%	-1.9%	-1.7%	-1.7%
L15	2707	2901	2863	99	3061	13.1%	5.5%	-1.8%	-1.6%	-1.5%
L16	3103	3320	3288	90	3468	11.8%	4.5%	-1.5%	-1.4%	-1.2%
L17	3001	3203	3174	84	3342	11.4%	4.3%	-1.5%	-1.3%	-1.2%
L18	2957	3136	3110	74	3259	10.2%	3.9%	-1.4%	-1.2%	-1.1%
L19	3066	3271	3241	84	3410	11.2%	4.3%	-1.5%	-1.3%	-1.2%
L20	2926	3114	3087	77	3241	10.8%	4.1%	-1.4%	-1.3%	-1.1%

Table G-4 – Semi-submersible platform. Bootstrap Results. All lines (simulation length of 3hr).

Semi-submersible platform							
Line #	**Short-Term Tension T_{Max} [kN]**	**Long-Term Tension T_{LT} [kN]**	**Bootstrap Mean Tension [kN]**	**Bootstrap Standard Deviation [kN]**	**Bootstrap Tension T_{100} [kN]**	$\frac{T_{100}}{T_{Max}}$	$\frac{T_{100}}{T_{LT}}$
L1	**4413**	**4414**	**4404**	**22**	**4448**	**0.8%**	**0.8%**
L2	4331	4332	4321	24	4368	0.8%	0.8%
L3	4409	4410	4400	23	4447	0.9%	0.8%
L4	4343	4344	4336	25	4386	1.0%	1.0%
L5	3268	3289	3233	82	3396	3.9%	3.3%
L6	3371	3394	3331	91	3512	4.2%	3.5%
L7	3336	3360	3309	76	3460	3.7%	3.0%
L8	3270	3293	3268	44	3357	2.7%	1.9%
L9	1570	1571	1569	3	1576	0.4%	0.3%
L10	1606	1606	1598	11	1620	0.9%	0.8%
L11	1617	1617	1605	17	1638	**1.3%**	**1.3%**
L12	1636	1636	1624	18	1659	1.4%	1.4%
L13	3514	3526	3489	86	3662	4.2%	3.9%
L14	3660	3672	3632	99	3830	4.7%	4.3%
L15	3676	3690	3648	106	3861	5.0%	4.6%
L16	3665	3682	3638	111	3861	5.3%	4.9%

Table G-5 – Semi-submersible platform. Bootstrap Results. All lines (simulation length of 15hr).

Semi-submersible platform										
Line #	**Short-Term Tension T_{Max} [kN]**	**Long-Term Tension T_{LT} [kN]**	**Bootstp Mean Tension [kN]**	**Bootstp S. D. [kN]**	**Bootstp Tension T_{100} [kN]**	$\frac{T_{100}}{T_{Max}}$	$\frac{T_{100}}{T_{LT}}$	$\frac{T_{15hr}}{T_{3hr}}$ (T_{LT})	$\frac{T_{15hr}}{T_{3hr}}$ (T_{100})	$\frac{T_{15hr}}{T_{3hr}}$ (T_{Max})
L1	**4412**	**4413**	**4404**	**17**	**4438**	**0.6%**	**0.6%**	**0.0%**	**-0.2%**	**0.0%**
L2	4331	4332	4320	18	4355	0.6%	0.5%	0.0%	-0.3%	0.0%
L3	4409	4410	4398	19	4436	0.6%	0.6%	0.0%	-0.3%	0.0%
L4	4343	4344	4334	23	4379	0.8%	0.8%	0.0%	-0.2%	0.0%
L5	3261	3278	3227	77	3382	3.7%	3.2%	-0.3%	-0.4%	-0.2%
L6	3363	3382	3325	86	3497	4.0%	3.4%	-0.3%	-0.4%	-0.2%
L7	3329	3348	3303	70	3444	3.5%	2.9%	-0.4%	-0.5%	-0.2%
L8	3262	3281	3260	40	3339	2.4%	1.8%	-0.4%	-0.5%	-0.2%
L9	1570	1571	1569	3	1574	0.3%	0.2%	0.0%	-0.1%	0.0%
L10	1606	1606	1597	11	1619	0.8%	0.8%	0.0%	0.0%	0.0%
L11	1617	1617	1602	18	1638	**1.3%**	**1.3%**	0.0%	0.0%	0.0%
L12	1636	1636	1621	18	1658	1.4%	1.3%	0.0%	0.0%	0.0%
L13	3511	3523	3486	81	3648	3.9%	3.6%	-0.1%	-0.4%	-0.1%
L14	3657	3669	3628	94	3815	4.3%	4.0%	-0.1%	-0.4%	-0.1%
L15	3673	3685	3643	101	3846	4.7%	4.4%	-0.1%	-0.4%	-0.1%
L16	3660	3675	3631	107	3845	5.1%	4.6%	-0.2%	-0.4%	-0.1%

Table G-6 – Turret-moored FPSO. Bootstrap Results. All lines (simulation length of 3hr).

Turret-moored FPSO							
Line #	**Short-Term Tension T_{Max} [kN]**	**Long-Term Tension T_{LT} [kN]**	**Bootstrap Mean Tension [kN]**	**Bootstrap Standard Deviation [kN]**	**Bootstrap Tension T_{100} [kN]**	$\frac{T_{100}}{T_{Max}}$	$\frac{T_{100}}{T_{LT}}$
L1	863	866	855	26	907	5.2%	4.7%
L2	**2145**	**2598**	**2363**	**422**	**3207**	49.5%	23.4%
L3	1482	1674	1640	88	1817	22.6%	8.5%
L4	1532	1863	1851	76	2003	30.7%	7.5%
L5	1142	1156	1146	19	1183	3.6%	2.4%
L6	1032	1037	1024	27	1077	4.3%	3.8%

Table G-7 – Turret-moored FPSO. Bootstrap Results. All lines (simulation length of 15hr)

Turret-moored FPSO										
Line #	**Short-Term Tension T_{Max} [kN]**	**Long-Term Tension T_{LT} [kN]**	**Bootstp Mean Tension [kN]**	**Bootstp S. D. [kN]**	**Bootstp Tension T_{100} [kN]**	$\frac{T_{100}}{T_{Max}}$	$\frac{T_{100}}{T_{LT}}$	$\frac{T_{15hr}}{T_{3hr}}$ (T_{LT})	$\frac{T_{15hr}}{T_{3hr}}$ (T_{100})	$\frac{T_{15hr}}{T_{3hr}}$ (T_{Max})
L1	865	869	857	30	917	6.0%	5.4%	0.3%	1.0%	0.2%
L2	**1888**	**2223**	**2044**	**320**	**2683**	**42.2%**	**20.7%**	**-14.4%**	**-16.3%**	**-12.0%**
L3	1372	1500	1471	68	1606	17.1%	7.1%	-10.4%	-11.6%	-7.4%
L4	1397	1605	1594	44	1682	20.4%	4.8%	-13.9%	-16.0%	-8.8%
L5	1135	1145	1126	30	1186	4.5%	3.6%	-0.9%	0.2%	-0.6%
L6	1035	1042	1025	32	1090	5.3%	4.6%	0.4%	1.2%	0.3%

Table G-8 – Turret-moored FPSO. Bootstrap Results. All lines (simulation length of 30hr).

Turret-moored FPSO										
Line #	**Short-Term Tension T_{Max} [kN]**	**Long-Term Tension T_{LT} [kN]**	**Bootstp Mean Tension [kN]**	**Bootstp S. D. [kN]**	**Bootstp Tension T_{100} [kN]**	$\frac{T_{100}}{T_{Max}}$	$\frac{T_{100}}{T_{LT}}$	$\frac{T_{30hr}}{T_{15hr}}$ (T_{LT})	$\frac{T_{30hr}}{T_{15hr}}$ (T_{100})	$\frac{T_{30hr}}{T_{15hr}}$ (T_{Max})
L1	865	870	855	33	920	6.3%	5.7%	0.1%	0.3%	0.1%
L2	**1894**	**2233**	**2112**	**311**	**2735**	**44.4%**	**22.5%**	**0.4%**	**1.9%**	**0.3%**
L3	1366	1494	1478	68	1614	18.2%	8.0%	-0.4%	0.5%	-0.4%
L4	1401	1606	1595	42	1680	19.9%	4.6%	0.0%	-0.1%	0.3%
L5	1133	1142	1126	27	1179	4.1%	3.2%	-0.2%	-0.6%	-0.2%
L6	1036	1043	1025	34	1093	5.6%	4.9%	0.1%	0.3%	0.1%